JUL 29
1957

REGISTERED No. M. 3121

UNIVERSITY OF MICHIGAN
JUL 2[illegible] 1957
PHYSICS LIBRARY.

PROCEEDINGS
OF THE
INDIAN ACADEMY
OF SCIENCES

VOL. XLV] *SECTION A* [No. 5

MAY 1957

Price Rs. 2 or 3 Sh. *Annual Subscription Rs. 18*

PRINTED AT THE BANGALORE PRESS, BANGALORE CITY, BY C. VASUDEVA RAO
SUPERINTENDENT AND PUBLISHED BY THE INDIAN ACADEMY OF
SCIENCES, BANGALORE

THE SPECIFIC HEATS OF CRYSTALS AND THE FALLACY OF THE THEORIES OF DEBYE AND BORN

By Sir C. V. Raman

(*Memoir No. 96 of the Raman Research Institute, Bangalore 6*)

Received May 9, 1957

1. Introduction

The first step in any attempt at a theoretical evaluation of the specific heats of crystals is to determine the nature of the disturbance in their structure produced by the thermal agitation. In an earlier publication[1] and more fully again in the address to the Conference of Nobel Laureates held at Lindau in June 1956 which was printed in these *Proceedings*,[2] this problem was discussed. A general theory of the specific heats of crystals embodying the ideas expressed in those memoirs has since been formulated and published.[3] The theory leads to a determination of the spectroscopic behaviour of crystals and simultaneously with it to an expression for their specific heats as a function of the temperature. The success of the theory in achieving these aims has been demonstrated by a series of fully worked-out examples and a comparison with the facts of experiment.[4]

The principles on which the present approach to specific heat theory is based may be briefly sketched here. While the classical mechanics is made use of in the theory, stress is laid on the necessity of paying due regard at the same time to the basic principles of thermodynamics and to the fundamental notions of the quantum theory. With these requirements in view, the crystal is regarded as an assembly in thermodynamic equilibrium of sets of *similar* oscillators in great number, the energies of vibration of which are *individually* quantised. The identification and enumeration of these oscillators and the determination of their modes and frequencies of vibration is accomplished by taking note of the three-dimensional periodicity of structure characteristic of crystals and applying to the elements of that structure essentially the same methods as those which are so successful in the field of molecular spectroscopy. The determination of the thermal energy of the crystal as a function of the temperature is then effected by the same procedure as that indicated by Einstein in his fundamental paper[5] of 1907 introducing the quantum theory of specific heats.

The present approach to specific heat theory rejects completely the ideas regarding the subject embodied in Debye's well-known paper[6] and also those set out by Born and his school in numerous publications.[7] As the present generation of physicists and chemists has been brought up to believe in these latter theories, it would not be superfluous to explain in some detail why their rejection is necessary. That indeed is the purpose of the present memoir, which is sought to be achieved by a searching examination of the premises underlying the theories of Debye and Born and of the consequences to which those theories lead. It emerges from the examination that those premises are untenable and that the conclusions derived from them are false.

2. THE HYPOTHESIS OF JEANS

The parent of the specific heat theories of Debye and Born and also of other similar theories was a publication[8] by J. H. Jeans which appeared in the *Philosophical Magazine* in the year 1909. Though the title of that paper indicated temperature radiation as its subject, actually it was devoted for the most part to a discussion of the thermal behaviour of material bodies on the basis of classical mechanics. It put forward and sought to establish a proposition which may be stated as follows:—*the thermal energy of material bodies is identifiable with the sum of the potential and kinetic energies of regular trains of waves traversing them and forming stationary wave-patterns filling their volume.* The reader familiar with Debye's specific heat theory will immediately recognise this as the thesis which Debye accepted and elaborated in his attempt to explain the experimental results for the specific heats of elementary solids at low temperatures. It is not surprising in these circumstances that Jeans became an enthusiastic supporter of Debye's theory and by his advocacy helped to promote a general belief in the validity of the thesis on which that theory was based.

The waves considered by Debye in his paper were the longitudinal and transversal waves in an isotropic solid contemplated by the classical theory of elasticity. The formulæ set out in the paper were based on an analysis of the modes of vibration of an elastic solid sphere whose external surface was assumed to be rigidly fixed, followed by their enumeration in terms of their frequencies of vibration. Debye restricted himself for the most part to a consideration of the cases of monatomic solids exhibiting cubic symmetry. No such restriction is contemplated in the theory put forward and developed by Born and his school, which claims to be valid for all crystals. While Debye considered it to be adequate for his purpose to regard the vibrating solid as a continuum, the Born theory claims to take account of the discrete

lattice structure of the crystal. The waves considered in it are also of a more general kind than those recognised by Debye. Nevertheless, the theory of Born, like that of Debye, is based on an acceptance of the same thesis, *viz.*, the hypothesis of Jeans.

3. The Fallacy of the Hypothesis

Simple considerations of a general character suffice to show that the hypothesis of Jeans is a wholly misconceived idea. We have only to remark that the specific heat of a solid is an atomistic property, since its value at any given temperature is completely determined by two quantities, one of which is the number of atoms comprised in unit mass of the substance, and the other is the effective average frequency of vibration of the atoms at that temperature. Any attempt to explain this situation theoretically has, of necessity, to base itself on an atomistic approach to the problem. In other words, we have to consider the individual atoms in the crystal and investigate their dynamic behaviour. *Per contra*, wave-motions and the stationary wave-patterns resulting from the presence of an external boundary limiting their travel are macroscopic concepts, which, it should be emphasised, do not require us to take any notice of the atomicity of structure of the material traversed by the waves. In these circumstances, it is obvious that the attempt to build a theory of specific heats on the assumption that the thermal agitation is identifiable with wave-motions is an illogical and illusory proceeding.

We may usefully enlarge upon the foregoing remarks. The specific heat theories based on the hypothesis of Jeans concern themselves with the enumeration of the stationary wave-patterns assumed to exist within the volume of the solid. But, since the atomicity of structure of the material need not at all be considered in the description and enumeration of the wave-patterns, it remains completely outside the problem. The identification of the thermal energy of the solids with the sum of the kinetic and potential energies of the wave-patterns is therefore incapable of leading us to any determination of their specific heats. The difficulty which arises here is one of pure logic and is fundamental. In the theories now under discussion, the difficulty is sought to be circumvented by introducing an additional assumption, *viz.*, that the total number of wave-patterns is equal to thrice the number of atoms comprised in the crystal. While this assumption may appear plausible, it cannot be pretended that such a fixation of the number of wave-patterns is a necessary consequence or concomitant of the wave hypothesis. Actually, of course, it is introduced in order "to make the theory work", in other words, in order that the results of the theory

might bear some resemblance to the experimental facts. In logic, such a proceeding would be described as *petitio principii*, or begging the question.

4. Thermodynamics and the Theory of Specific Heats

It can be readily shown that the notions underlying the theories of Debye and Born are irreconcilable with the statistical concept of the nature of thermal energy which lies at the very base of the science of thermodynamics. A crystal is an assembly of an immense number of individual atoms which are capable of moving from their positions of equilibrium. Hence, the state of the system can only be described in terms of the values of a very large number of independent variables. No doubt, the atoms are held together by their mutual interactions to form the ordered assemblage which we call a crystal and which can be regarded as a unit in the macroscopic sense. But the statistical concept of thermal energy forbids us from regarding the entire assembly as a single unit in the thermodynamic sense. We cannot, for example, identify the thermal energy of the crystal with the energy of stationary wave-patterns of any sort. Indeed, the constancy of amplitude and coherence of phase relationship over extended regions of space and large periods of time which the formation of such wave-patterns presupposes are excluded by reason of the very nature of thermal energy. *Per contra*, it is to be expected that the thermal energy of a solid exhibits fluctuations in space and in time which preclude any definitive description of it except for domains of space and periods of time which are very small in comparison with macroscopic standards.

5. Classical Mechanics and the Theory of Specific Heats

That the theories of Debye and Born are untenable becomes evident also when we examine them from the standpoint of classical mechanics. For, specific heat theory starts from the well-known theorem that all the possible vibrations of a system of connected particles are superpositions of a set of normal modes in each of which the particles oscillate with the same frequency and in the same or opposite phases. The particles in the present problem are the individual atoms in the crystal and hence we are here concerned with the determination of the normal modes of vibration of *the atoms* in the sense of the theorem just stated. Instead of considering this question, the theories of Debye and Born concern themselves with an entirely different and indeed irrelevant subject, *viz.*, the normal modes of vibration of a macroscopic solid as determined by the form of its external boundary. Their treatment of specific heat theory thus stands revealed as a purely fanciful approach devoid of any validity or significance.

A straightforward application of the standard methods of classical dynamics enables us to determine the characteristic modes and frequencies with which the atoms in a three-dimensionally periodic array can oscillate about their positions of equilibrium. It emerges from the investigation that these characteristic modes can be enumerated and that they are related in a precisely definable manner to the structure and symmetry properties of the atomic groupings in the crystal. In the theories of Debye and Born, on the other hand, which assume that the modes of vibration are determined by the external boundary conditions and further, that the total number of wave-patterns is equal to thrice the number of atoms included in the crystal, we encounter results of an altogether different character. According to these theories, the great majority of the stationary wave-patterns which they contemplate have "wave-lengths" of the same order of magnitude as the lattice-spacings of the crystal. But these wave-lengths are all different and represent different frequencies of vibration. As a consequence, the "cells" of the wave-pattern in which the phase of vibration alternates bear no relation whatever to the structure of the crystal, while the wave-patterns themselves appear in immense numbers and are all different from each other. Such a description of the dynamical behaviour of the atoms linked with one another in the geometrically ordered structure of a crystal is, on the face of it, a fantastic misrepresentation. It is, in effect, a *reductio ad absurdum* of the theories which lead up to it.

6. The Quantum Theory of Specific Heats

The ideas which connect the hypothesis of energy quanta with the theory of specific heats were very clearly expounded in Einstein's classic paper[5] of 1907. If it be assumed that radiation is emitted or absorbed in energy-quanta proportional to the frequency, it follows as a necessary consequence that the mechanical energy of the oscillator which thus emits or absorbs would itself diminish or increase respectively by finite steps of the same amount. Generalising this result, Einstein postulated that the energy of any elementary structure capable of mechanical vibration would likewise obey the quantum rule. He then coupled this with the concept of thermodynamic probability embodied in Boltzmann's principle and showed that the relative probabilities of the oscillator being in different energy states could be determined with the aid of the principle. The next step is the evaluation of the average energy of an oscillator in an assembly consisting of a great number of such oscillators having a common frequency of vibration. This leads at once to the evaluation of the thermal energy of the whole assembly. The basic ideas of the quantum theory were further clarified and illumined by

Einstein in the famous paper[9] of 1917 in which he showed that the exchange of energy between a radiation field and the oscillators located in it can properly be described only in terms of statistical concepts. The probability of the oscillator being in any given state appears in the paper as the product of two factors, one of which is the thermodynamic probability factor given by the Boltzmann formula and the other is the intrinsic statistical weight of that state.

The foregoing remarks are made to emphasise that the quantum theory of specific heats rests on thermodynamic-statistical concepts which are wholly alien to the determinism of macroscopic physics. In other words, the theory of energy-quanta possesses a meaning and significance only in relation to the behaviour of the ultimate units of which matter is composed; *per contra* it is wholly out of place in any considerations regarding the behaviour of matter in bulk. For example, we can speak of the energy states of rotation or vibration of a molecule of benzene, but it would be nonsensical to discuss the problem of quantising the vibrations of a tuning fork or the rotations of a fly-wheel.

It will be clear from the foregoing remarks that Debye and Born fell grievously into error when they rejected the basic ideas of Einstein's theory and sought to build a theory of the specific heats of crystals on the behaviour of macroscopic solids. In doing this, not only did they ignore all considerations of logic as well as the physical principles bearing on the subject, but they also sought to impose on the quantum theory a fantastic and altogether meaningless interpretation.

7. THE SPECTROSCOPIC BEHAVIOUR OF CRYSTALS

The specific heats of crystals and their spectroscopic behaviour are intimately related properties since they are both determined by the frequencies of vibration of the atoms about their positions of equilibrium. This relationship is conveyed more precisely by the statement that the elementary oscillators in the crystal which are the carriers of its heat energy are also the oscillators capable of absorbing, emitting or scattering the radiations incident on it. It follows that any valid specific heat theory contains within itself a complete description of the vibration spectrum of a crystal: *vice versa*, a theory of the spectroscopic behaviour of crystals which correctly describes the facts of observation in that field necessarily contains within itself all the data needed for the evaluation of the specific heat as a function of the temperature.

From the foregoing remarks, it follows that the theories of Debye and Born which are based on erroneous assumptions regarding the carriers of the thermal energy in crystals also lead to a false picture of their vibration spectra. That is actually the case, for the assumptions made in these theories lead to the conclusion that the vibration frequencies of a crystal are immensely numerous and are all different from each other and hence that the vibration spectrum exhibits a continuous band of frequencies stretching over the entire range. *Per contra*, the atomistic theory of specific heats shows that the vibration spectrum of a crystal consists of a finite number of discrete monochromatic frequencies accompanied by a residual spectrum with a relatively small statistical weight which may be considered as continuous and which goes down to very low frequencies.

Spectroscopy is an exact science, and the vibration spectra of crystals are accessible to precise study and investigation by several different techniques and with a great variety of materials. In every case, the experimental results support and confirm the results of the atomistic theory in an unequivocal fashion. They are therefore also an objective demonstration of the falsity of the Debye and Born theories.

8. Summary

It is shown that the hypothesis, originally proposed by Jeans and adopted in the theories of Debye and Born, that the thermal energy of a solid is identifiable with the energy of wave-motions in its interior is not logically sustainable as a basis for a theory of their specific heats. The constancy of amplitude and of phase-relationships in extended volumes and periods of time demanded by the hypothesis is irreconcilable with the statistical-thermodynamical concept of the nature of thermal energy, and the idea that the theory of specific heats can be treated as a boundary-value problem in the physics of macroscopic solids is therefore misconceived. It is shown that such an approach is repugnant both to classical mechanics and to the principles of the quantum theory. It must therefore give place to a purely atomistic approach which gives us a wholly different picture of the nature of the thermal agitation in the solid and of its vibration spectrum.

9. References

1. Raman, C. V. .. Memoir No. 77 of the Raman Research Institute, *Proc. Ind. Acad. Sci.*, 1955, **42 A**, 163.

2. ———— .. Memoir No. 85 of the Raman Research Institute, *Ibid.*, .. 1956, **43 A**, 327.

3. Raman, C. V. .. Memoir No. 87 of the Raman Research Institute, *Proc. Ind. Acad. Sci.*, 1956, **44 A**, 153.

4. ———— .. Memoirs 86, 87, 91 and 93 of the Raman Research Institute' *Ibid.*, 1956, **44 A**, 99, 160 and 367; 1957, **45 A**, 1, 7, 59 and 139.

5. Einstein, A. .. *Ann. Der. Physik.*, 1907, **22**, 180.

6. Debye, P. .. *Ibid.*, 1912, **39**, 789.

7. Born and Karman .. *Physik., Zeits.*, 1912, **13**, 297.

8. Jeans, J. H. .. *Phil. Mag.*, 1909, **17**, 229.

9. Einstein, A. .. *Physik. Zeits.*, 1917, **18**, 121.

ON SUPERPOSABLE FLOWS

By P. L. Bhatnagar
(Indian Institute of Science, Bangalore)
AND
P. D. Verma
(Maharaja's College, Jaipur)

Received March 1, 1957

Let (q_1, p_1, Ω_1) and (q_2, p_2, Ω_2) be the two flows of an incompressible fluid of uniform density ρ and kinematic viscosity ν, where as usual $\vec{q}$ is the velocity vector, p the pressure and Ω the force potential from which the external forces are assumed to be derived. Following Ram Ballabh[1] we shall call these flows as superposable if it is possible to determine a pressure $p_1 + p_2 + \pi$ such that $(\vec{q}_1 + \vec{q}_2,\ p_1 + p_2 + \pi,\ \Omega_1 + \Omega_2)$ is also a solution of Stokes-Navier equations with the necessary modification in the initial and boundary conditions. In the present note we shall consider the two-dimensional flows due to a (i) vortex, (ii) spiral-vortex, (iii) vortex-doublet and (iv) a radial flow from the point of view of superposability. We may note that in a recent paper Prem Prakash[2] has studied radial flow but we are reconsidering it here in order to bring out some important points about it.

In the first section we have obtained the general condition for superposability of two flows and other necessary expressions working through vectors in order to make the treatment independent of the choice of co-ordinate system. In particular, we deduce the condition of superposability of axi-symmetrical flows and discuss them from the point of view of superposability. As far as the plane flows are concerned we have not obtained any new result in this section but the discussion of axi-symmetrical flows appears to be new. Besides, we have included this deduction here as it is short and elegant and we use the condition of superposability in the text in the form deduced here.

1. Denoting vorticity by $\vec{\omega}$, the equations of continuity and motion for the two flows are:

$$\operatorname{div} \vec{q}_1 = 0 \tag{1.1}$$

$$\frac{\partial \vec{q}_1}{\partial t} + \operatorname{grad}\left(\tfrac{1}{2}\vec{q}_1^{\,2} + \frac{p_1}{\rho} + \Omega_1\right) + \vec{\omega}_1 \times \vec{q}_1 = -\nu \operatorname{curl} \vec{\omega}_1 \tag{1.2}$$

$$\operatorname{div} \vec{q}_2 = 0 \tag{1.3}$$

$$\frac{\partial \vec{q}_2}{\partial t} + \text{grad}\left(\tfrac{1}{2}\vec{q}_2^{\,2} + \frac{p_2}{\rho} + \Omega_2\right) + \vec{\omega}_2 \times \vec{q}_2 = -\nu \,\text{curl}\, \vec{\omega}_2 \tag{1.4}$$

We first note that condition of integrability of the equation of motion is

$$\frac{d\vec{\omega}}{dt} = (\vec{\omega} \cdot \nabla)\vec{q} + \nu \triangle \vec{\omega} \tag{1.5}$$

as will be seen by taking the curl of both sides of the equation of motion.

Adding (1.1) and (1.3) we find that the equation of continuity

$$\text{div}\,(\vec{q}_1 + \vec{q}_2) = 0 \tag{1.6}$$

for the superposed motion is satisfied.

Adding (1.2) and (1.4), we have

$$\frac{\partial}{\partial t}(\vec{q}_1 + \vec{q}_2) + \text{grad}\left[\tfrac{1}{2}(\vec{q}_1 + \vec{q}_2)^2 + \frac{p_1 + p_2 + \pi}{\rho} + (\Omega_1 + \Omega_2)\right]$$
$$+ (\vec{\omega}_1 + \vec{\omega}_2) \times (\vec{q}_1 + \vec{q}_2) - \left[\text{grad}\left(\frac{\pi}{\rho} + \vec{q}_1 \cdot \vec{q}_2\right)\right.$$
$$\left. + \vec{\omega}_2 \times \vec{q}_1 + \vec{\omega}_1 \times \vec{q}_2\right]$$
$$= -\nu \,\text{curl}\,(\vec{\omega}_1 + \vec{\omega}_2) \tag{1.7}$$

Hence the two flows are superposable if

$$\text{grad}\left[\frac{\pi}{\rho} + \vec{q}_1 \cdot \vec{q}_2\right] + \vec{\omega}_2 \times \vec{q}_1 + \vec{\omega}_1 \times \vec{q}_2 = 0\Big] \tag{1.8}$$

Or

$$\text{grad}\,\pi = -\rho\,[\text{grad}\,(\vec{q}_1 \cdot \vec{q}_2) + \vec{\omega}_2 \times \vec{q}_1 + \vec{\omega}_1 \times \vec{q}_2] \tag{1.9}$$

The equation (1.9) determines π. Performing curl operation on (1.8) we have

$$\text{curl}\,(\vec{\omega}_2 \times \vec{q}_1) + \text{curl}\,(\vec{\omega}_1 \times \vec{q}_2) = 0 \tag{1.10}$$

(1.10) gives the necessary condition for superposability of the two flows.

From (1.10) we conclude that there exists a scalar function χ such that

$$\vec{\omega}_2 \times \vec{q}_1 + \vec{\omega}_1 \times \vec{q}_2 = \text{grad}\,\chi \tag{1.11}$$

so that from (1.8) we have

$$\frac{\pi}{\rho} = \text{constant} - \vec{q}_1 \cdot \vec{q}_2 - \chi \tag{1.12}$$

In view of (1.11) and (1.12) it is easy to see that (1.10) is also a sufficient condition.

For the self-superposability of the flow $(\vec{q}, p, \Omega)$ the necessary and sufficient condition is

$$\text{curl}\,(\vec{\omega} \times \vec{q}) = 0 \tag{1.13}$$

so that

$$\vec{\omega} \times \vec{q} = \text{grad}\,\overline{\chi} \tag{1.14}$$

and

$$\frac{\pi}{\rho} = \text{constant} - \vec{q}^2 - \overline{\chi} \tag{1.15}$$

We may note the condition of superposability and the expression for π do not contain t explicitly and hence the difference in the consideration of steady and non-steady cases arises only through the condition of integrability (1.5).

If one flow, say with suffix 1, be irrotational then the condition of superposability of a rotational flow, with suffix 2, on it is

$$(\vec{q}_1 \cdot \nabla)\,\vec{\omega}_2 = (\vec{\omega}_2 \cdot \nabla)\,\vec{q}_1 \tag{1.16}$$

Considerable simplification results if we restrict our consideration to only the two-dimensional flows. In this particular case the above conditions reduce to

$$(\vec{q}_2 \cdot \nabla)\,\vec{\omega}_1 + (\vec{q}_1 \cdot \nabla)\,\vec{\omega}_2 = 0, \tag{1.17}$$

for the superposition of rotational flows,

$$(\vec{q}_1 \cdot \nabla)\,\vec{\omega}_2 = 0 \tag{1.18}$$

for the superposition of a rotational flow on an irrotational flow, and

$$(\vec{q} \cdot \nabla)\,\vec{\omega} = 0 \tag{1.19}$$

for the self-superposition of a rotational flow.

We may notice that the two irrotational flows always satisfy the condition of superposability.

We shall now consider the axi-symmetrical viscous flows. We shall take the x-axis along the axis of symmetry and as usual denote the perpendicular distance from the axis by $\widehat{\omega}$. The discussion simplifies considerably if we work through Stokes' stream function ψ such that

$$q_x = -\frac{1}{\widehat{\omega}}\frac{\partial\psi}{\partial\widehat{\omega}},\quad q_{\widehat{\omega}} = \frac{1}{\widehat{\omega}}\frac{\partial\psi}{\partial x} \tag{1.20}$$

and

$$\omega = \frac{1}{\widehat{\omega}}\mathrm{E}^2\psi,\quad \mathrm{E}^2 \equiv \frac{\partial^2}{\partial x^2} + \frac{\partial^2}{\partial\widehat{\omega}^2} - \frac{1}{\widehat{\omega}}\frac{\partial}{\partial\widehat{\omega}}. \tag{1.21}$$

In terms of the stream function the condition of integrability (1.5) for steady motion reduces to

$$\widehat{\omega}\,\mathrm{J}\begin{pmatrix}\psi, & \widehat{\omega}^{-2}\mathrm{E}^2\psi\\ x, & \widehat{\omega}\end{pmatrix} = \nu\,\mathrm{E}^4\psi, \tag{1.22}$$

while the condition of superposability of axi-symmetrical flows with stream functions ψ_1 and ψ_2 takes the form

$$\mathrm{J}\begin{pmatrix}\psi_1, & \widehat{\omega}^{-2}\mathrm{E}^2\psi_2\\ x, & \widehat{\omega}\end{pmatrix} + \mathrm{J}\begin{pmatrix}\psi_2, & \widehat{\omega}^{-2}\mathrm{E}^2\psi_1\\ x, & \widehat{\omega}\end{pmatrix} = 0, \tag{1.23}$$

where J denotes the Jacobian. We may note that in deducing (1.23) we have used the equations of continuity for both the flows.

From (1.23) we find that the condition of self-superposability is

$$\mathrm{J}\begin{pmatrix}\psi, & \widehat{\omega}^{-2}\mathrm{E}^2\psi\\ x, & \widehat{\omega}\end{pmatrix} = 0 \tag{1.24}$$

while the condition of superposability of a rotational flow, with suffix 2, on an irrotational flow, with suffix 1, is

$$\mathrm{J}\begin{pmatrix}\psi_1, & \widehat{\omega}^{-2}\mathrm{E}^2\psi_2\\ x, & \widehat{\omega}\end{pmatrix} = 0 \tag{1.25}$$

From (1.23) we conclude that the two flows will be superposable if

(i) they are irrotational,

(ii) vorticity of each flow is proportional to $\widehat{\omega}$,

(iii) $\omega_1/\widehat{\omega}$ is constant along the stream lines of flow 2, while $\omega_2/\widehat{\omega}$ is constant along the stream lines of flow 1.

From (1.24) we see that an axi-symmetrical flow will be self-superposable if its vorticity ω is of the form

$$\omega = \widehat{\omega} f(\psi) \tag{1.26}$$

and then the condition of integrability (1.22) reduces to

$$E^4\psi = 0 \tag{1.27}$$

From (1.25) we note that a rotational flow ψ_2 is superposable on an irrotational flow ψ_1, if in general

$$\omega_2 = \widehat{\omega} f(\psi_1) \tag{1.28}$$

and then the condition of integrability becomes

$$\widehat{\omega}\, J\left(\begin{matrix}\psi_2, & f(\psi_1)\\ x, & \widehat{\omega}\end{matrix}\right) = \nu E^2[\widehat{\omega}^2 f(\psi_1)]. \tag{1.29}$$

We may regard (1.29) as an equation to determine ψ_2 when ψ_1 is prescribed.

2. *Two-dimensional vortex.*—Let a two-dimensional vortex of strength K be placed at the origin. Then its complex potential is

$$W = iK \log Z \tag{2.1}$$

so that its velocity potential is

$$\phi = -K\theta \tag{2.2}$$

We investigate the general motion which can be superposed on it. The condition of superposability (1.18) here becomes

$$\frac{\partial \omega_2}{\partial \theta} = 0 \tag{2.3}$$

so that

$$\omega_2 = F(r), \tag{2.4}$$

where F is an arbitrary function of r.

Substituting this in the condition of integrability (1.5) we get

$$\frac{\partial \psi_2}{\partial \theta} = -\nu\left[r\frac{F''}{F'} + 1\right], \tag{2.5}$$

where ψ_2 is the stream function of the motion with suffix 2, so that

$$\psi_2 = -\nu\theta H(r) + G(r), \tag{2.6}$$

where

$$H(r) = r\frac{F''}{F'} + 1 \tag{2.7}$$

and G (r) is an arbitrary function of r.

Now since

$$\omega_2 = \triangle\psi_2 \tag{2.8}$$

We have

$$\omega_2 = -\nu\theta\left[H'' + \frac{1}{r}H'\right] + \left[G'' + \frac{1}{r}G'\right] \tag{2.9}$$

From (2.4) ω_2 is function of r only, this is possible, if

$$H'' + \frac{1}{r}H' = 0 \tag{2.10}$$

and

$$F(r) = G'' + \frac{1}{r}G' \tag{2.11}$$

i.e., if

$$H = A\log r + B. \tag{2.12}$$

Hence from (2.7)

$$\omega_2 = F(r) = D + C\int^{\log r} \exp\left(\tfrac{1}{2}AZ^2 + BZ\right) dZ \tag{2.13}$$

and from (2.6)

$$\psi_2 = \theta\,[A\log r + B] + G(r) \tag{2.14}$$

where G (r) is determined by (2.11) and (2.13).

From (2.13) we conclude that the vorticity in the motion which can be superposed on the flow due to a vortex is constant on concentric circles having the centre at the origin.

3. *Two-dimensional spiral vortex.*—Let a two-dimensional spiral vortex, *i.e.*, a source and a vortex, be situated at the origin, then the complex potential is given by Milne-Thompson[3]

$$W = (-m + iK)\log Z$$

so that its stream function ψ_1 is

$$\psi_1 = -m\theta + K\log r \tag{3.1}$$

We now investigate the general motion which is superposable on this irrotational flow. Here the condition of superposability is

$$mr\frac{\partial\omega_2}{\partial r} + K\frac{\partial\omega_2}{\partial\theta} = 0 \tag{3.2}$$

so that

$$\omega_2 = F(\tau), \tag{3.3}$$

where

$$\tau = re^{-\frac{m}{K}\theta}. \tag{3.4}$$

Also the condition of integrability in terms of the stream function ψ_2 becomes

$$\frac{\partial\psi_2}{\partial\theta} + \frac{m}{K} r \frac{\partial\psi_2}{\partial r} = -\nu\left(1 + \frac{m^2}{K^2}\right)\left(\tau\frac{F''}{F'} + 1\right) \tag{3.5}$$

The complete solution of (3.5) is

$$\psi_2 = -\nu\left(1 + \frac{m^2}{K^2}\right) H(\tau)\,\theta + G(\tau), \tag{3.6}$$

Where $G(\tau)$ is an arbitrary function of τ.

and

$$H(\tau) = \tau\frac{F''}{F'} + 1 \tag{3.7}$$

using (3.6) we get

$$\omega_2 = \triangle\psi_2 = -\nu\left(1 + \frac{m^2}{K^2}\right)^2\left(H'' + \frac{1}{\tau}H'\right)\left(\theta e^{-2\frac{m}{K}\theta}\right)$$

$$+ \left(1 + \frac{m^2}{K^2}\right)e^{-\frac{2m}{K}\theta}\left[2\frac{m\nu}{K}\frac{H'}{\tau} + \left(G'' + \frac{1}{\tau}G'\right)\right] \tag{3.8}$$

From (3.3), ω_2 is function of τ only and in view of (3.8) it is possible only if

$$H'' + \frac{1}{\tau}H' = 0 \tag{3.9}$$

and

$$2\frac{m}{K}\nu\frac{H'}{\tau} + \left(G'' + \frac{1}{\tau}G'\right) = 0 \tag{3.10}$$

but then

$$\omega_2 = 0 \tag{3.11}$$

Therefore we conclude that on the flow due to spiral vortex only an irrotational flow can be superposed.

We may note that when $m = 0$, (3.8) reduces to (2.9) because then $\tau = r$.

4. *Two-dimensional vortex doublet.*—We shall now investigate the general flow which can be superposed on the flow due to a vortex doublet situated at the origin along the axis of y. The velocity potential here is

$$\phi = \mu \frac{\cos \theta}{r} \tag{4.1}$$

so that the condition of superposability of flow (ψ_2, ω_2) on it is

$$r \frac{\partial \omega_2}{\partial r} + \tan \theta \frac{\partial \omega_2}{\partial \theta} = 0 \tag{4.2}$$

The complete solution of (4.2) is

$$\omega_2 = \mathrm{F}(\tau) \tag{4.3}$$

where F is an arbitrary function and

$$\tau = \frac{\sin \theta}{r} \tag{4.4}$$

Also the condition of integrability for the flow with suffix 2 is

$$r \sin \theta \frac{\partial \psi_2}{\partial \theta} + r^2 \cos \theta \frac{\partial \psi_2}{\partial r} = \nu \frac{\mathrm{F}''}{\mathrm{F}'} \tag{4.5}$$

The complete solution of (4.5) is

$$\psi_2 = -\nu \mathrm{H}(\tau) \frac{\cos \theta}{\tau} + \mathrm{G}(\tau), \tag{4.6}$$

where $\mathrm{G}(\tau)$ is an arbitrary function of τ

and

$$\mathrm{H}(\tau) = \mathrm{F}''/\mathrm{F}'. \tag{4.7}$$

From (4.6)

$$\omega_2 = \triangle \psi_2 = -\nu \frac{(1 - r^2\tau^2)^{\frac{1}{2}}}{r^5} \mathrm{H}'' + \frac{1}{r^4} \mathrm{G}'' \tag{4.8}$$

From (4.3) we find that ω_2 is function of τ only. This is possible if in (4.8)

$$\mathrm{H}'' = 0 \tag{4.9}$$

and

$$\mathrm{G}'' = 0 \tag{4.10}$$

but then

$$\omega_2 = 0 \tag{4.11}$$

so that only irrotational flow can be superposed on the flow due to a vortex-doublet.

5. *Radial flow.*—with velocity components[4]

$$(q_r)_2 = \frac{1}{r} f(\theta) \tag{5.1}$$

$$(q_\theta)_2 = 0 \tag{5.2}$$

and vorticity

$$\omega_2 = -\frac{1}{r^2} f'(\theta). \tag{5.3}$$

The condition of integrability of the Stokes Navier equation reduces to

$$2ff' + \nu(f^{IV} + 4f'') = 0 \tag{5.4}$$

We shall now determine the most general irrotational flow that can be superposed on it. Let the stream function of the irrotational flow be ψ_1, then the condition of superposability is

$$\frac{f'}{f''}\frac{\partial \psi_1}{\partial \theta} + \tfrac{1}{2} r \frac{\partial \psi_1}{\partial r} = 0 \tag{5.5}$$

The complete solution of (5.5) is

$$\psi_1 = \mathrm{F}(\omega_2) \tag{5.6}$$

Now, since ψ_1 is the stream function of irrotational motion,

$$\triangle \psi_1 = 0$$

i.e.,

$$\left[\left(\frac{\partial \omega_2}{\partial r}\right)^2 + \left(\frac{\partial \omega_2}{r \partial \theta}\right)^2\right] \mathrm{F}'' + (\triangle \omega_2)\, \mathrm{F}' = 0 \tag{5.7}$$

or

$$\omega_2 \frac{\mathrm{F}''}{\mathrm{F}'} = -\frac{(4f' + f''')f'}{4(f')^2 + (f'')^2}. \tag{5.8}$$

Prem Prakash, working through cartesian co-ordinates, obtains an equation corresponding to (5.8) and his satisfying that equation in a particular manner amounts to taking

$$\mathrm{F}'' = 0 \tag{5.9}$$

and

$$\triangle \omega_2 = 0 \tag{5.10}$$

in (5.7). Hence he has investigated only a particular case of the radial motion for which the vorticity is harmonic. Further, in this case from (1.5) the condition of integrability will be independent of viscosity and (5.4) reduces to

$$ff' = 0 \tag{5.11}$$

which means

$$f' = 0, \text{ i.e., } f = \text{constant} \tag{5.12}$$

so that

$$(q_r)_2 = \frac{\text{constant}}{r}. \tag{5.13}$$

Hence the radial flow which he considers is due to either a source or a sink under his assumptions.

We may regard (5.8) as an equation in two independent variables θ and $\omega_2 = -1/r^2 f'(\theta)$ and hence it will be satisfied if each side is taken equal to a constant k, say, *i.e.*, if

$$\omega_2 \frac{F''}{F'} = k \tag{5.14}$$

and

$$\frac{(4f' + f''')f'}{4(f')^2 + (f'')^2} = -k \tag{5.15}$$

The complete solution of (5.14) is

$$\psi_1 = F(\omega_2) = \frac{K}{k+1} \omega_2^{k+1} + L \tag{5.16}$$

where K and L are arbitrary constants.

On integrating (5.15) we have

$$f'' = \left[\frac{M^2}{(f')^{2k}} - 4(f')^2\right]^{\frac{1}{2}} \tag{5.17}$$

$$f' = \left(\frac{M}{2}\right)^{\lambda} \sin^{\lambda}\left(\frac{2\theta}{\lambda} + N\right) \tag{5.18}$$

and

$$f = \left(\frac{M}{2}\right)^{\lambda} \int \sin^{\lambda}\left(\frac{2\theta}{\lambda} + N\right) d\theta + P, \tag{5.19}$$

where M, N, P are arbitrary constants, and

$$\lambda = \frac{1}{k+1} \tag{5.20}$$

Now the superposition of an irrotational motion on the radial flow is possible only if f obtained in (5.19) satisfies the condition of integrability (5.4). Substituting the values of f', f'', f^{IV} in it, we get

$$f + \frac{4\nu(\lambda-1)(\lambda-2)}{\lambda^2}\cos\left(\frac{2\theta}{\lambda}+\mathrm{N}\right)\operatorname{cosec}^3\left(\frac{2\theta}{\lambda}+\mathrm{N}\right)=0.$$

Differentiating the above relation and substituting for f we get

$$t^{\lambda+4} + 2at^2 - 3a = 0$$

where

$$t = \sin\left(\frac{2\theta}{\lambda}+\mathrm{N}\right)$$

and

$$a = \left(\frac{2}{\mathrm{M}}\right)^{\lambda}\frac{8\nu(\lambda-1)(\lambda-2)}{\lambda^3}.$$

This cannot hold for all t. Hence we conclude that it is not possible to superpose an irrotational motion on the radial flow in general.

6. In conclusion, we may note that in the cases of the flows due to spiral-vortex, vortex-doublet and the radial flow we prove the non-existence of the rotational flows in the case of the first two and of irrotational flow in the case of the third which can be superposed on them. Such a conclusion, however, is not unexpected and it is in the very nature of the inverse approach[5] which we have adopted here. In the case of the flow due to a vortex we could find a family of rotational flows which are superposable on it. In these flows the isocurls are concentric circles.

Summary

In the first section of the present paper we obtain the condition of superposability working through vectors and in particular give explicitly the condition of superposability of axi-symmetrical flows. This enables us to make some general remarks on the possibility of superposition of two axi-symmetrical flows. The rest of the paper is devoted to the consideration of the possibility of superposition of general rotational flow on the flows due to a vortex, spiral-vortex and vortex-doublet and of irrotational flow on a radial flow in two-dimensions.

In case of the flow due to a vortex, we find that a family of rotational flows for which the isocurls are concentric circles is superposable on it. In

the case of the remaining three flows we find that the contemplated types of flows do not exist.

REFERENCES

1. Ram Ballabh .. *Proc. Banaras Math. Soc.*, 1940, **2**, 70–79.
2. Prem Prakash .. *Ganit*, 1954, **5**, 21–24.
3. Milne-Thompson, L. M. .. *Theoretical Hydrodynamics*, 1949 p. 325.
4. Durand, W. F. .. *Aerodynamics Theory*, 1935, **3**, 167.
5. Nemenyi, P. F. .. *Advances in Applied Mechanics*, 1951, p. 124.

A NEW SYNTHESIS OF DALBERGIN AND METHYL DALBERGIN AND A SYNTHESIS OF ALLO-DALBERGIN

By V. K. Ahluwalia, A. C. Mehta and T. R. Seshadri, F.A.Sc.

(Department of Chemistry, University of Delhi, Delhi)

Received March 18, 1957

In an earlier paper,[1] 4-phenyl coumarins occurring in nature were considered to be related to benzophenone derivatives. This was supported by the ready oxidation of the former into the latter. The oxidation of methyl dalbergin (I *a*) producing 2-hydroxy-4: 5-dimethoxy benzophenone (II *a*) has already been described.[1] Under the same conditions, 4-phenyl-7-methoxy coumarin (I *b*) yields 2-hydroxy-4-methoxy benzophenone (II *b*). The reverse change of a benzophenone into a 4-phenyl coumarin has been used in the past in two cases. Limaye and Ramkrishna[2] boiled 2: 4-dihydroxy benzophenone with acetic anhydride and sodium acetate and obtained 4-phenyl umbelliferone acetate. Similarly using 2: 6-dihydroxy benzophenone, Seshadri and Varadarajan[3] prepared 4-phenyl-5-hydroxy coumarin and its derivatives. This method has now been applied for the synthesis of dalbergin (I *c*) and methyl dalbergin (I *a*) using 2: 5-dihydroxy-4-methoxy benzophenone (II *c*) and 2-hydroxy-4: 5-dimethoxy benzophenone (II *a*) respectively. In exploratory experiments for working out the best conditions of the reaction 2-hydroxy-4-methoxy benzophenone (II *b*) was employed for conversion into 4-phenyl-7-methoxy coumarin (I *b*). The yields by this method at their best are not satisfactory as compared with the application of the Pechmann's reaction using benzoyl acetic ester.[1, 4, 5]

However, the benzophenone method is convenient for the preparation of 4-phenyl-5-methoxy-6-hydroxy coumarin, which can be called allo-dalbergin. As already mentioned Seshadri and Varadarajan[3] prepared 4-phenyl-5-hydroxy and 4-phenyl-5-methoxy coumarins by this method. The alternative method of preparing these compounds using β-resorcylic ester and benzoyl acetic ester along with aluminium chloride in nitrobenzene medium did not work satisfactorily. 4-Phenyl-5-methoxy coumarin undergoes nuclear oxidation to yield allo-dalbergin whose methyl ether and acetate have also been prepared.

Ahluwalia, Mehta and Seshadri[5] reported that partial methylation of nor-dalbergin (4-phenyl-6: 7-dihydroxy coumarin) was successful in

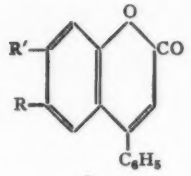

I

(*a*) R = R′ = OCH_3
(*b*) R = H; R′ = OCH_3
(*c*) R = OH; R′ = OCH_3

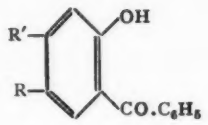

II

providing a convenient synthesis of dalbergin (I *c*). It has now been found that the method of partial demethylation can also be successfully employed. When methyl dalbergin (I *a*) is heated at 100° with hydrobromic acid in acetic acid, a mixture of dalbergin and nor-dalbergin is formed. But by using hydriodic acid at 115–20° for half an hour a better yield of dalbergin is obtained. The separation of the mixture could be effected by taking advantage of the property of nor-dalbergin to form a water-soluble complex with borax.

One of the extraordinary properties of dalbergin and methyl dalbergin has been the bright colour reactions they give with magnesium and alcoholic hydrochloric acid. In this respect there is resemblance to the flavonoids. A study has been made here of the behaviour of a number of 4-phenyl coumarins in this reaction. As will be seen from the results presented below, most of the 4-phenyl coumarins give the colour reaction, but it is most prominent with 6: 7-disubstituted compounds and least with 5- and 5: 7-substituted coumarins. The methyl ethers yield brighter colours as compared with hydroxy compounds.

The 3-phenyl coumarin derivatives do not give this colour reaction. The following methoxy and hydroxy-3-phenyl coumarins have been examined in this connection: 7-methoxy, 7-hydroxy, 7: 8-dimethoxy, 7: 8-dihydroxy, 6: 7-dimethoxy and 6: 7-dihydroxy. It would appear that there is something specific in regard to the substitution in the 4-position. Hence, in order to examine if a methyl group in this position will serve the same purpose as a phenyl group, a number of 4-methyl coumarins have been tested. Their reactions are positive though the colours are less intense as compared with the 4-phenyl coumarins. The same effect of position of the methoxy and hydroxy substituents is found here too.

In order to examine the combined effect of 3-phenyl along with the 4-methyl substituent the following 3-phenyl-4-methyl coumarins have been examined and they do not give any colour: 7-hydroxy, 6-methoxy, 6-hydroxy and 5-hydroxy.

The colour reaction with magnesium and alcoholic hydrochloric acid (known as the anthocyanin colour reaction) has been largely used in the field of flavonoids; generally a deep red or pink colour is observed. The flavanone, plathymenin was recorded by King *et al.*[5a] to give rise to pink and intense blue colour in this reaction. It has not been used before in the case of coumarins. From what has been recorded in the previous paragraphs, it would appear that this colour reaction is capable of being used for distinguishing between differently substituted coumarins.

Experimental

4-Phenyl-7-methoxy coumarin.—2-Hydroxy-4-methoxy benzophenone, (10 g.),[4,6,7] fused sodium acetate (5 g.) and acetic anhydride (11 c.c.) were heated in an oil-bath (165–70°) for 24 hrs., adding 2·5 c.c. of acetic anhydride after every six hours. The mixture was poured into water and the product (2 g.) crystallised from alcohol, m.p. 116–17°, undepressed by the sample prepared by using the Pechmann's reaction.[4]

Permanganate oxidation of 4-phenyl-7-methoxy coumarin.—4-Phenyl-7-methoxy coumarin in acetone was oxidised with potassium permanganate added in small quantities. When the product was worked up following the procedure described in a recent paper[1] it gave benzoic acid, oxalic acid and 2-hydroxy-4-methoxy benzophenone.

4-Phenyl-6-hydroxy-7-methoxy coumarin (dalbergin).—2: 5-Dihydroxy-4-methoxy benzophenone[7] (10 g.) gave acetyl dalbergin (3 g.) which crystallised from alcohol, m.p. 157–58°, undepressed by the acetate obtained from natural dalbergin.[8] On deacetylation it yielded dalbergin, m.p. 209–10°, undepressed by the natural sample.[8]

4-Phenyl-6: 7-dimethoxy coumarin (methyl dalbergin).—2-Hydroxy-4: 5-dimethoxy benzophenone[7,9] (10 g.) gave on cyclisation in a similar way methyl dalbergin (2 g.), m.p. and mixed m.p. with the natural sample[8] 144–45°.

Partial demethylation of methyl dalbergin:

(*a*) *With hydrobromic acid.*—Methyl dalbergin (2 g.) in glacial acetic acid (20 c.c.) was heated on a boiling water-bath with hydrobromic acid (66%; 20 c.c.) for 1 hr. The solution was poured into ice and the solid product filtered. It was digested with a warm (60–70°) solution of borax (5 g. in 30 c.c. water). The insoluble portion (0·6 g.) crystallised from methanol, m.p. 209–10°; mixed m.p. with natural dalbergin[8] was undepressed. The borax solution was treated with dilute sulphuric acid and the product (0·5 g.) obtained crystallised from alcohol, m.p. 267–68°; mixed m.p. with an authentic sample of nor-dalbergin[8] was undepressed.

(*b*) *With hydriodic acid.*—Methyl dalbergin (2 g.) in acetic anhydride (20 c.c.) was heated with hydriodic acid (20 c.c.) at 115–20° for half an hour. The solution was poured into saturated aqueous sodium bisulphite and the solid product filtered. It was separated into dalbergin (1·0 g.) and nor-dalbergin (0·6 g.) as in the above case.

4-Phenyl-5-methoxy-6-hydroxy coumarin (*Allo-dalbergin*).—It was prepared by the nuclear oxidation of 4-phenyl-5-methoxy coumarin[3] (2·7 g.) in aqueous sodium hydroxide (3 g. in 60 c.c. water) with potassium persulphate (4·8 g. in 100 c.c. water) following the procedure described in a recent paper.[5] It (1·5 g.) crystallised from benzene as colourless stout rectangular tablets, m.p. 178–79° (Found: C, 71·1; H, 4·8; $C_{16}H_{12}O_4$ requires C, 71·6; H, 4·5%).

The acetate (acetic anhydride and pyridine method) crystallised from methanol as colourless stout prisms, m.p. 114–16°. The methyl ether was prepared by means of methyl sulphate and anhydrous potassium carbonate in acetone solution. It crystallised from methanol as colourless thick rhombohedral plates, m.p. 134–36°.

Colour reactions:

Procedure.—A solution of about 5–10 mg. of the coumarin was dissolved in alcohol (5 c.c.) and an equal volume of concentrated hydrochloric acid added. The solution was treated with magnesium powder in small lots a number of times.

4-Phenyl coumarins.—(1) 4-Phenyl-7-hydroxy coumarin—pink red changing to green and finally fading to dirty yellow on standing. (2) 4-Phenyl-7-methoxy coumarin—red quickly changing to green and red on standing. (3) 4-Phenyl-7: 8-dihydroxy coumarin—pink changing to deep red. (4) 4-Phenyl-7: 8-dimethoxy coumarin—red changing to brown and again deep red; slowly fades to brown yellow on further addition of magnesium and hydrochloric acid. (5) 4-Phenyl-6: 7-dihydroxy coumarin (nor-dalbergin)—pink red changing to green and finally deep red on standing. (6) 4-Phenyl-6: 7-dimethoxy coumarin (methyl-dalbergin)—same as (5). (7) 4-Phenyl-6-hydroxy-7-methoxy coumarin (dalbergin)—same as (5). (8) 4-Phenyl-6-methoxy-7-hydroxy coumarin (iso-dalbergin)—pink red changing to green and finally pink. (9) 4-Phenyl-5-methoxy coumarin—red, fades slowly. (10) 4-Phenyl-5-hydroxy coumarin—orange yellow; fades slowly. (11) 4-Phenyl-5-methoxy-6-hydroxy coumarin (allo-dalbergin)—red; fades quickly. (12) 4-Phenyl-5: 6-dimethoxy coumarin—deep red changing to brown

red and finally fades. (13) 4-Phenyl-5: 7-dimethoxy coumarin—red fading slowly to yellow. (14) 4-Phenyl-5: 7-dihydroxy coumarin—orange, fades slowly.

4-*Methyl coumarins.*—(1) 4-Methyl-7-hydroxy coumarin—pink with slight green tinge changing finally to pink. (2) 4-Methyl-7-methoxy coumarin—pink changing to blue and finally to red. (3) 4-Methyl-6: 7-dihydroxy coumarin—red changing to pink and finally red. (4) 4-Methyl-6: 7-dimethoxy coumarin—pink changing to blue and finally deep red. (5) 4-Methyl-5: 7-dihydroxy coumarin—no colour. (6) 4-Methyl-5: 7-dimethoxy coumarin—no colour. (7) 4-Methyl-5: 6-dihydroxy coumarin—no colour. (8) 4-Methyl-5: 6-dimethoxy coumarin-red colour.

Summary

Though the benzophenone method of synthesis is not quite advantageous for dalbergin and methyl dalbergin, it is more convenient for the preparation of allo-dalbergin (4-phenyl-5-methoxy-6-hydroxy coumarin) and its methyl ether. These compounds and other 4-phenyl coumarins give markedly coloured solutions when treated with alcohol, hydrochloric acid and magnesium; a number of 4-methyl coumarin derivatives also give similar colour reactions. On the other hand 3-phenyl and 3-phenyl-4-methyl coumarin derivatives do not respond to this test which may therefore be of diagnostic value.

Acknowledgement

Our thanks are due to the Council of Scientific & Industrial Research for a research grant.

References

1. Ahluwalia and Seshadri .. *J.C.S.*, 1957, 970.
2. Limaye and Ramkrishna .. *Rasayanam*, 1937, **1**, 80.
3. Seshadri and Varadarajan .. *Proc. Ind. Acad. Sci.*, 1952, **35 A**, 80.
4. Kostanecki and Tambor .. *Ber.*, 1895, **28**, 2305.
5. Ahluwalia, Mehta and Seshadri *Proc. Ind. Acad. Sci.*, 1957, **45 A**, 15.

5*a*. King, King and Neill .. *J.C.S.*, 1953, 1055.

6. Kauffmann *et al.* .. *Ber.*, 1910, **43**, 1208.
7. Laumas, Neelakantan and Seshadri Unpublished work.
8. Ahluwalia, Sawhney and Seshadri *Jour. Sci. Ind. Res.*, 1956, **15 B**, 66.
9. Bargellini and Martegiani .. *Atti. R. Acad. Lincei.*, 1911, **20**, 183.

STUDIES ON THE DEPENDENCE OF OPTICAL ACTIVITY ON CHEMICAL CONSTITUTION

Part XLVI. The Rotatory Dispersion of *d*-Camphor-β-sulphonyl-nitrophenylamides (*o*-, *m*- and *p*-), *d*-camphor-β-sulphonylphenylenediamines (*o*-, *m*- and *p*-) and (*o*-, *m*- and *p*-) phenylene-*bis*-*d*-camphor-β-sulphonylamides

By Bawa Kartar Singh and Shiva Mohan Verma

Received October 30, 1956

In continuation of Part XLIII,[1] we describe the effect of the substitution of nitro, amino and *d*-camphor-β-sulphonylamido ($C_{10}H_{15}OSO_2NH$-) radicals in place of a hydrogen atom of the phenyl group of *d*-camphor-β-sulphonyl-phenylamide on the rotatory dispersion of the compounds.

Position Isomerism and Rotatory Power.—We find that Frankland's *lever-arm* hypothesis[2] and its electrostatic modification of Rule[3] do not hold for these compounds in any solvent, whereas Cohen's[4] rule is obeyed in all solvents for camphor-β-sulphonyl-nitrophenylamides (Tables I–III) and camphor-β-sulphonylphenylenediamines (Tables IV–VI) but not for phenylene-*bis*-*d*-camphor-β-sulphonylamides (Tables VII–IX). Whereas the *p*-, and *m*-isomerides of *d*-camphor-β-sulphonyl-nitrophenylamide are dextro rotatory, the *o*-isomeride is lævo rotatory.

Influence of Solvent on Rotatory Power.—It is found that the specific rotatory power, $[\alpha]_{5461}^{35°C.}$, in different solvents, generally increases with the decreasing value of the dielectric constant* of the solvent but in the following cases a reverse order has been found: *d*-camphor-β-sulphonyl-*o*-nitrophenyl-amide in chloroform gives $[\alpha]_{5461}^{35°C.} = -30·5°$ and in ethyl alcohol $[\alpha]_{5461}^{35°C.} = -36·0°$; *m*-, and *p*-isomerides of *d*-camphor-β-sulphonyl-nitrophenyl-amide and *o*- and *m*-isomerides of phenylene-*bis*-*d*-camphor-β-sulphonyl-amide show higher rotatory power in methyl alcohol than in ethyl alcohol.

'*Characteristic*' *Wavelengths derived from Dispersion Constants of Drude's Equation.*—The compounds now described exhibit '*simple*' rotatory dispersion in all the solvents as they can be expressed by the *one-term* Drude's equation. The '*characteristic*' wavelengths deduced from the dispersion equation vary from 4415 Å to 1622 Å. In solvents of ~~high~~ low and medium dielectric constants they vary generally from 2394 Å to 1622 Å (figures in italics in Tables I–IX). These high frequency absorption bands correspond to the

* Solvents in the decreasing order of the dielectric constant: methyl alcohol (31·5); ethyl alcohol (25·8); acetone (21·5); pyridine (12·4); ethyl acetate (6·11); chloroform (5·2); and benzene (2·28).

TABLE A. *Physical Properties of the Compounds*

Name of the compound	M. P. °C.	Crystalline form	Analysis % found	% required	Solubility
1 Camphor-β-sulphonyl-*p*-nitrophenyl-amides	*d* 146·5°	Amber-coloured prismatic needles	N=8·1		Soluble in A, B, C, E, M; insoluble in water
	dl 184·0°	Light yellow prismatic needles	S =9·1		
2 Camphor-β-sulphonyl-*m*-nitrophenyl-amides	*d* 146·0°	Fine pale yellow needles	S=9·06	For $C_{16}H_{20}O_5N_2S$,	do.
	dl 177·0°	Pale yellow prismatic needles	S =9·12	N=7·95 S =9·09	do.
3 Camphor-β-sulphonyl-*o*-nitrophenyl-amides	*d* 134·0°	Pale yellow rectangular plates	S =8·86		do.
	dl 132·0°	do.	S =9·20		do.
4 Camphor-β-sulphonyl-*p*-phenylenedia-mines	*d* 187·0°	Acicular prisms[6]			Less Soluble in B, M and EtOAC.
	dl 162·0°	do.	N=8·93		
5 Camphor-β-sulphonyl-*m*-phenylenedia-mines	*d* 118·0°	Fine prismatic needles	N=8·97	For $C_{16}H_{22}N_2SO_3$, N=8·7	Soluble in A, B, C, E, M and EtOAC
	dl 101·0°	Amorphous powder	N=8·88		
6 Camphor-β-sulphonyl-*o*-phenylenedia-mines	*d* 133·0°	Fine colourless needles	N=8·81		do.
	dl 143·0°	Colourless needles	N=8·89		do.
7 *p*-phenylene-*bis*-camphor-β-sulphonyl-amides	*d* 185·0°	Fine needles	N=5·26		Soluble in A, E and M; less soluble in EtOAC, B, E
	dl 191·0°	do.	N=5·29		
8 *m*-phenylene-*bis*-camphor-β-sulphonyl-amides	*d* 203·0°	Colourless prismatic needles	N=5·51	For $C_{26}H_{36}O_6S_2N_2$, N=5·22	Soluble in A, B, C, E, M
	dl 200·0°	do.	N=5·39		
9 *o*-phenylene-*bis*-camphor-β-sulphonyl-amides	*d* 92·0°	Amorphous powder	N=5·4		do.
	dl 83·84°	do.	N=5·38		do.

Where A = Acetone, B = Benzene, C = Chloroform, E = Ethyl alcohol, M = Methyl alcohol and EtOAC = Ethyl acetate.

TABLE I. *Rotatory Dispersion of* d-*Camphor-β-sulphonyl*-p-*nitrophenylamide, m.p.* 146·5° C.

Solvents	Methyl alcohol		Ethyl alcohol		Acetone		Ethyl acetate		Chloroform		Benzene	
Conc. in gm. per 100 c.c.	1·000		1·000		1·000		1·000		1·000		1·000	
Calc. $[\alpha]_\lambda^{35°}$	$\frac{8·493}{\lambda^2-3·0643}$		$\frac{6·154}{\lambda^2-0·0983}$		$\frac{9·876}{\lambda^2-0·0272}$		$\frac{13·032}{\lambda^2-0·0296}$		$\frac{18·23}{\lambda^2}$		$\frac{30·90}{\lambda^2}$	
Calc. λ_0 (Å)	2536		3134		*1649*		*1721*		..		..	
Lines	*o*	*c*	*o*	*c*	*o*	*c*	*o*	*c*	*o*	*c*	*o*	*c*
6708 ..	22·0	22·02	17·5	17·5	23·5	23·36	31·0	30·99	40·0	40·42	69·5	68·68
6438 ..	24·0	24·26	19·5	19·46	25·5	25·51	34·5	33·86	44·0	44·0	73·5	72·86
6104 ..	27·0	27·55	22·5	22·42	28·5	28·61	38·5	38·0	48·0	48·95	83·5	83·1
5893 ..	30·0	30·02	25·0	24·74	31·0	30·87	41·5	41·02	52·0	52·5	89·0	89·08
5780 ..	31·5	31·48	26·0	26·10	32·0	32·18	43·0	42·79	54·5	54·58	91·5	92·5
5468 ..	35·5	36·19	30·0	30·67	36·5	36·34	47·5	48·35	61·0	60·96	102·5	103·4
5460 ..	36·0	36·31	30·5	30·78	36·5	36·44	48·0	48·51	61·5	61·12	103·0	103·6
5209 ..	41·0	41·03	35·5	35·58	40·0	41·4	54·0	53·87	66·5	67·21	113·0	113·9
5086 ..	44·5	43·71	38·0	38·40	42·5	42·69	57·0	56·9	71·0	70·5	118·5	119·5
4799 ..	52·0	50·98	47·0	46·41	47·5	48·61	65·0	64·89	80·0	79·0	134·5	133·9
4678 ..	..	..	51·0	50·97	50·0	51·56	69·0	68·85	84·0	83·32	140·5	141·2
4603 ..	..	..	54·0	54·22	53·5	53·51	71·5	71·5	88·5	86·08	145·0	146·0
4358 ..	..	..	67·0	67·07	59·0	60·67	80·0	81·23	94·0	95·94	161·0	162·7

TABLE II. *Rotatory Dispersion of* d-*Camphor-β-sulphonyl*-m-*nitrophenylamide, m.p.* 146·5° *C.*

Solvents	Methyl alcohol		Ethyl alcohol		Acetone		Pyridine		Ethyl acetate		Chloroform		Benzene	
Conc. in gm. per 100 c.c.	1·000		1·000		0·5000		1·000		1·000		0·5000		0·5000	
Calc. $[\alpha]_\lambda^{35°}$	$\frac{9·708}{\lambda^2-0·069}$		$\frac{8·108}{\lambda^2-0·0903}$		$\frac{8·916}{\lambda^2-0·0753}$		$\frac{10·99}{\lambda^2-0·055}$		$\frac{10·182}{\lambda^2-0·0926}$		$\frac{30·4031}{\lambda^2}$		$\frac{21·474}{\lambda^2}$	
Calc. λ_0 (Å)	2627		3005		2744		*2345*		3042		..		..	
Lines	*o*	*c*	*o*	*c*	*o*	*c*	*o*	*c*	*o*	*c*	*o*	*c*	*o*	*c*
6708 ..	25·5	25·49	22·5	22·54	23·5	23·8	28·0	27·83	28·5	28·49	48·0	47·72	69·0	69·13
6438 ..	28·0	28·1	25·0	25·01	26·0	26·28	30·5	30·58	31·5	31·61	52·0	51·8	74·0	73·35
6104 ..	32·0	32·0	29·0	28·74	30·0	30·0	35·0	34·61	36·5	36·36	58·0	57·63	81·0	81·62
5893 ..	35·0	34·9	31·5	31·56	33·0	32·79	38·0	37·61	40·0	39·97	62·0	61·72	87·0	87·56
5780 ..	37·0	36·63	33·0	33·26	34·5	34·45	39·0	39·39	42·0	42·14	64·0	64·27	91·0	91·01
5468 ..	43·0	42·22	38·5	38·85	40·0	39·86	44·5	45·02	49·0	49·3	72·0	71·8	102·0	101·5
5460 ..	43·0	42·36	39·0	38·99	40·0	40·0	45·0	45·2	50·0	49·42	72·0	71·99	102·5	102·0
5209 ..	48·0	47·99	44·5	44·79	46·0	45·48	50·0	51·12	57·0	56·96	79·0	79·2	110·0	112·0
5087 ..	52·0	51·21	47·5	48·16	50·0	48·68	54·0	53·99	60·5	61·31	84·0	83·03	116·0	117·5

TABLE III. *Rotatory Dispersion of* d-*Camphor-β-sulphonyl-o-nitrophenylamide, m.p.* 134° *C.*

Solvents	Methyl alcohol		Ethyl alcohol		Acetone		Ethyl acetate		Chloroform		Benzene	
Conc. in gm. per 100 c.c.	1·000		0·5000		1·000		1·000		1·000		1·000	
Calc. $[\alpha]_\lambda^{35°}$	$\frac{-4\cdot155}{\lambda^2-0\cdot1175}$		$\frac{-4\cdot041}{\lambda^2-0\cdot1837}$		$\frac{-3\cdot993}{\lambda^2-0\cdot1429}$		$\frac{-1\cdot7857}{\lambda^2-0\cdot1949}$		$\frac{-7\cdot71}{\lambda^2-0\cdot0444}$		$\frac{-8\cdot583}{\lambda^2-0\cdot1552}$	
Calc. λ_0 (Å)	3472		4209		3781		4415		*2107*		3937	
Lines	*o*	*c*	*o*	*c*	*o*	*c*	*o*	*c*	*o*	*c*	*o*	*c*
6708 ..	−12·5	−12·49	−15·0	−15·17	−13·0	−13·0	−7·0	−7·0	−19·0	−19·01	−29·0	−29·12
6438 ..	14·0	13·98	17·5	17·51	15·0	15·04	8·0	8·13	21·0	20·84	33·0	33·11
6104 ..	16·0	16·29	20·0	20·4	17·0	17·39	10·0	10·06	23·5	23·51	39·5	39·5
5893 ..	18·0	18·10	25·0	24·72	19·5	19·5	12·0	11·73	25·5	25·47	45·0	44·71
5780 ..	19·0	19·18	27·0	26·87	20·5	20·87	13·0	12·83	26·0	26·62	48·5	47·98
5468 ..	23·0	22·89	35·0	35·05	26·0	25·58	17·5	17·16	30·0	30·29	60·0	59·7
5460 ..	23·0	23·0	36·0	35·3	26·0	25·71	17·5	17·30	30·5	30·38	60·0	60·03
5209 ..	28·0	27·02	45·0	46·13	31·0	31·1	23·0	23·37	34·0	33·98	73·5	73·92
5087 ..	30·5	29·44	54·0	53·95	34·5	34·51	28·0	28·04	36·0	35·99	83·00	83·22

TABLE IV. *Rotatory Dispersion of* d-*Camphor-β-sulphonyl*-p-*phenylene diamine, m.p.* 187° *C.*

Solvents	Ethyl alcohol		Acetone		Pyridine		Chloroform	
Conc. in gm. per 100 c.c.	0·5000		1·000		0·5000		1·000	
Calc. $[\alpha]_\lambda^{35°}$	$\frac{9·56}{\lambda^2-0·0732}$		$\frac{10·666}{\lambda^2-0·1098}$		$\frac{13·115}{\lambda^2-0·0857}$		$\frac{29·68}{\lambda^2}$	
Calc. λ_0 (Å)	2705		3315		2927		..	
Lines	*o*	*c*	*o*	*c*	*o*	*c*	*o*	*c*
6708 ..	26·0	25·37	32·0	31·34	36·0	35·99	67·0	65·97
6438 ..	28·0	28·01	35·0	35·0	40·0	39·76	71·0	71·61
6104 ..	32·0	31·95	40·5	40·61	46·0	45·72	79·5	79·69
5893 ..	35·0	34·89	45·0	44·93	50·0	50·16	85·5	85·49
5780 ..	37·0	36·64	48·0	47·57	53·0	52·81	90·0	88·86
5468 ..	42·0	42·33	56·0	56·36	63·0	61·48	99·0	99·26
5461 ..	43·0	42·49	56·0	56·59	63·0	61·72	99·0	99·54
5209 ..	48·0	48·35	67·0	66·06	70·0	70·65	110·5	109·4
5087 ..	52·0	51·57	73·0	71·63	79·0	75·86	114·0	114·8
4800 ..	61·0	60·81	89·0	88·49	91·0	90·61	127·0	128·5
4678 ..	66·0	65·66	100·0	97·86	..	..	135·5	135·6
4603 ..	69·0	68·98	107·0	104·6	104·0	104·0	141·5	140·2
4358 ..	82·0	81·85	133·0	133·0	..	..	..	..

TABLE V. *Rotatory Dispersion of* d-*Camphor-β-sulphonyl*-m-*phenylene diamine, m.p.* 118° *C.*

Solvents	Methyl alcohol		Ethyl alcohol		Acetone		Pyridine		Ethyl acetate		Chloroform		Benzene	
Conc. in gm. per 100 c.c.	1·000		1·000		1·000		1·000		1·000		1·000		1·000	
Calc. $[\alpha]_{\lambda}^{35°}$	$\frac{6·253}{\lambda^2-0·0927}$		$\frac{7·413}{\lambda^2-0·0674}$		$\frac{10·195}{\lambda^2-0·0791}$		$\frac{11·92}{\lambda^2-0·0763}$		$\frac{15·783}{\lambda^2-0·0402}$		$\frac{23·275}{\lambda^2-0·0556}$		$\frac{31·949}{\lambda^2-0·0682}$	
Calc. λ_0 (Å)	3044		2596		2812		2762		*2005*		*2357*		2611	
Lines	*o*	*c*	*o*	*c*	*o*	*c*	*o*	*c*	*o*	*c*	*o*	*c*	*o*	*c*
6708 ..	17·5	17·5	19·0	19·37	27·5	27·49	31·5	31·63	38·5	38·51	59·0	59·02	85·0	83·7
6438 ..	19·0	19·16	22·5	21·36	30·0	30·4	35·0	34·91	42·0	42·17	65·0	64·85	93·0	92·26
6104 ..	22·0	22·35	24·5	24·3	34·5	34·73	40·0	39·81	47·5	47·5	75·0	73·45	105·0	105·0
5893 ..	24·5	24·57	26·5	26·5	38·0	38·02	43·5	43·48	51·5	51·41	79·0	79·82	114·0	114·5
5780 ..	25·5	25·9	28·0	27·8	40·0	39·97	45·5	45·67	53·0	53·71	83·5	83·58	122·0	120·1
5468 ..	30·0	30·31	31·5	32·01	46·5	46·35	52·5	52·77	61·0	60·98	95·0	95·63	138·0	138·5
5460 ..	30·5	30·42	32·0	32·12	46·5	46·55	52·5	52·94	61·0	61·17	95·0	95·94	138·5	139·0
5209 ..	36·0	35·01	36·0	36·72	53·5	53·04	60·0	60·15	68·0	68·29	107·5	107·9	156·0	157·3
5087 ..	38·0	37·69	39·0	39·17	57·0	56·78	64·0	64·25	73·0	73·26	114·5	114·7	168·0	167·8
4800 ..	45·0	45·25	45·5	45·47	67·0	67·16	75·5	75·54	83·5	83·75	134·0	132·8	197·0	197·0
4678 ..	50·0	49·6	49·0	48·97	73·0	72·95	82·0	81·81	89·5	87·84	143·0	142·7	212·0	212·1
4603 ..	52·5	52·5	51·0	51·34	75·5	76·71	87·0	85·92	92·0	92·02	149·0	149·0	223·0	223·4
4358 ..	66·0	64·27	61·0	60·46	90·0	91·83	102·0	102·0	106·0	105·4	172·0	173·2	259·5	262·1

TABLE VI. *Rotatory Dispersion of* d-*Camphor-β-sulphonyl-o-phenylenediamine, m.p.* 133° *C.*

Solvents	Methyl alcohol		Ethyl alcohol		Acetone		Pyridine		Ethyl acetate		Chloroform		Benzene	
Conc. in gm. per 100 c.c.	0·5000		0·5000		0·5000		0·5000		0·5000		0·5000		0·5000	
Calc. $[\alpha]_\lambda^{35°}$	$\frac{6·804}{\lambda^2-0·1295}$		$\frac{7·88}{\lambda^2-0·1112}$		$\frac{10·55}{\lambda^2-0·1200}$		$\frac{7·41}{\lambda^2-0·1446}$		$\frac{20·42}{\lambda^2-0·0573}$		$\frac{36·857}{\lambda^2-0·0701}$		$\frac{42·73}{\lambda^2-0·0685}$	
Calc. λ_0 (Å)	3600		3334		3464		3801		*2394*		2647		2615	
Lines	*o*	*c*	*o*	*c*	*o*	*c*	*o*	*c*	*o*	*c*	*o*	*c*	*o*	*c*
6708 ..	21·0	21·23	23·0	23·1	32·0	31·98	24·0	24·26	52·0	51·99	97·0	97·01	112·0	112·0
6438 ..	24·0	23·88	26·0	25·98	36·0	35·83	28·0	27·45	58·0	57·16	108·0	107·0	125·0	123·5
6104 ..	28·0	28·0	30·0	30·16	41·0	41·78	32·5	32·52	65·0	64·77	122·0	121·8	142·0	140·6
5893 ..	31·0	31·25	33·0	33·39	47·0	46·44	37·0	36·57	71·0	70·43	130·0	132·9	154·0	153·3
5780 ..	33·0	33·28	36·0	35·05	50·0	49·28	39·0	39·09	74·0	73·75	139·0	139·6	159·0	160·9
5468 ..	40·0	40·16	42·0	41·96	60·0	58·92	48·0	47·99	84·0	84·5	160·0	161·0	185·0	185·5
5461 ..	40·0	40·33	43·0	42·14	61·0	59·21	48·0	48·23	85·0	84·76	160·0	161·5	185·0	186·0
5209 ..	48·0	47·99	49·0	49·21	71·0	69·74	59·0	58·48	96·0	95·41	183·0	183·1	213·0	210·7
5087 ..	54·0	52·71	54·0	53·46	76·0	76·12	65·0	65·0	104·0	101·4	197·0	195·4	225·0	224·8
4800 ..	..	..	67·0	66·10	94·0	95·68	..	..	118·0	118·0	230·0	229·9	264·0	264·0
4678 ..	..	..	74·0	73·21	110·0	106·8	..	..	125·0	126·5	250·0	249·5	282·0	284·3
4603 ..	..	..	78·0	78·34	115·0	114·9	..	..	130·0	132·1	262·0	260·1	296·0	298·2
4358 ..	..	..	100·0	100·0	148·0	150·8	..	..	153·0	153·8	305·0	307·3	352·0	351·8

TABLE VII. *Rotatory Dispersion of* p-*phenylene*-bis-d-*camphor-β-sulphonylamide, m.p.* 185° *C.*

Solvents	Methyl alcohol		Ethyl alcohol		Acetone		Pyridine		Ethyl acetate		Chloroform	
Conc. in gm. per 100 c.c.	0·5000		0·5000		0·5000		0·5000		0·5000		0·5000	
Calc. $[\alpha]_{\lambda}^{35°}$	$\frac{8\cdot186}{\lambda^2-0\cdot0779}$		$\frac{9\cdot012}{\lambda^2-0\cdot0895}$		$\frac{11\cdot151}{\lambda^2-0\cdot0711}$		$\frac{15\cdot325}{\lambda^2-0\cdot073}$		$\frac{14\cdot0}{\lambda^2-0\cdot0554}$		$\frac{21\cdot25}{\lambda^2-0\cdot0838}$	
Calc. λ_0 (Å)	2791		2992		2666		2702		*2354*		2895	
Lines	*o*	*c*	*o*	*c*	*o*	*c*	*o*	*c*	*o*	*c*	*o*	*c*
6708 ..	22·0	22·0	25·0	25·0	30·0	29·43	38·0	37·99	36·0	35·47	58·0	58·0
6438 ..	25·0	24·32	28·0	27·73	32·0	32·46	42·0	41·94	40·0	39·98	63·0	64·25
6104 ..	28·0	27·6	32·0	31·84	37·0	36·98	48·0	47·82	45·0	44·09	74·0	73·58
5893 ..	31·0	30·4	35·0	34·97	40·0	40·37	52·0	51·23	48·0	47·97	79·0	80·65
5780 ..	32·0	31·97	37·0	36·84	42·0	42·38	55·0	54·88	50·0	50·23	86·0	84·89
5468 ..	37·0	37·02	43·0	43·01	48·5	48·93	63·0	63·37	57·0	57·46	99·0	98·74
5461 ..	37·0	37·16	43·0	43·17	49·0	49·09	63·0	63·59	58·0	57·66	99·0	99·1
5209 ..	42·5	42·33	50·0	49·57	54·0	55·69	73·0	72·21	63·0	64·85	112·0	113·3
5087 ..	45·0	45·31	53·0	53·29	58·5	59·32	78·0	77·16	68·0	68·9	121·0	121·5
4799 ..	53·0	53·69	64·0	63·93	70·0	69·98	91·0	91·0	80·0	80·0	144·0	144·9
4678 ..	58·0	58·19	70·0	69·69	74·0	75·48	100·0	98·22	85·0	85·67	158·0	157·4
4603 ..	61·0	61·13	74·0	73·69	81·0	79·25	..	..	90·0	89·52	166·0	166·0
4358 ..	73·0	73·03	89·0	89·69	93·0	93·71	..	..	105·0	104·0	200·0	200·0

TABLE VIII. *Rotatory Dispersion of* m-*phenylene*-bis-d-*camphor*-β-*sulphonylamide, m.p.* 203° *C.*

Solvents	Methyl alcohol		Ethyl alcohol		Acetone		Pyridine		Ethyl acetate		Chloroform	
Conc. in gm. per 100 c.c.	0·5000		0·5000		0·5000		0·5000		0·5000		0·5000	
Calc. $[\alpha]_{\lambda}^{35°}$	$\frac{12\cdot992}{\lambda^2-0\cdot068}$		$\frac{10\cdot8}{\lambda^2-0\cdot09}$		$\frac{13\cdot797}{\lambda^2-0\cdot0771}$		$\frac{16\cdot926}{\lambda^2-0\cdot0664}$		$\frac{20\cdot61}{\lambda^2-0\cdot0378}$		$\frac{24\cdot554}{\lambda^2-0\cdot0263}$	
Calc. λ_0 (Å)	2608		3000		2776		*2375*		*1944*		*1622*	
Lines	*o*	*c*	*o*	*c*	*o*	*c*	*o*	*c*	*o*	*c*	*o*	*c*
6708 ..	34·0	34·01	30·0	30·0	37·0	37·01	43·0	42·99	50·0	50·0	58·0	57·97
6438 ..	37·0	37·5	33·0	33·29	41·0	40·9	48·0	47·26	54·0	54·71	62·0	63·27
6104 ..	43·0	42·67	38·0	38·27	47·0	46·71	54·0	53·55	62·0	61·59	71·0	70·92
5893 ..	46·0	46·54	42·0	42·0	51·0	51·07	59·0	58·20	65·0	66·61	75·0	76·54
5780 ..	49·0	48·82	44·0	44·24	53·0	53·69	61·0	60·96	70·0	69·59	79·0	79·8
5468 ..	56·0	56·24	51·0	51·68	61·0	62·19	70·0	69·76	78·0	78·93	88·0	90·05
5461 ..	56·0	56·44	51·0	51·87	61·0	62·4	70·0	70·0	79·0	79·14	89·0	90·33
5209 ..	64·0	65·4	59·0	59·57	71·0	71·06	80·0	78·75	88·0	88·26	100·0	100·2
5087 ..	69·0	68·17	64·0	64·04	76·0	76·02	85·0	83·7	93·0	93·37	106·0	105·7
4799 ..	80·0	80·0	74·0	76·93	90·0	90·0	..	..	107·0	107·0	121·0	120·3
4678 ..	87·0	86·18	83·0	83·83	97·0	97·38	..	..	114·0	113·9	130·0	127·6
4603 ..	93·0	92·47	89·0	88·67	102·0	102·4	..	..	120·0	118·5	132·0	132·3
4358 ..	109·0	106·5	108·0	108·0	120·0	122·3	..	..	134·0	135·4	149·0	150·01

TABLE IX. *Rotatory Dispersion of* o-*phenylene*-bis-d-*camphor-β-sulphonylamide, m.p.* 92° *C.*

Solvents	Methyl alcohol		Ethyl alcohol		Acetone		Pyridine		Ethyl acetate		Chloroform		Benzene	
Conc. in gm. per 100 c.c.	0·5000		0·5000		0·5000		0·5000		0·5000		0·5000		0·5000	
Calc. $[\alpha]_\lambda^{35°}$	$\frac{9·6133}{\lambda^2-0·09395}$		$\frac{8·415}{\lambda^2-0·1135}$		$\frac{15·74}{\lambda^2-0·0565}$		$\frac{15·031}{\lambda^2-0·0527}$		$\frac{17·115}{\lambda^2-0·0475}$		$\frac{24·376}{\lambda^2-0·0396}$		$\frac{16·5312}{\lambda^2-0·0564}$	
Calc. λ_0 (Å)	3065		3370		*2377*		*2296*		*2178*		*1990*		*2375*	
Lines	*o*	*c*	*o*	*c*	*o*	*c*	*o*	*c*	*o*	*c*	*o*	*c*	*o*	*c*
6708 ..	27·0	27·00	25·0	25·0	40·0	40·0	38·0	37·83	45·0	45·0	60·0	59·53	42·0	42·0
6438 ..	29·0	29·99	28·0	27·96	44·0	43·96	41·0	41·54	49·0	49·34	65·0	65·01	46·0	46·16
6104 ..	34·0	34·51	32·0	32·49	50·0	49·8	47·0	47·0	55·0	55·72	73·0	73·21	52·0	52·3
5893 ..	38·0	37·96	36·0	36·0	54·0	54·16	50·0	51·04	61·0	60·42	79·0	79·23	57·0	56·84
5780 ..	40·0	40·02	38·0	38·14	58·0	56·7	53·0	53·4	63·0	63·19	83·0	82·77	60·0	59·53
5468 ..	46·0	46·87	45·0	45·36	64·0	64·91	60·0	61·02	71·5	71·97	95·0	93·96	68·0	68·14
5461 ..	47·0	47·09	45·0	45·57	64·0	65·13	61·0	61·22	72·0	72·24	95·0	94·26	69·0	68·37
5209 ..	54·0	54·18	53·0	53·33	72·5	73·28	68·0	68·74	80·0	80·94	105·0	105·2	77·0	76·93
5087 ..	58·0	58·37	57·0	57·99	77·0	77·87	73·0	72·98	87·0	85·78	111·0	111·3	82·0	81·75
4799 ..	70·0	70·46	71·0	71·77	90·0	90·53	84·0	84·1	99·0	99·0	128·0	127·7	95·0	95·01
4678 ..	77·0	77·0	80·0	79·93	97·0	96·99	91·0	90·46	108·0	105·7	136·0	136·0	102·0	101·8
4608 ..	82·0	81·55	83·0	85·63	104·0	101·4	..	..	..	..	142·0	141·6	107·0	106·4
4358 ..	103·0	101·0	110·0	110·0	..	..	..	..	..	..	..	..	125·0	123·7

general absorption of the saturated molecules. In continuation[1,5] with our previous work the authors have noticed that in five cases the rotatory dispersion can be expressed by Biot's equation and in other cases the low frequency of the absorption band is replaced by a high frequency in solvents of low dielectric constants, namely, ethyl acetate, chloroform and benzene. This result in which the low frequency corresponding to the keto group of the compound has been replaced by the high frequency corresponding to the saturated molecule and brought about by solvents of low dielectric constants needs elucidation by direct measurement of ultraviolet absorption of these compounds.

Experimental

(*d*- and -*dl*) Camphor-β-sulphonyl (*o*-, *m*- and *p*-) nitrophenylamides, $C_{10}H_{15}OSO_2NHC_6H_4NO_2$ and (*d*- and *dl*-) camphor-β-sulphonyl (*o*-, *m* and *p*-) phenylenediamines, $C_{10}H_{15}OSO_2NHC_6H_4NH_2$.

Camphor-β-sulphonylnitrophenylamides were prepared by condensing camphor-β-sulphonyl chloride (1 mole.) with nitroanilines (2 moles) in presence of toluene according to the method of Morgan and Micklethwait.[6] Camphor-β-sulphonylphenylenediamines were obtained by reducing the nitro compounds with iron and acetic acid. The physical properties of these compounds are recorded in Table A (1–6).

(o-, m- *and* p-) *phenylene*-bis-*camphor-β-sulphonylamides* (d- *and* dl-), $C_{10}H_{15}OSO_2NH \cdot C_6H_4NH \cdot SO_2C_{10}H_{15}O$

These compounds were prepared by heating camphor-β-sulphonyl-chloride with phenylenediamines in equimolecular proportions on the water-bath for two hours. The products thus obtained were washed with water and then extracted with alcohol. They were crystallised from dilute aqueous alcohol, when colourless crystals were obtained. The physical properties of *d*-, and *dl*-isomerides of (*o*-, *m*- and *p*-) phenylene-*bis*-camphor-β-sulphonyl-amides are recorded in Table A (7–9).

The rotatory dispersion measurements were made in a 2-decimeter jacketed tube at 35° C. and are given in Tables I–IX. The values of λ_0 in these tables are given in Å units.

Summary

The rotatory dispersion of the compounds (Tables I–IX) have been determined in 7 solvents for 13 wavelengths ($\lambda = 6708$ Å to $\lambda = 4358$ Å) in the visible region of the spectrum. It is found to be '*simple*' as it can be expressed by *one-term* Drude's equation, $[\alpha]_{\lambda}^{35^\circ C.} = \frac{k}{\lambda^2 - \lambda_0^2}$. It is controlled

generally by a low frequency corresponding to the ketonic group of camphor and sometimes by a high frequency 'characteristic' of saturated molecules. In solvents of low dielectric constants such as ethyl acetate, chloroform and benzene the high frequency corresponding to the saturated molecules generally replaces the low frequency pertaining to the ketonic group. The effect of position isomerism and the influence of the solvent on the rotatory power have been also discussed.

ACKNOWLEDGEMENT

We wish to make grateful acknowledgement to the Banaras Hindu University, for the provision of research facilities and to the Government of India, for the award of a Senior Research Scholarship to one of us (S. M. Verma).

REFERENCES

1. Singh *et al.* .. *Proc. Ind. Acad. Sci.*, 1956, **43 A**, 21.
2. Frankland, P. F. .. *J.C.S.*, 1896, **69**, 284.
3. Rule, H. G. .. *Ibid.*, 1924, **125**, 1122.
4. Cohen, J. B. .. *Ibid.*, 1910, **97**, 1739; 1911, **99**, 1061.
5. Singh, B. K. and (Miss) Amma, M. K. P. *Jour. Ind. Chem. Soc.*, 1954, **31**, 657.
6. Morgan and Micklethwait .. *J.C.S.*, 1905, **87**, 177.

MULTIPLE PROCESSES IN ELECTRON-PHOTON CASCADES

By Alladi Ramakrishnan, F.A.Sc., S. K. Srinivasan, N. R. Ranganathan and R. Vasudevan

(Department of Physics, University of Madras)

Received March 18, 1957

Abstract

Recent experiments on high energy electron-photon cascades suggest the possibility of the following multiple processes:—

(i) Electron scattering with pair creation,

(ii) Electron scattering with the emission of two photons, and

(iii) Photon scattering with pair creation.

The cross-section for the first process predicted by Bhabha has been recalculated recently by the standard Feynman technique. Using the same technique, we here present the calculations for the cross-sections of processes (ii) and (iii).

Introduction

The analysis of high energy electron-photon showers in cosmic rays suggests the necessity of considering third order processes of the following type:

(i) Electron scattering with pair creation, *i.e.*, 'trident' production,

(ii) Electron scattering with emission of two photons. The usual 'bremsstrahlung' of Bethe and Heitler (1934) deals with the emission of one photon,

(iii) Photon scattering with pair creation. In the usual treatment, pair creation is due to the annihilation of the photon. Here we postulate the emergence of a photon after collision.

Pair production by electrons was predicted by Bhabha as early as 1935 while the possibility of process (ii) is mentioned in explicit terms by Heitler (1954). Recently Murota *et al.* (1956) have recalculated the cross-section for the production of 'tridents' (pair + scattered electron) by the Feynman-Dyson technique. The experimental data of Koshiba and Kaplon (1955) seem to confirm the production of electron pairs by electrons. Recently Seeman and Glasser (1956) have observed an event in which a helium nucleus

having an energy of the order of 10^5 Gev. gives rise to a shower containing very many pairs of electrons. The results of Fay (1956)* at Gottingen seem to show that the number of pairs is much greater than can be expected from the standard cascade theory. The processes (i) to (iii) we have mentioned above may explain some of the new data relating to high energy electron photon cascades.

The object of the present paper is to obtain the differential cross-sections for processes (ii) and (iii) using the Feynman-Dyson techniques. The standard notation of Feynman will be used and explanation will be given only when necessary.

ELECTRON SCATTERING WITH CREATION OF TWO PHOTONS

(*a*) *Matrix elements and their reduction.*—Throughout this paper, we use the natural units $\hbar = 1$ and $c = 1$ and the following notation:

$a.b \equiv a_t b_t - a_x b_x - a_y b_y - a_z b_z$: The four dimensional scalar product of the vectors*** a and b whose components are (a_t, a_x, a_y, a_z) and (b_t, b_x, b_y, b_z) respectively.

$p \equiv (E, \vec{p})$: The energy-momentum four vector of electron. Subscripts will be used to distinguish between different electrons.

$q \equiv (\omega, \vec{q})$: The energy-momentum four vector of a photon. Subscripts will be used to distinguish between different photons.

$e \equiv (0, \vec{e})$: The spatial vector representing the direction of polarization of a photon.

m: The rest mass of the electron.

In addition to those we shall use the 'dagger' notation of Feynman (1953). The daggered operator $\mathbf{a}$** of any four vector a is defined as

$$\mathbf{a} \equiv a_t\gamma_t - a_x\gamma_x - a_y\gamma_y - a_z\gamma_z$$
$$\equiv a_0\gamma_0 - a_1\gamma_1 - a_2\gamma_2 - a_3\gamma_3 \qquad (1)$$

* Private communication.

** The daggered operator of a four vector a is represented as $\not{a}$ by Feynman. For convenience of printing we use the corresponding bold face letter.

*** For convenience ordinary italics are used for four-vectors. No confusion will arise with ordinary numbers since in the paper four-vectors occur only in scalar products.

where γ's are the well-known Dirac matrices (*see* for example, Bethe and Schweber, 1955). The γ's are characterised by the following relations:

$$\begin{aligned} \gamma_\mu\gamma_\nu + \gamma_\nu\gamma_\mu &= 0 && \mu \neq \nu \\ &= +2 && \mu = \nu = 0 \\ &= -2 && \mu = \nu = 1, 2, 3. \end{aligned} \tag{2}$$

While the matrices γ_x, γ_y and γ_z are anti-Hermitian, γ_t is Hermitian.

In this process, a free electron of momentum p_1 is incident and we obtain after its collision with the nucleus, a free electron of momentum p_2 and two photons of momenta q_1, q_2. The initial and final state electron wave functions are given by

$$\begin{aligned} \psi_1 &= u_1 e^{-p_1 \cdot r} \\ \psi_2 &= u_2 e^{-p_2 \cdot r} \end{aligned} \tag{3}$$

where u_1, u_2 are the four component spinor parts of the free particle wave function corresponding to the momenta p_1 and p_2 respectively.

$$\begin{aligned} \mathbf{p}_1 u_1 &= m u_1, \ \mathbf{p}_2 u_2 = m u_2 \\ p_1 \cdot p_1 &= p_2 \cdot p_2 = m^2 \end{aligned} \tag{4}$$

r is a four vector with components (t, x, y, z). The potentials corresponding to the emitted photons are given by

$$\begin{aligned} \mathrm{A}_{1\mu} &= e_{1\mu} e^{-iq_1 \cdot r} \\ \mathrm{A}_{2\mu} &= e_{2\mu} e^{-iq_2 \cdot r} \end{aligned} \tag{5}$$

where

$$e_1 \cdot q_1 = 0 = e_2 \cdot q_2, \ q_1 \cdot q_1 = 0 = q_2 \cdot q_2 \tag{6}$$

The Coulomb potential due to the nucleus of charge Z is given by

$$\vec{\mathrm{A}} = 0, \ \mathrm{A}_t = \phi = \frac{Ze}{|\vec{r}|} . \tag{7}$$

As we shall be working in momentum representation, it is convenient to define $\mathbf{V}(q)$ as

$$\begin{aligned} \mathbf{V}(q) &= \frac{1}{(2\pi)^4} \int \mathbf{A}(r)\, e^{iq \cdot r} d^4 r \\ &= \frac{4\pi Ze}{\vec{\mathrm{Q}} \cdot \vec{\mathrm{Q}}} \delta(q_4)\gamma_t = v(\mathrm{Q})\, \delta(q_4)\, \gamma_t \end{aligned} \tag{8}$$

where $\vec{\mathrm{Q}}$ is the spatial part of the momentum and δ the Dirac delta function.

We shall choose a co-ordinate system in which the nucleus does not move and take the direction of propagation of the photon with momentum q_1 as the z-axis and the plane containing the directions of propagation of the photons as the y-z plane. Let the angle between the directions of propagation of the photons be θ. Thus

$$\mathbf{q}_1 = \omega_1 (\gamma_t - \gamma_z) \tag{9}$$

$$\mathbf{q}_2 = \omega_2 (\gamma_t - \gamma_z \cos\theta - \gamma_y \sin\theta) \tag{10}$$

$$\mathbf{p}_1 = \mathrm{E}_1 \gamma_t - p_{1x}\gamma_x - p_{1y}\gamma_y - p_{1z}\gamma_z \tag{11}$$

$$\mathbf{p}_2 = \mathrm{E}_2 \gamma_t - p_{2x}\gamma_x - p_{2y}\gamma_y - p_{2z}\gamma_z. \tag{12}$$

The photon beam corresponding to (9) can be resolved into two types of polarization which will be designated as type A and type B.

(A) $\mathbf{e}_1 = \gamma_x$ (B) $\mathbf{e}_1 = \gamma_y$.

Similarly the beam corresponding to (10) can be resolved into two types of polarization:

(A′) $\mathbf{e}_2 = \gamma_x$ (B′) $\mathbf{e}_2 = \gamma_z \sin\theta - \gamma_y \cos\theta$.

The lowest order Feynman diagrams for the present process are given below.

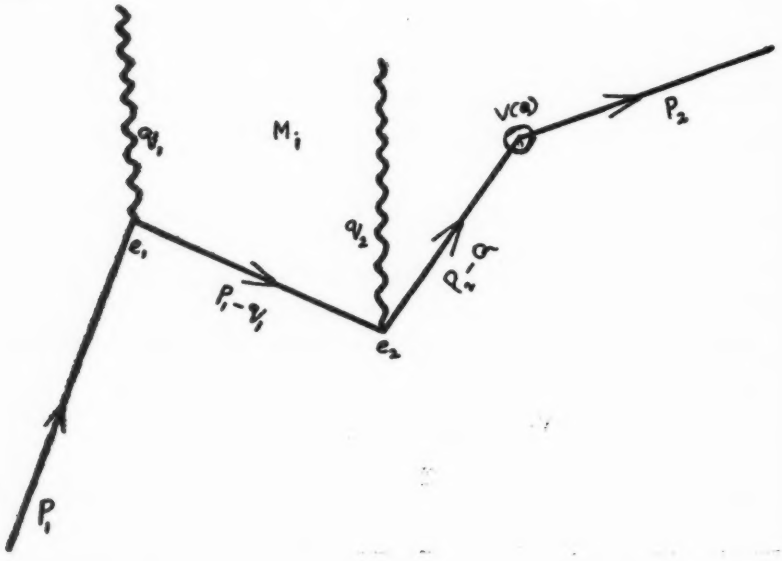

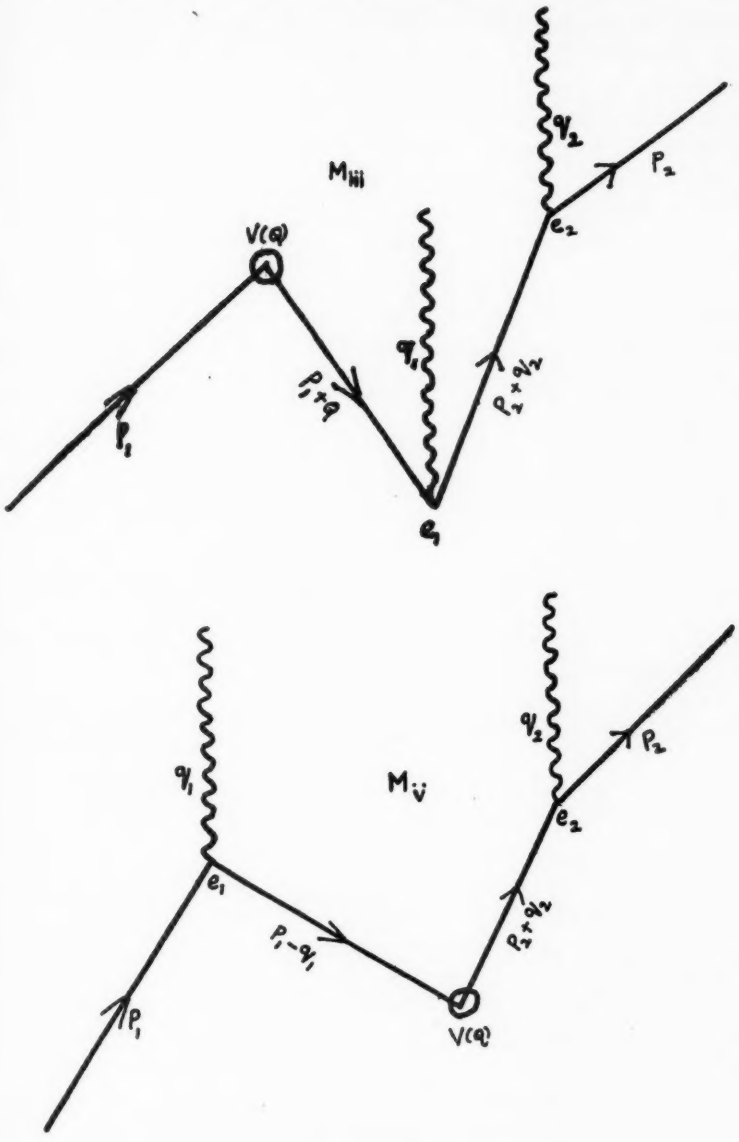

FIG. 1. Electron scattering with emission of two photons.

There are six different Feynman diagrams for the process yielding six matrix elements, M_i, M_{ii}, M_{iii}, M_{iv}, M_v, M_{vi}. In the figure, we have shown only three and the other three can be obtained by interchanging the photons. For convenience we pair the matrix elements corresponding to the interchange of photons. The matrix elements are given by

$$M_i + M_{ii} = -4\pi ie^3 v(Q)\,\tilde{u}_2 \left\{ \gamma_t \frac{1}{\mathbf{p}_2 - \mathbf{Q} - m} \mathbf{e}_2 \frac{1}{\mathbf{p}_1 - \mathbf{q}_1 - m} \mathbf{e}_1 + \gamma_t \frac{1}{\mathbf{p}_2 - \mathbf{Q} - m} \mathbf{e}_1 \frac{1}{\mathbf{p}_1 - \mathbf{q}_2 - m} \mathbf{e}_2 \right\} u_1 \tag{13}$$

$$M_{iii} + M_{iv} = -4\pi ie^3 v(Q)\,\tilde{u}_2 \left\{ \mathbf{e}_2 \frac{1}{\mathbf{p}_2 + \mathbf{q}_2 - m} \mathbf{e}_1 \frac{1}{\mathbf{p}_1 + \mathbf{Q} - m} \gamma_t + \mathbf{e}_1 \frac{1}{\mathbf{p}_2 + \mathbf{q}_1 - m} \mathbf{e}_2 \frac{1}{\mathbf{p}_1 + \mathbf{Q} - m} \gamma_t \right\} u_1 \tag{14}$$

$$M_v + M_{vi} = -4\pi ie^3 v(Q)\,\tilde{u}_2 \left\{ \mathbf{e}_2 \frac{1}{\mathbf{p}_2 + \mathbf{q}_2 - m} \gamma_t \frac{1}{\mathbf{p}_1 - \mathbf{q}_1 - m} \mathbf{e}_1 + \mathbf{e}_1 \frac{1}{\mathbf{p}_2 + \mathbf{q}_1 - m} \gamma_t \frac{1}{\mathbf{p}_1 - \mathbf{q}_2 - m} \mathbf{e}_2 \right\} u_1. \tag{15}$$

We shall demonstrate the reduction of R.H.S. of (13). Rationalisation of the denominators yields

$$M_i + M_{ii} = -4\pi ie^3 v(Q)\,\tilde{u}_2 \left\{ \frac{\gamma_t (\mathbf{p}_2 - \mathbf{Q} + m) \mathbf{e}_2 (\mathbf{p}_1 - \mathbf{q}_1 + m) \mathbf{e}_1}{[(\mathbf{p}_2 - \mathbf{Q})^2 - m^2]\ [(\mathbf{p}_1 - \mathbf{q}_1)^2 - m^2]} + \frac{\gamma_t (\mathbf{p}_2 - \mathbf{Q} + m) \mathbf{e}_1 (\mathbf{p}_1 - \mathbf{q}_2 + m) \mathbf{e}_2}{[(\mathbf{p}_2 - \mathbf{Q})^2 - m^2]\ [(\mathbf{p}_1 - \mathbf{q}_2)^2 - m^2]} \right\} u_1. \tag{16}$$

To simplify the numerator, we write

$$\begin{aligned} &\tilde{u}_2 \gamma_t (\mathbf{p}_2 - \mathbf{Q} + m) \mathbf{e}_2 (\mathbf{p}_1 - \mathbf{q}_1 + m) \mathbf{e}_1 u_1 \\ &= \tilde{u}_2 \gamma_t (\mathbf{p}_2 - \mathbf{Q} + m) \mathbf{e}_2 (-\mathbf{e}_1 \mathbf{p}_1 + 2p_1 . e_1 - \mathbf{q}_1 \mathbf{e}_1 + m\mathbf{e}_1) u_1 \\ &= \tilde{u}_2 \gamma_t (\mathbf{p}_2 - \mathbf{Q} + m) \mathbf{e}_2 (2p_1 . e_1 - \mathbf{q}_1 \mathbf{e}_1) u_1. \end{aligned} \tag{17}$$

We next use the relations

$$\mathbf{p}_2 - \mathbf{Q} = \mathbf{p}_1 - \mathbf{q}_1 - \mathbf{q}_2. \tag{18}$$

$$\mathbf{p}_1 \mathbf{a} = -\mathbf{a}\mathbf{p}_1 + 2p_1 . a \tag{19}$$

and eliminate $\mathbf{p}_1$ from (16) with the help of (4). Reducing the other part in a similar manner, we obtain after some simplification

$$M_I + M_{II} = -4\pi e^3 v(Q)\frac{u_2\gamma_t}{Q.Q-2p_2.Q}\left\{2\frac{p_1.e_1}{p_1.q_1}(q_1.e_2-p_1.e_2)\right.$$
$$+\frac{2p_1.e_1}{p_1.q_2}(q_2.e_1-p_1.e_1)+2e_1.e_2+\mathbf{q}_1\mathbf{e}_1\left(\frac{p_1.e_2}{p_1.q_2}\right.$$
$$\left.+\frac{p_1.e_2}{p_1.q_1}-\frac{e_2.q_1}{p_1.q_1}\right)+\mathbf{q}_2\mathbf{e}_2\left(\frac{p_1.e_1}{p_1.q_1}+\frac{p_1.e_1}{p_1.q_2}-\frac{e_1.q_2}{p_1.q_2}\right)$$
$$\left.+\frac{\mathbf{q}_1\mathbf{e}_1\mathbf{e}_2\mathbf{q}_2}{2p_1.q_2}+\frac{\mathbf{q}_2\mathbf{e}_2\mathbf{e}_1\mathbf{q}_1}{2p_1.q_1}\right\}u_1. \tag{20}$$

Proceeding in an exactly same manner, we reduce the R.H.S. of (14) and (15). The total matrix element M is given by

$$M = -4\pi ie^3 v(Q)\,\tilde{u}_2\{A_1\gamma_t + A_2\gamma_t\,\mathbf{e}_1\mathbf{q}_1 + A_3\gamma_t\,\mathbf{e}_2\mathbf{q}_2 + A_4\mathbf{e}_1$$
$$+ A_5\mathbf{e}_2 + A_6\mathbf{e}_1\mathbf{q}_1\gamma_t\mathbf{e}_2\mathbf{q}_2 + A_7\mathbf{e}_2\mathbf{q}_2\gamma_t\mathbf{e}_1\mathbf{q}_1 + A_8\omega_2\mathbf{e}_1\mathbf{q}_1\mathbf{e}_2$$
$$+ A_9\omega_2\mathbf{e}_2\mathbf{e}_1\mathbf{q}_1 + A_{10}\omega_1\mathbf{e}_1\mathbf{e}_2\mathbf{q}_2 + A_{11}\omega_1\mathbf{e}_2\mathbf{q}_2\mathbf{e}_1\}\,u_1 \tag{21}$$

where

$$A_1 = -\frac{p_2.e_2}{p_1.q_1}\frac{p_1.e_1}{p_2.q_1} - \frac{p_2.e_1}{p_1.q_2}\frac{p_1.e_2}{p_2.q_1} + \left[\frac{p_2.e_1}{p_2.q_1}e_2.q_1 + \frac{p_2.e_2}{p_2.q_2}e_1.q_2\right.$$
$$\left. - e_1.e_2 + \frac{p_2.e_2}{p_2.q_2}p_2.e_1 + \frac{p_2.e_2}{p_2.q_1}p_2.e_1\right]\frac{2}{Q.Q+2p_1.Q}$$
$$+\left[\frac{p_1.e_1}{p_1.q_1}e_2.(q_1-p_1) + \frac{p_1.e_2}{p_1.q_2}e_1.(q_2-p_1)\right.$$
$$\left. + e_1.e_2\right]\frac{2}{Q.Q-2p_2.Q}$$

$$A_2 = \frac{1}{Q.Q+2p_1.Q}\left(\frac{p_2.e_2}{p_2.q_2}+\frac{p_2.e_2}{p_2.q_1}+\frac{e_2.q_1}{p_2.q_1}\right)+\frac{1}{Q.Q-2p_2.Q}$$
$$\times\left(\frac{e_2.q_1}{p_1.q_1}-\frac{p_1.e_2}{p_1.q_2}-\frac{p_1.e_2}{p_1.q_1}\right)-\left(\frac{p_1.e_2}{2p_1.q_2\,p_2.q_1}+\frac{p_2.e_2}{2p_1.q_1\,p_2.q_2}\right)$$

$$A_3 = \frac{1}{Q.Q+2p_1.Q}\left(\frac{p_2.e_1}{p_2.q_1}+\frac{p_2.e_1}{p_2.q_2}+\frac{e_1.q_2}{p_2.q_2}\right)$$
$$+\frac{1}{Q.Q-2p_2.Q}\left(-\frac{p_1.e_1}{p_1.q_1}-\frac{p_1.e_1}{p_1.q_2}+\frac{e_1.q_2}{p_1.q_2}\right)$$
$$-\left(\frac{p_2.e_1}{2p_1.q_2\,p_2.q_1}+\frac{p_1.e_1}{2p_1.q_1\,p_2.q_2}\right)$$

$$A_4 = \frac{2\omega_1}{Q.Q + 2p_1.Q}\left(\frac{p_2.e_2}{p_2.q_2} + \frac{p_2.e_2}{p_2.q_1} + \frac{e_2.q_1}{p_2.q_1}\right) - \frac{p_1.e_2\omega_1}{p_1.q_1\, p_2.q_2}$$

$$A_5 = \frac{2\omega_2}{Q.Q + 2p_1.Q}\left(\frac{p_2.e_1}{p_2.q_1} + \frac{p_2.e_1}{p_2.q_2} + \frac{e_1.q_2}{p_2.q_2}\right) - \frac{p_1.e_1}{(p_1.q_1\ p_1.q_2)}\,\omega_2$$

$$A_6 = -\frac{1}{(2p_1.q_2)\,(Q.Q - 2p_2.Q)} + \frac{1}{(2p_2.q_1)\,(Q.Q + 2p_1.Q)} - \frac{1}{4(p_1.q_2)(p_2.q_1)}$$

$$A_7 = -\frac{1}{(2p_1.q_1)\,(Q.Q - 2p_2.Q)} + \frac{1}{(2p_2.q_2)\,(Q.Q + 2p_1.Q)} - \frac{1}{(4p_1.q_1)(p_2.q_2)}$$

$$A_8 = \frac{1}{(p_2.q_1)\,(Q.Q + 2p_1.Q)}$$

$$A_9 = \frac{1}{(p_1.q_1)\,(Q.Q - 2p_2.Q)}$$

$$A_{10} = \frac{1}{(p_1.q_2)\,(Q.Q - 2p_2.Q)}$$

$$A_{11} = \frac{1}{(p_2.q_2)\,(Q.Q + 2p_1.Q)}\,. \tag{22}$$

Using the relations (9) to (12) we can still further reduce the matrix element corresponding to various combinations of polarizations and express it finally in terms of the γ-matrices and the products of γ-matrices. Let M_1, M_2, M_3 and M_4 be the matrix elements corresponding to the polarizations AA′, AB′, BA′ and BB′ respectively. After considerable calculation and simplification, we obtain

$$M_i = -4\pi e^3 v\,(Q)\,\bar{u}_2\{a_{i1}\gamma_t + a_{i2}\gamma_x + a_{i3}\gamma_y + a_{i4}\gamma_z + a_{i5}\gamma_t\gamma_x\gamma_y + a_{i6}\gamma_t\gamma_y\gamma_z + a_{i7}\gamma_t\gamma_z\gamma_x + a_{i8}\gamma_x\gamma_y\gamma_z\}\,u_1 \tag{23}$$

where

$$a_{11} = A_1 - \omega_1\omega_2\,(A_6 + A_7)\,(1 + \cos\theta) + \omega_1\omega_2\,(A_8 - A_9) - A_{10} + A_{11}$$
$$a_{12} = A_2 + A_3 - \omega_2 A_5 - \omega_1 A_4$$
$$a_{13} = \omega_1\omega_2\,(A_6 + A_7)\sin\theta + \omega_1\omega_2\,(A_{10} - A_{11})\sin\theta$$
$$a_{14} = \omega_1\omega_2\,(A_6 + A_7)\,(1 + \cos\theta) + \omega_1\omega_2\,(A_9 - A_8) + \omega_1\omega_2\,(A_{10} - A_{11})\cos\theta$$

$$a_{15} = -\omega_2 A_5 \sin\theta$$
$$a_{16} = \omega_1\omega_2 (A_7 - A_6) \sin\theta$$
$$a_{17} = \omega_1 A_4 + \omega_2 A_5 \cos\theta$$
$$a_{18} = 0 \tag{24}$$

$$a_{21} = A_1$$
$$a_{22} = A_2 - \omega_1 A_4 - \omega_1\omega_2 (A_6 + A_7 - A_8 + A_9) \sin\theta$$
$$a_{23} = (\omega_2 A_5 - A_3) \cos\theta$$
$$a_{24} = (A_3 - \omega_2 A_5) \sin\theta$$
$$a_{25} = \omega_1\omega_2 (-A_6 + A_7)(1 + \cos\theta) + \omega_1\omega_2 (A_8 + A_9 - A_{10} - A_{11}) \cos\theta$$
$$a_{26} = \omega_2 A_5$$
$$a_{27} = \omega_1 A_4 + \omega_1\omega_2 (-A_6 + A_7 + A_8 + A_9 - A_{10} - A_{11}) \sin\theta$$
$$a_{28} = \omega_1\omega_2 A_6 (1 + \sin\theta) - \omega_1\omega_2 A_7 (1 + \cos\theta) - \omega_1\omega_2 (A_8 + A_9) \cos\theta + \omega_1\omega_2 (A_{10} + A_{11}) \tag{25}$$

$$a_{31} = A_1$$
$$a_{32} = A_3 + \omega_2 A_5 - \omega_1\omega_2 A_6 \sin\theta - \omega_1\omega_2 A_7 \sin\theta - \omega_1\omega_2 A_{10} \sin\theta + \omega_1\omega_2 A_{11} \sin\theta$$
$$a_{33} = A_2 - \omega_1 A_4$$
$$a_{34} = 0$$
$$a_{35} = \omega_2 A_5 \sin\theta - \omega_1\omega_2 A_6 (1 + \cos\theta) + \omega_1\omega_2 A_7 (1 + \cos\theta) + \omega_1\omega_2 (A_8 + A_9 - A_{10} - A_{11})$$
$$a_{36} = -\omega_1 A_4$$
$$a_{37} = -\omega_2 A_5 \cos\theta - \omega_1\omega_2 A_6 \sin\theta + \omega_1\omega_2 A_7 \sin\theta$$
$$a_{38} = \omega_1\omega_2 A_6 (1 + \cos\theta) - \omega_1\omega_2 A_7 (1 + \cos\theta) + \omega_1\omega_2 (-A_8 - A_9 + A_{10}) + \omega_1\omega_2 A_{11} \cos\theta \tag{26}$$

$$a_{41} = A_1 + \omega_1\omega_2 A_6 (1 + \cos\theta) + \omega_1\omega_2 A_7 (1 + \cos\theta) + \omega_1\omega_2 (-A_8 + A_9 + A_{10} - A_{11}) \cos\theta$$
$$a_{42} = a_{45} = a_{46} = a_{48} = 0$$
$$a_{43} = A_2 - A_3 \cos\theta + \omega_2 A_5 \cos\theta + \omega_1\omega_2 (-A_6 - A_7 + A_8 - A_9) \sin\theta$$
$$a_{44} = A_3 \sin\theta - \omega_2 A_5 \sin\theta - \omega_1\omega_2 A_6 (1 + \cos\theta) - \omega_1\omega_2 A_7 (1 + \cos\theta) + \omega_1\omega_2 (A_8 - A_9) \cos\theta + \omega_1\omega_2 (-A_{10} + A_{11})$$
$$a_{47} = -\omega_1 A_4 + \omega_2 A_5 + \omega_1\omega_2 (A_6 - A_7 - A_8 - A_9 + A_{10} + A_{11}) \sin\theta. \tag{27}$$

SPUR CALCULATION

The differential cross-section for any particular polarization is given by

$$d\sigma_i = 2\pi \frac{E_1}{p_1} \cdot (\text{normalisation factor}) \cdot \tfrac{1}{2} \cdot \sum_{\text{spins 1}} \sum_{\text{spins 2}} |M_i|^2 \cdot (\text{density of final states}). \tag{28}$$

where we have summed over the final spin states of the electron and averaged over the initial spin states. In this section, we shall evaluate

$$\sum_{\text{spins 1}} \sum_{\text{spins 2}} |M_i|^2.$$

It is well known that if

$$M = \tilde{u}_2 M u_1 \tag{29}$$

then

$$\sum_{\text{spins 1}} \sum_{\text{spins 2}} |M^2| = Sp\,|(\mathbf{p}_2 + m)\, M\, (\mathbf{p}_1 + m)\, M'| \tag{30}$$

where

$$M' = \gamma_t \tilde{M}. \tag{31}$$

Now M_i is given by

$$M_i = a_{i1}\gamma_t + a_{i2}\gamma_x + a_{i3}\gamma_y + a_{i4}\gamma_z + a_{i5}\gamma_t\gamma_x\gamma_y + a_{i6}\gamma_t\gamma_y\gamma_z + a_{i7}\gamma_t\gamma_z\gamma_x + a_{i8}\gamma_x\gamma_y\gamma_z. \tag{32}$$ ‡

It is easily verified by direct multiplication that

$$\mathbf{p}_2 M_i = l_{i1}\mathrm{I} + l_{i2}\gamma_t\gamma_x + l_{i3}\gamma_t\gamma_y + l_{i4}\gamma_t\gamma_z + l_{i5}\gamma_x\gamma_y + l_{i6}\gamma_y\gamma_z + l_{i7}\gamma_z\gamma_x + l_{i8}\gamma_t\gamma_x\gamma_y\gamma_z \tag{33}$$

$$\mathbf{p}_1 M_i' = m_{i1}\mathrm{I} + m_{i2}\gamma_t\gamma_x + m_{i3}\gamma_t\gamma_y + m_{i4}\gamma_t\gamma_z + m_{i5}\gamma_x\gamma_y + m_{i6}\gamma_y\gamma_z + m_{i7}\gamma_z\gamma_x + m_{i8}\gamma_t\gamma_x\gamma_y\gamma_z \tag{34}$$

where

$$\begin{aligned}
l_{i1} &= E_2 a_{i1} + p_{2x} a_{i2} + p_{2y} a_{i3} + p_{2z} a_{i4} \\
l_{i2} &= E_2 a_{i2} + p_{2x} a_{i1} + p_{2y} a_{i5} - p_{2z} a_{i7} \\
l_{i3} &= E_2 a_{i3} - p_{2x} a_{i5} + p_{2y} a_{i1} + p_{2z} a_{i6} \\
l_{i4} &= E_2 a_{i4} + p_{2x} a_{i7} - p_{2y} a_{i6} + p_{2z} a_{i1} \\
l_{i5} &= E_2 a_{i5} - p_{2x} a_{i3} + p_{2y} a_{i2} + p_{2z} a_{i8} \\
l_{i6} &= E_2 a_{i6} + p_{2x} a_{i8} - p_{2y} a_{i4} + p_{2z} a_{i3} \\
l_{i7} &= E_2 a_{i7} + p_{2x} a_{i4} + p_{2y} a_{i8} - p_{2z} a_{i2} \\
l_{i8} &= E_2 a_{i8} + p_{2x} a_{i6} + p_{2y} a_{i7} + p_{2z} a_{i5}
\end{aligned} \tag{35}$$

‡ We omit the factor $-4\pi i e^3 v(Q)$ since it has no role in the calculation of the spur. We shall restore the factor when we substitute for $|M_i|^2$ in equation (28).

$$
\begin{aligned}
m_{i1} &= \mathrm{E}_1 a_{i1} + p_{1x} a_{i2} + p_{1y} a_{i3} + p_{1z} a_{i4} \\
m_{i2} &= \mathrm{E}_1 a_{i2} + p_{1x} a_{i1} - p_{1y} a_{i5} + p_{1z} a_{i7} \\
m_{i3} &= \mathrm{E}_1 a_{i3} + p_{1x} a_{i5} + p_{1y} a_{i1} - p_{1z} a_{i6} \\
m_{i4} &= \mathrm{E}_1 a_{i4} - p_{1x} a_{i7} + p_{1y} a_{i6} + p_{1z} a_{i1} \\
m_{i5} &= -\mathrm{E}_1 a_{i5} - p_{1x} a_{i3} + p_{1y} a_{i2} - p_{1z} a_{i8} \\
m_{i6} &= -\mathrm{E}_1 a_{i6} - p_{1x} a_{i8} + p_{1y} a_{i4} + p_{1z} a_{i3} \\
m_{i7} &= -\mathrm{E}_1 a_{i7} + p_{1x} a_{i4} - p_{1y} a_{i8} - p_{1z} a_{i2} \\
m_{i8} &= -\mathrm{E}_1 a_{i8} - p_{1x} a_{i6} - p_{1y} a_{i7} - p_{1z} a_{i5}
\end{aligned} \qquad (36)
$$

and I is the unit matrix.

Now (30) can be written as

$$
\begin{aligned}
\sum_{\text{spins 1}} \sum_{\text{spins 2}} |\mathrm{M}_i|^2 &= Sp\,|(\mathbf{p}_2 + m)\, M_i\, (\mathbf{p}_1 + m)\, M_i'| \\
&= Sp\,|\mathbf{p}_2\, M_i\, \mathbf{p}_1\, M_i'| + m^2\, Sp\,|M_i M_i'| \\
&\quad + m\, Sp\,|\mathbf{p}_2\, M_i M_i'| + m\, Sp\,|M_i \mathbf{p}_1 M_i'|. \qquad (37)
\end{aligned}
$$

Using the well-known properties of γ-matrices, it can be proved that

$$
\begin{aligned}
Sp\,|M_i \mathbf{p}_1 M_i'| &= 0 \\
Sp\,|\mathbf{p}_2 M_i M_i'| &= 0 \\
Sp\,|\mathbf{p}_2 M_i \mathbf{p}_1 M_i'| &= 4 \sum_{j=1}^{8} l_{ij} m_{ij}\, \epsilon(j) \\
Sp\,|M_i M_i'| &= 4 \sum_{j=1}^{8} a_{ij}^2\, \epsilon'(j)
\end{aligned}
$$

$$
\begin{aligned}
\epsilon(j) &= +1 \text{ for } j = 1, 2, 3, 4. \qquad & \epsilon'(j) &= +1 \text{ for } j = 1, 5, 6, 7. \\
&= -1 \text{ for } j = 5, 6, 7, 8. & &= -1 \text{ for } j = 2, 3, 4, 8.
\end{aligned} \qquad (38)
$$

Thus we obtain

$$
\sum_{\text{spins 1}} \sum_{\text{spins 2}} |\mathrm{M}_i|^2 = 4\,|4\pi e^3 v\,(\mathrm{Q})|^2 \sum_{j=i}^{8} [l_{ij} m_{ij}\, \epsilon(j) + m^2 a_{ij}^2 \epsilon'(j)]. \qquad (39)
$$

Density of States

The density of states for a 4-particle system can be easily derived as

$$
\mathrm{D} = (2\pi)^{-9} \frac{p_3^2 dp_3 d\Omega_3 p_4^2 dp_4 d\Omega_4 \mathrm{E}_5 \mathrm{E}_6 p_5^3 d\Omega_5}{(\mathrm{E} - \mathrm{E}_3 - \mathrm{E}_4)\, p_5^2 - \mathrm{E}_5 \{(p - p_3 - p_4) \cdot p_5\}} \qquad \S(40)
$$

§ We use the subscripts 3, 4, 5 and 6 to denote the four particles instead of 1, 2, 3, 4 just to avoid any confusion with the use of subscripts 1 and 2 for the initial and final states of the electron in the problem.

Adapting (40) to our problem, we make the substitutions

$$E_6 = \infty, \quad p_3 \equiv p_2, \quad p_4 \equiv \omega_1, \quad p_5 \equiv \omega_2.$$

We then obtain

$$D = (2\pi)^{-9}\, p_2^2 dp_2 d\Omega_2 \omega_1^2 d\omega_1 d\Omega_{\omega_1} \omega_2^2 d\Omega_{\omega_2}. \tag{41}$$

Hence $d\sigma_i$ is given by

$$d\sigma_i = \frac{2\pi}{2E_1 \cdot 2\omega_1 \cdot 2\omega_2 \cdot 2E_2} \cdot \frac{E_1}{p_1} (2\pi)^{-9}\, p_2^2 dp_2 \omega_1^2 d\omega_1 d\Omega_{\omega 1} \omega_2^2 d\Omega_{\omega 2}$$

$$\times\, 2\,[4\pi e^3 v\,(Q)]^2 \sum_{j=1}^{8} [l_{ij} m_{ij} \epsilon\,(j) + m^2 a_{ij}^2 \epsilon'\,(j)]. \tag{42}$$

If we are not interested in any particular polarization, we can sum over all polarizations. This is done by asumming $d\sigma_i$ over i.

We shall consider a particular case when the two photons are weak. In this case, the cross-section reduces to a very simple form. The matrix element (13) can be expressed purely in terms of $\mathbf{q}_1$ and $\mathbf{q}_2$ as

$$M_1 + M_{11} = -\,4\pi i e^3 v\,(Q)\, \tilde{u}_2 \gamma_t \frac{1}{\mathbf{p}_1 - \mathbf{q}_1 - \mathbf{q}_2 - m}$$

$$\times \left(\mathbf{e}_2 \frac{1}{\mathbf{p}_1 - \mathbf{q}_1 - m} \mathbf{e}_1 + \mathbf{e}_1 \frac{1}{\mathbf{p}_1 - \mathbf{q}_2 - m} \mathbf{e}_2 \right) u_1. \tag{43}$$

Rationalising the denominator and neglecting $\mathbf{q}_1$ and $\mathbf{q}_2$ in the numerator and $q_1 \cdot q_2$ in the denominator, we obtain

$$M_1 + M_{11} = -\,4\pi i e^3 v\,(Q)\, \frac{\tilde{u}_2 \gamma_t\, (\mathbf{p}_1 - m)}{4 p_1 \cdot (q_1 + q_2)}$$

$$\times \left[\mathbf{e}_2 \frac{(\mathbf{p}_1 - m)\, \mathbf{e}_1}{p_1 \cdot q_1} + \frac{\mathbf{e}_1\, (\mathbf{p}_1 - m)}{p_1 \cdot q_2} \mathbf{e}_2 \right] u_1. \tag{44}$$

Reducing still further by the method now familiar, we obtain

$$M_1 + M_{11} = -\,4\pi i e^3 v\,(Q)\, \tilde{u}_2 \gamma_t u_1 \frac{p_1 \cdot e_1}{p_1 \cdot q_1} \frac{p_1 \cdot e_2}{p_1 \cdot q_2}. \tag{45}$$

In a similar manner, we reduce the other two pairs of elements and obtain

$$M_1 = -\,4\pi i e^3 v\,(Q)\, \tilde{u}_2 \gamma_t u_1 \left(\frac{p_2 \cdot e_1}{p_2 \cdot q_1} - \frac{p_1 \cdot e_1}{p_1 \cdot q_1} \right) \left(\frac{p_2 \cdot e_2}{p_2 \cdot q_2} - \frac{p_1 \cdot e_2}{p_1 \cdot q_2} \right). \tag{46}$$

On making the spur calculation, the cross-section can be written as

$$d\sigma_i = \frac{E_1}{p_1} \left[\frac{2\pi e^2}{4 E_1 E_2} |v\,(Q)|^2 \frac{E_2 p_2 d\Omega_2}{(2\pi)^3} 4\,(m^2 + 2E_1 E_2 - p_1 \cdot p_2) \right]$$

$$\times\left[\frac{e^2 d\omega_1 d\Omega\omega_1}{(2\pi)^2\omega_1}\left(\frac{p_2\cdot e_1}{p_2\cdot\frac{q_1}{\omega_1}}-\frac{p_1\cdot e_1}{p_1\cdot\frac{q_1}{\omega_1}}\right)^2\right]$$

$$\times\left[\frac{e^2 d\omega_2 d\Omega\omega_2}{(2\pi)^2\omega_2}\left(\frac{p_2\cdot e_2}{p_2\cdot\frac{q_2}{\omega_2}}-\frac{p_1\cdot e_2}{p_1\cdot\frac{q_2}{\omega_1}}\right)^2\right] \tag{47}$$

so that the last two factors can be interpreted as the probability of emission of the weak photons, if there is elastic scattering from momentum p_1 to p_2 (*see* Feynman, 1953).

Scattering of a Photon with Pair Creation

In this process a photon of momentum q_1 and polarization e_1 is incident and after its collision with the nucleus, we obtain a photon of momentum q_2 and polarization e_2 besides a positron-electron pair of momentum p_+ and p_- respectively. The lowest order Feynman diagrams for this process are given below. As in the previous section, we have given only three diagrams since the other three can be obtained by the exchange of the positions of the photons.

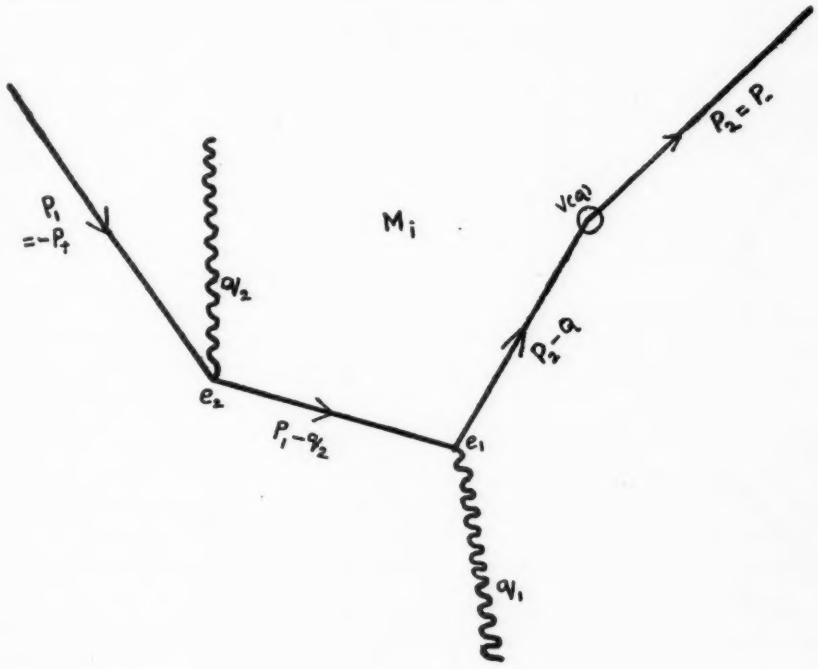

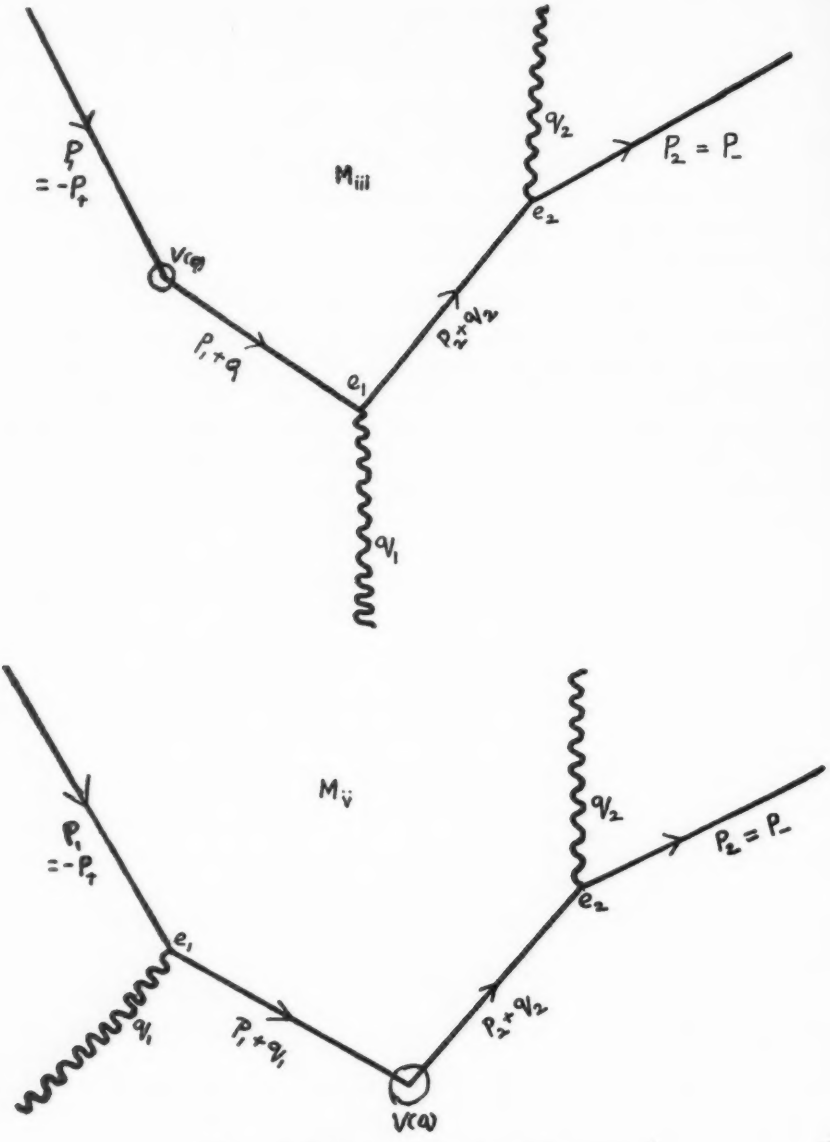

FIG. 2. Scattering of photon with a pair creation.

With respect to the directions of the arrows and without regard to the directions of increasing time, these diagrams look exactly like those for the process discussed in the previous section (*cf.* Fig. 1). However when the direction of time is taken into account, we notice that

(1) p_1 is the momentum of the electron travelling backward in time, *i.e.*, $p_1 = -p_+$.

(2) The photon q_1 is absorbed instead of being emitted.

(3) $p_2 = p_-$.

Hence we can obtain the matrix elements corresponding to these diagrams from those of process (ii) if only we replace $\mathbf{p}_1$ by $-\mathbf{p}_+$, $\mathbf{q}_1$ by $-\mathbf{q}_1$ and $\mathbf{p}_2$ by $\mathbf{p}_-$. However the density of final states is different in this case since the particles in the final states are now a photon, an electron and a positron. Thus $d\sigma_i$ the differential cross-section for a polarization of i-th type is given by

$$d\sigma_i = \frac{2\pi}{2E_-2\omega_1 2\omega_2 2E_+}(2\pi)^{-9}p_+^2 dp_+ d\Omega_+ p_-^2 dp_- d\Omega_- \omega_2^2 d\Omega\omega_2$$

$$\times 2\,[4\pi e^3 v\,(Q)]^2 \sum_{j=1}^{8}{}' [l_{ij}m_{ij}\epsilon\,(j) + m^2 a_{ij}^2 \epsilon'\,(j)]' \qquad (48)$$

where the prime over the square bracket under summation sign indicates that we have to make the following substitutions

$$-p_+ \text{ for } p_1; \qquad -E_+ \text{ for } E_1$$

$$p_- \text{ for } p_2; \qquad E_- \text{ for } E_2$$

and

$$-\omega_1 \text{ for } \omega_1.$$

If we are not interested in a particular state of polarization of the photons, we average over the polarization of the incoming photon and sum over polarization of the outgoing photon. This is done by summing over i and dividing by 2.

We hope that this process will be of considerable interest in high energy electron-photon cascades since it yields a photon, in addition to a pair. In a later contribution we hope to discuss these cross-sections under some useful approximations. We also propose to include these processes in the usual soft cascade theory and study the fluctuations in the number of electron pairs.

Two of us (S. K. S. and R. V.) are grateful to the Madras University for the Government of India Scholarship and the other (N. R. R.) expresses his gratitude to the Madras University for a generous stipend.

REFERENCES

1. Bhabha, H. J. .. *Proc. Roy. Soc.*, 1935, **152 A,** 559.
2. Bethe, H. A. and Heitler, W. *Ibid.*, 1934, **146 A,** 83.
3. ——— and Scheweber .. *Mesons and Fields*, 1955, **1** (Row, Peterson and Co., New York).
4. Feynman, R. P. .. *Quantum Electrodynamics*, 1953. Lectures given at the Californian Institute of Technology.
5. Heitler, W. .. *Quantum Theory of Radiation*, 1954, Oxford.
6. Koshiba, M. and Kaplon, M. F. *Phys. Rev.*, 1955, **97,** 193; 1955, **100,** 327.
7. Murota, T., Ueda, A. and Tanaka, H. *Prog. Theo. Phys.*, 1956, **16,** 482.
8. Seeman, N. and Glasser, R. G. *Report of the Sixth Rochester Conference on High Energy Physics*, 1956, Interscience, New York.

INHIBITION OF SHRINKAGE IN NUCLEAR EMULSIONS

By P. N. Krishnamoorthy

(*Tata Institute of Fundamental Research, Bombay*)

Received March 18, 1957

(Communicated by Prof. B. Peters, F.A.SC.)

Summary

A method of inhibiting shrinkage in nuclear emulsions has been developed. It consists of replacing the silver halide in the emulsion, which is removed during the fixing stage of the processing, by canada balsam. This method can be employed with advantage in the study of neutron spectra with nuclear emulsions, as it will yield improved energy resolution. Another field in which this process of shrinkage inhibition can be advantageously employed is the study of gamma ray spectra, with heavy water loaded emulsions. Here again, improved energy resolution is possible. In fact, this technique can be employed with advantage in all nuclear emulsion work, as it will (*a*) result in overall reduction of distortion in emulsions, (*b*) improve conditions for the measurement of tracks, and (*c*) improve the stability and keeping qualities of processed emulsions.

Introduction

It has come to be recognised that the most generally useful technique for neutron spectroscopy in the energy region 0·5–15·0 MeV is the nuclear emulsion technique. In this method, the trajectories of proton recoils are employed to determine the energies of the incident neutrons. In effect one needs to measure the range and orientation of the recoil protons. The ultimate precision with which these quantities can be measured, together with the range straggling of the protons, determines the resolution of the method and the energy region in which it can be usefully employed. It has not been possible hitherto, to extend measurements on recoil protons to energies below 0·5 MeV and thus extend the measurable energy range of the neutron spectrum. The reasons are twofold. One is the relatively large number of background grains resulting from the gamma radiation which is invariably present during neutron exposures. As a result, there is considerable straggling in range for low energy tracks. Furthermore, measurement of tracks containing less than a few grains is almost impossible due to the difficulty of distinguishing random background grain patterns from true tracks. Secondly, there is the difficulty of determining with any degree of accuracy,

the dip angles of tracks which are smaller in length than 5·5 microns (or 0·5 MeV protons). This arises from the finite depth of focus of the microscopes used.

The finite depth of focus can contribute errors in the measurement of long range protons as well. Firstly, it is the first few microns of any recoil proton track, which gives accurately the direction of the recoil proton relative to the incident neutron direction. The direction is thus determined with dubious accuracy in those cases where the initial portion of the proton track is not favourably situated for the measurement of the dip angle. Such inaccuracy in the measurement of a number of tracks results in the broadening of the neutron energy peaks finally obtained. Secondly, the total length of a track is composed of many independent segments, and the inaccuracies in the measurement of individual segments arising again from the finite value of the depth of focus of the microscope, all add up to contribute a dispersion in the final values of the ranges.

It will thus be seen that the precision with which the ranges and orientations of the recoil protons could be measured, is limited severely by the phenomenon of shrinkage of the emulsion during processing. This shrinkage results from the removal, during the fixing stage of the development, of unsensitized silver halides. The emulsion layer, thus devoid of the silver halide, contracts in thickness during the drying process. Such shrinkage leads to several types of distortions:

1. actual contraction perpendicular to the plane of the emulsion,

2. relative displacement of emulsion layers parallel to the plane of the emulsion, and

3. in cases where foreign substances like wires and capillaries are present in the emulsion, volume distortion by contraction of the emulsion round the wire or capillary. If a suitable substance could be found to fill the voids in the emulsion, so as to bring it back to almost its original thickness, this would minimise the distortions in the emulsion, and enable dip angle measurements to be made with an accuracy comparable to that with which the horizontal angles are measured.

Another field in which the desirability of shrinkage inhibition has been recognised, is the study of gamma ray spectra with heavy water loaded emulsions. Gibson *et al.*,[1, 2] have shown that this method of using heavy water loaded emulsions can be valuable for the measurement of gamma ray energies in the interval 4–12 Mev. In this method, the range and orientation of protons resulting from the photodisintegration of the deutrons from the heavy

water are measured, and are used to infer the energies of the gamma rays. Here the precision with which the dip angles of the protons can be measured is limited by the shrinkage of the emulsions, to an even greater extent. Whereas the shrinkage factor, *i.e.*, the ratio of the thickness of the emulsion during exposure to that after processing is $\sim 2{\cdot}5$ in neutron spectroscopy, the value of this factor in gamma ray spectroscopy lies between $9{\cdot}5$ and $11{\cdot}0$. This is because the nuclear plate, at the time of exposure to gamma radiation, is soaked in heavy water and is swollen to about four times its initial thickness. The accuracy attainable in dip angle measurements is therefore even more restricted. Gibson *et al.*[2] have indicated that even if the final thickness of the processed emulsion could be increased by no more than a factor of two, the errors in the measurement of dip angle would be halved, and the energy resolution considerably improved.

Thus, in the fields referred to above, as in many other fields of investigations employing the nuclear emulsion technique, the desirability of inhibiting shrinkage is now well recognised. The advantages of shrinkage inhibition could be listed as follows:

1. Angles of dip of tracks can be measured with accuracy comparable to that with which the horizontal angles in the plane of the emulsion can be measured.

2. Vertical projections of tracks are more than in shrunk emulsions, and hence range measurements can be made with improved accuracy.

3. As compared with a shrunk emulsion, the average background grain density is reduced by a factor which is the ratio of the shrinkage factors of the shrunk and shrinkage inhibited emulsions. This reduction in background will be of particular value in the range measurement of low energy tracks—protons around $0{\cdot}5$ MeV and low energy electrons.

4. Accidental coincidences between distinct tracks is minimised.

Previous Methods

After the washing stage, and prior to drying, it is customary to soak nuclear emulsions in a 5% solution of glycerine, to minimise strains which are set up in the emulsions during the drying process. It was found by Meulemans and Mignone[3] that a concentration of 10–11% of glycerine gave a shrinkage factor close to unity. Glycerine however is not the best shrinkage inhibiting agent because (1) its refractive index is slightly different from that of gelatine and the immersion oils, and hence the optical quality of the emulsions is impaired, (2) it is hygroscopic—the glycerine treated

plates must therefore be stored and analysed at constant relative humidity; this is a major shortcoming of this technique, and (3) the emulsion becomes soft and tends to melt under the intense beam of light in the microscope. In spite of these difficulties, this method has been employed, for the sake of improved energy resolution, in the study of the fission neutron spectrum of U^{235} by Cranberg *et al.*[4]

Another method has been developed by Dansyz and Yekutieli,[5] in which after the washing stage, the water in the emulsion is replaced by alcohol, by immersion in a succession of baths of gradually increasing concentration of alcohol. The plates are then soaked in a solution of 30 gm. of resin in 100 c.c. of alcohol. A 300 micron emulsion thus soaked for a period of 48 hours gave a shrinkage factor close to unity.

OUR METHOD

A systematic examination of the various substances available for incorporation into the emulsion revealed that canada balsam was by far the best substance. It has a refractive index same as that of the emulsion, and unlike glycerine it is found to insulate the emulsion from humidity variations of the surroundings. It is only partially soluble in alcohol, and hence cannot be incorporated in the emulsion by the method of Dansyz and Yekutieli. It is however very soluble in benzene which in turn is miscible with alcohol, but not water. We did a preliminary experiment to ensure that benzene did not damage a processed emulsion. The following procedure was then adopted to impregnate the emulsion with canada balsam.

After washing, the plates were leached of water by immersion in successively increasing concentrations of alcohol in water. The alcohol concentration was increased in 10% steps, and the plates were maintained in each stage for a period of time which depended upon their thickness—75 minutes for 200 micron plates and 6 hours for 400 micron plates. After the 100% alcohol stage, the plates were immediately put in a 10% solution of benzene in alcohol. They were then taken through benzene-alcohol mixtures, with the benzene concentration increasing in 10% steps, the time for each stage being the same as that for the water alcohol mixtures. After the 100% benzene stage, the plates were immediately transferred into a solution of canada balsam in benzene, the optimum concentration of which was arrived at after a series of trials. A concentration of 100 gm. of canada balsam in 25 c.c. of benzene with a soaking time of 12 hours for 200 micron emulsions (Ilford C2), gave a shrinkage factor close to or lesser than unity. After removal from the canada balsam, the plates are allowed to dry and then cleaned with benzene soaked in cotton wool. The actual value of the shrinkage factor depends

not only on the concentration of the canada balsam-benzene solution, but also on the type, history and pretreatment of the plates. This aspect will be discussed separately. The times for the water-alcohol and alcohol-benzene stages, and the soak in the canada balsam-benzene solutions are indicated in Table I.

TABLE I

Thickness in microns ..	100	200	400	600	1000
Water-alcohol or alcohol-benzene stage	35 min.	75 min.	6 hrs.	10 hrs.	12 hrs.
Benzene-canada balsam solution	6 hrs.	12 hrs.	60 hrs.	100 hrs.	120 hrs.

The temperatures of all the above solutions are kept below 10° C. In all stages of the processing and particularly in the canada balsam stage it is important to maintain the plates in well levelled trays.

DETERMINATION OF THE SHRINKAGE FACTOR

To establish the reliability of this method of shrinkage inhibition, a simple yet accurate method has been employed for the determination of the shrinkage factor. Before processing, the thickness of the emulsion along with the glass backing is measured at six different points on the plate, using a dial gauge. The measurements are accurate to within one micron. The thickness of the processed emulsion with the glass backing is again measured at the same points. The thickness of the processed emulsion only at these points is then measured with a microscope. From the set of three measurements at each point, the thickness of the unprocessed emulsion and hence the shrinkage factor at that point can be obtained.

For any particular plate, the value of the shrinkage factor at six different points is thus obtained, and from these, the mean value of the shrinkage factor for the whole plate is obtained. This mean value which lies around unity for the shrinkage inhibited plate, has a standard deviation of 0·03. In the case of some plates which were not held horizontal during processing, in particular during the canada balsam stage, the standard deviation for the shrinkage factor of a plate was as high as 0·07. Experiments have however shown that by carefully controlling conditions, it is possible to achieve uniform impregnation of canada balsam, and thus obtain values of shrinkage factor with standard deviation as small as 0·01. In a typical experiment six Ilford 200 micron C2 plates belonging to the same batch and hence with the same

history, were identically processed and subjected to the canada balsam treatment. The thickness of the unprocessed emulsions varied from 187 microns to 228 microns. The variations on individual plates were much less—189 to 204 and 220 to 228 in two typical cases. The values of shrinkage factors for individual plates, obtained as a mean of six independent determinations at six different points on each plate, were $0{\cdot}80 \pm 0{\cdot}02$, $0{\cdot}75 \pm 0{\cdot}01$, $0{\cdot}78 \pm 0{\cdot}01$, $0{\cdot}81 \pm 0{\cdot}02$, $0{\cdot}79 \pm 0{\cdot}01$ and $0{\cdot}78 \pm 0{\cdot}02$. The average value of the shrinkage factor for all the six plates is $0{\cdot}79 \pm 0{\cdot}02$. Four other Ilford C2—200 micron plates which were processed and dried in the conventional manner (alcohol drying without glycerine) gave shrinkage factors of $2{\cdot}53 \pm 0{\cdot}03$, $2{\cdot}51 \pm 0{\cdot}02$, $2{\cdot}49 \pm 0{\cdot}03$, and $2{\cdot}61 \pm 0{\cdot}03$. The average value for the four plates was $2{\cdot}52 \pm 0{\cdot}06$. It will thus be seen that a plate treated with canada balsam yields a value of shrinkage factor which is constant within experimental errors over the whole of the plate.

As indicated earlier, the value of the shrinkage factor differs from plate to plate, depending upon the type, history and pretreatment. For example, various 200 micron plates processed and shrinkage inhibited by identical processes, gave shrinkage factors varying from 0·7 to 1·2. The important factor however, was the constancy of the value of the shrinkage factor over the whole of any individual plate. Therefore, in any shrinkage inhibited plate, it will be sufficient to make the various thickness measurements at say, three points. The emulsion thickness before processing at these points is thus known, and the shrinkage factor of the emulsion at any time when track measurements are being made, can be determined by measuring the emulsion thickness at these points under the microscope. We can thereby eliminate errors due to minor variations in the thickness of a plate due to various factors like time, storage conditions, etc.

In order that gamma ray measurements with heavy water loaded emulsions may be improved further, an attempt was made to increase the final thickness of the emulsions by increasing the concentration of canada balsam. Four plates from the same batch were identically processed and shrinkage inhibited in the following manner. Two were placed in a solution of the already recommended concentration, *viz.*, 100 gm. of canada balsam in 25 c.c. of benzene. The other two were placed in a solution of 150 gm. of canada balsam in 25 c.c. of benzene. The former two plates gave a shrinkage factor of $1{\cdot}07 \pm 0{\cdot}02$, while the latter two gave $1{\cdot}08 \pm 0{\cdot}03$. It will thus be seen that any sizeable reduction in the value of the shrinkage factor cannot be achieved by increasing the concentration of canada balsam. The exact nature of the dependence of the value of the shrinkage factor on the history and pretreatment of the plates has not been investigated.

Uniformity of Shrinkage Inhibition in Depth

To ensure further, that the shrinkage inhibition was uniform throughout the depth of the emulsion the following investigation was undertaken. The ratio of the number of background grains in equal areas of the shrunk and shrinkage inhibited emulsions (from the same batch and processed identically) was determined at various depths. If the shrinkage inhibition is uniform, this ratio should be the same for all depths, and should be equal to the ratio of the shrinkage factors of the shrunk and shrinkage inhibited emulsions. In a typical study, the ratio of the shrinkage factors of 2 plates was 3·11. The ratio of the grain counts made at three different depths gave the values 3·46, 3·28 and 3·29. In addition, emulsions soaked in benzene-canada balsam solution for times much larger than those given in Table I, *e.g.*, 18 hours for 200 μ emulsions and 90 hours for 400 μ emulsions, did not have shrinkage factors different from those emulsions which had been normally treated.

Variation of Thickness with Humidity

In view of the hygroscopic nature of glycerine, it would be expected that the thickness of a glycerine impregnated emulsion would be sensitive to humidity variations of the surroundings. A canada balsam treated plate, however, should be expected to render the plate almost immune to such humidity variations. In order to study the behaviour of differently treated emulsions under conditions of varying humidity, the following experiment was undertaken.

Five plates were treated as follows: The first plate was removed from the 100% alcohol stage and allowed to dry. The second plate after removal from the alcohol stage, was subjected to a 5% glycerine treatment. The third plate was treated similarly to plate 2, except that 15% glycerine was used. Plate 4 was removed from the 100% benzene stage and allowed to dry. Plate 5 was subjected to the canada balsam treatment. All the five plates were then placed in a humidity chamber. The humidity in the chamber was held constant at any particular value by using solutions of glycerine in water of suitable concentrations.[6] At the various values of humidity, emulsion thicknesses were measured under the microscope, at three well defined points on each plate. Care was taken to ensure that the emulsion thickness at any particular value of humidity had reached equilibrium. This was done by maintaining the emulsions at a particular humidity value until thickness readings taken at any time were reproducible atleast 48 hours later. These readings were then taken as the thicknesses corresponding to the particular value of humidity.

The results obtained are represented in Fig. 1. It will be seen from the graph that whereas the glycerine soaked plates are extremely sensitive to humidity variations, the other plates are not. Table II gives the ratios of the thicknesses at the two extreme values of humidity at which measurements were made.

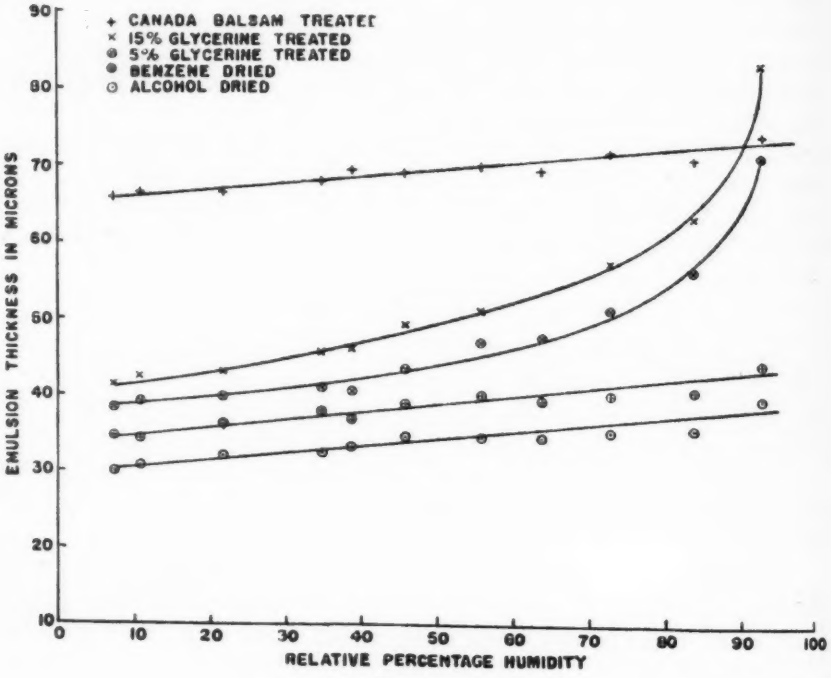

FIG. 1

TABLE II

Emulsion treatment	Alcohol dried	5% glycerine	15% glycerine	Benzene dried	Canada Balsam
Thickness at 93% humidity / Thickness at 7·5% humidity	1·31	1·88	1·97	1·26	1·13

The 15% glycerine plate shows a slightly larger thickness variation than the 5% glycerine plate. The difference in the ratios between the alcohol and benzene dried plates and the canada balsam treated plate is ascribable to the

fact that gelatine is itself hygroscopic and hence the addition of canada balsam improves its thickness preserving qualities by inhibiting water absorption. It was further observed that the optical properties of glycerine treated plates deteriorated progressively with increase in humidity. At values of humidity above 70% the glycerine plates were misty especially in the lower regions, and observations under the microscope were rendered extremely difficult. At low humidities, the alcohol and benzene dried plates tended to peel off from the glass backing, whereas the glycerine and canada balsam treated plates remained completely unaffected.

Discussion

From the above findings, it is obvious that the canada balsam treated plate has distinct advantages over the glycerine treated one. The canada balsam treated plate can be stored and measured in a laboratory where facilities do not exist for controlling humidity. The uniformity of the shrinkage factor value over the whole of a canada balsam treated plate having been established, it should now be possible to make accurate measurements to determine the mean angle of scattering of a track by vertical deflections, by the method of Mabboux.[7] Further, it should be possible to work with relative ease with emulsions in which foreign bodies like wires and capillaries have been incorporated. Stripped emulsions processed without glass backing could be shrinkage inhibited with canada balsam and the emulsion could then be rolled on to a glass plate, thus ensuring perfect optical contact between emulsion and the backing glass.

Acknowledgements

The author's thanks are due to Dr. R. Ramanna for advice and encouragement and to Messrs. K. N. Iyengar and M. R. Hiranandani for general assistance and microscope work.

References

1. Gibson, W. M., Grotdal, T. Orlin, J. J. and Trumpy, B. — *Phil. Mag.*, 1951, **42**, 555.
2. ———— .. *Ibid.*, 1952, **43**, 457.
3. Meulemans, G. and Mignone, G. — *P.Sc. and Ind. Phot.*, 1951, **23 A**, 309.
4. Cranberg, L., Frye, G., Nereson, N. and Rosen, L. — *Phys. Rev.*, 1956, **103**, 662.
5. Dansyz, M. and Yekutieli, G., — *Phil. Mag.*, 1951, **42**, 1185.
6. Wexler, A. and Brombacher, W. G. — *Natl. Bur. Standards, Instrumentation* 5 (25), No. 6.
7. Mabboux, M. C. .. *Comptes Rendus*, 1951, **232**, 1091, 2309.

NON-RELATIVISTIC APPROXIMATION OF BHABHA'S EQUATION

By K. K. Gupta

(*Tata Institute of Fundamental Research, Bombay* 1)

Received February 9, 1957

(Communicated by Dr. J. H. Bhabha, F.R.S., F.A.SC.)

A relativistic irreducible wave equation for a particle having the two mass and spin states $(m, 3/2)$ and $(\lambda m, \frac{1}{2})$ and positive-definite charge was proposed by Bhabha.[1] It can be rewritten[2] in a form analogous to that of the Rarita-Schwinger[3] equations for particles of half odd-integral spins. The purpose of this paper is to write down the non-relativistic approximation of the equations in an external magnetic field, with a view to determining the magnetic moment of the particle in the two states. It is convenient to use the Rarita-Schwinger form of the theory for this purpose, since only the Dirac matrices occur in the equations in this form, rather than the complicated 20×20 matrices of the original theory. We follow the method of Tiomno[4] who obtained the non-relativistic approximation of the Fierz-Pauli spin 3/2 equations. The magnetic moment in the spin 3/2 state is found to be $e/3m\,\vec{\Sigma}$, which is also the value for the pure spin 3/2 case. The value for the spin 1/2 state is $e/2\lambda m\,\{1 + 2\lambda d^2(1 + \lambda)\}$, and differs from that of a Dirac particle.

1. The equations of motion in the presence of an electro-magnetic field are

$$(\mathrm{P}_\tau\gamma^\tau + m)\,\psi_k - \tfrac{1}{3}(\mathrm{P}_l\gamma_k + \mathrm{P}_k\gamma_l)\,\psi^l + \tfrac{1}{3}\gamma_k(\mathrm{P}_\tau\gamma^\tau - m)\,\gamma_s\psi^s + d\mathrm{P}_k\psi = 0, \quad (1)$$

$$(\mathrm{P}_\tau\gamma^\tau + \lambda m)\,\psi - \mathrm{P}_\tau\psi^\tau = 0, \quad (2)$$

where

$$\mathrm{P}_k = i\frac{\partial}{\partial x_k} - e\mathrm{A}_k,$$

and A_k is the 4-potential of the external field. Multiplying (1) by γ^k and P^k and summing over k we obtain, respectively,

$$\tfrac{2}{3}\mathrm{P}_\tau\psi^\tau - \tfrac{1}{3}m\gamma_\tau\psi^\tau + d\mathrm{P}_\tau\gamma^\tau\psi = 0 \quad (3)$$

and

$$\tfrac{2}{3}\mathrm{P}_\tau\gamma^\tau\mathrm{P}_s\psi^s - \frac{m}{3}\mathrm{P}_\tau\gamma^\tau\gamma_s\psi^s + m\mathrm{P}_\tau\psi^\tau + ie\,\mathrm{F}_{lm}\gamma^l\psi^m$$

$$- \tfrac{1}{3}ie\,\mathrm{F}_{lm}\gamma^l\gamma^m\gamma_\tau\psi^\tau + d\mathrm{P}^s\psi = 0, \quad (4)$$

where

$$F_{lm} = \frac{\partial A_m}{\partial x^l} - \frac{\partial A_l}{\partial x^m}.$$

Multiplying (3) by $P_s\gamma^s$ and subtracting from (4), we get

$$m\,P_r\psi^r = -\,ie\,F_{lm}\gamma^l\psi^m + \tfrac{1}{6}\,ie\,F_{lm}\,\gamma^l\gamma^m\gamma_r\psi^r - \frac{d}{2}\,ie\,F_{lm}\gamma^l\gamma^m\psi. \tag{5}$$

From (2) and (3) we have

$$P_r\psi^r = \frac{1}{(2+3d^2)}\{m\gamma_r\psi^r + 3d\lambda m\psi\} \tag{6}$$

and

$$P_r\gamma^r\psi = \frac{1}{(2+3d^2)}\{dm\gamma_r\psi^r - 2\lambda m\psi\}. \tag{7}$$

Equations (5) and (6) now give

$$\gamma_r\psi^r = -\,3d\lambda\psi + \frac{(2+3d^2)}{m^2}\{-\,ie\,F_{lm}\gamma^l\psi^m + \tfrac{1}{6}\,ie\,F_{lm}\,\gamma^l\gamma^m\gamma_r\psi^r$$

$$-\frac{d}{2}\,ie\,F_{lm}\,\gamma^l\gamma^m\psi\}. \tag{8}$$

2. In the non-relativistic approximation the equations of motion should involve only two independent components for the spin 1/2 state and four independent components for the spin 3/2 state. We shall write down the equations of motion for the two cases as Schrödinger equations, the Hamiltonian being correct to terms of order $1/m$. One can then remove the small components by means of a Foldy-Wouthuysen transformation.

From (8) we have, to terms of order $(1/m)^2$,

$$\gamma_r\psi^r = -\,3d\lambda\psi + \frac{(2+3d^2)\,ie}{m^2}\{-\,F_{lm}\gamma^l\psi^m - \frac{d}{2}(1+\lambda)\,F_{lm}\gamma^l\gamma^m\psi\}. \tag{9}$$

We now wish to calculate $P\gamma\,(\gamma_r\psi^r)$ to terms of order $1/m$. For this purpose we assume that the external field is a constant, weak magnetic field, $\vec{H} = (-F_{12}, -F_{23}, -F_{31})$ and that

$$|P_k\psi| \ll m|\psi|.$$

Note also that, substituting for $P_r\psi^r$ from (6), equation (1) can be written as

$$(P_r\gamma^r + m)\,\psi^k - \frac{(1+d^2)}{(2+3d^2)}\,m\gamma^k\gamma_r\psi^r - \frac{d\lambda m}{(2+3d^2)}\,\gamma^k\psi - \tfrac{1}{3}\,P^k\gamma_r\psi^r$$

$$+\,\tfrac{1}{3}\,\gamma^k P_r\gamma^r\,(\gamma_s\psi^s) + dP^k\psi = 0, \tag{10}$$

Making use of (7), (10) and (9) we obtain, to terms of order $1/m$,

$$P_s\gamma^s(\gamma_r\psi^r) = 3d\lambda^2 m\psi + \frac{ie(3d^2\lambda - 3d^2 - 2)}{m} F_{lm}\gamma^l\psi^m$$

$$- \frac{3ied\lambda}{m} F_{lm}\gamma^l\gamma^m\psi. \tag{11}$$

Substituting for $\gamma_r\psi^r$ from (9) and for $P_r\gamma^r(\gamma_s\psi^s)$ from (11), equation (10) for $k = 1, 2, 3$ becomes

$$(P_r\gamma^r + m)\psi^k + d\lambda m(1 + \lambda)\gamma^k\psi + \frac{ie}{3m}(1 + 3d^2\lambda)\gamma^k F_{lm}\gamma^l\psi^m$$

$$+ \frac{ied}{2m}(1 + d^2 - \lambda + \lambda d^2)\gamma^k F_{lm}\gamma^l\gamma^m\psi = 0. \tag{12}$$

Similarly, making use of (6) and (9), equation (2) becomes

$$(P_r\gamma^r + \lambda m)\psi + \frac{ied}{m} F_{lm}\gamma^l\psi^m + \frac{ied^2(1 + \lambda)}{2m} F_{lm}\gamma^l\gamma^m\psi = 0. \tag{13}$$

3. Let us now consider the spin 3/2 state. In the force free case, in this state ψ is identically zero. In the presence of an external field we must therefore have

$$\psi = a F_{lm}\gamma^l\psi^m, \tag{14}$$

where a is a constant. Substituting this expression for ψ in (13) and making use of (12) one easily obtains

$$a = -\frac{ied}{m^2(1 + \lambda)}$$

Equation (12) now becomes

$$(P_r\gamma^r + m)\psi^k + \frac{ie}{3m}\gamma^k F_{lm}\gamma^l\psi^m = 0, \tag{15}$$

neglecting terms involving squares of the field strengths. This is just the non-relativistic approximation of the pure spin 3/2 equations obtained by Tiomno, and has been further reduced by him, by means of a Foldy-Wouthuysen transformation, to the form

$$i\frac{\partial\phi}{dt} = \left\{\frac{1}{2m}(\vec{p} - e\vec{A})^2 + eA_0 - \frac{e}{3m}\vec{\Sigma}\cdot\vec{H}\right\}\phi,$$

where ϕ is a four component quantity. The three components of $\vec{\Sigma}$ are the 3×3 matrices representing an angular momentum of 3/2. The magnetic moment of the particle in the spin 3/2 state is thus $e/3m\,\vec{\Sigma}$.

4. For the spin 1/2 case the wave-functions ψ^k can be determined from ψ. In the force free case we have, in the non-relativistic approximation [*see* equation (21 *a*) of A],

$$\psi^k = -\,d\lambda\,\gamma^k\psi. \tag{17}$$

In the presence of an external field this relation will be of the form

$$\psi^k = -\,d\lambda\,\gamma^k\psi + \text{terms involving } F_{lm}. \tag{18}$$

Substituting (18) in (13) we obtain

$$(P_r\gamma^r + \lambda m)\,\psi + \frac{ied^2}{2m}(1-\lambda)\,F_{lm}\gamma^l\gamma^m\psi = 0. \tag{19}$$

This may be rewritten as

$$i\frac{\partial\psi}{\partial t} = \left\{eA_0 + (\vec{p} - e\vec{A})\,\gamma^0\vec{\gamma} - \lambda m\gamma^0 - \frac{ied^2}{2m}\,\gamma^0\,(1-\lambda)\,F_{lm}\gamma^l\gamma^m\right\}\psi. \tag{20}$$

By means of a Foldy-Wouthuysen transformation this equation can be transformed to

$$i\frac{\partial\psi}{\partial t} = \left\{-\,\gamma^0\,\lambda m + eA_0 - \frac{\gamma^0}{2\lambda m}(\vec{p} - e\vec{A})^2 + \gamma^0\,\vec{H}\cdot\left(\frac{ed^2\,(1-\lambda)}{m} - \frac{e}{2\lambda m}\right)\vec{\sigma}\right\}\psi. \tag{21}$$

For the positive energy states only the first two components of ψ are non-zero. Making the tranformation

$$\psi \;\rightarrow\; e^{i\lambda mt}\psi$$

we obtain, for positive energy states,

$$i\frac{\partial\psi}{\partial t} = \left\{eA_0 + \frac{1}{2\lambda m}(\vec{p} - e\vec{A})^2 - \vec{H}\cdot\left(\frac{ed^2\,(1-\lambda)}{m} + \frac{e}{2\lambda m}\right)\vec{\sigma}\right\}\psi, \tag{22}$$

ψ being now a two component spinor. The particle thus has the magnetic moment

$$\vec{M} = \frac{e}{2\lambda m}\{1 + 2\lambda d^2\,(1-\lambda)\}\vec{\sigma}. \tag{23}$$

Note that it reduces to the value for a Dirac particle if $\lambda = 1$, *i.e.*, if the masses in the two states are equal.

It is a pleasure to thank Dr. M. K. Sundaresan for stimulating discussions.

REFERENCES

1. Bhabha, H. J. .. *Phil. Mag.*, 1952, **43**, 33.
2. Gupta, K. K. .. *Proc. Roy. Soc.*, 1954, **222 A**, 118; hereafter referred to as A. We use the notation of this paper.
3. Rarita, W. and Schwinger, J. *Phys. Rev.*, 1940, **60**, 61.
4. Tiomno, J. .. *Centro Brasileiro de Perquisas Fisicas, Notas de Fisica*, 1952, No. 9.

AN INTERPRETATION OF THE SOLAR ANISOTROPY OF PRIMARY COSMIC RADIATION

By N. W. Nerurkar

(*Physical Research Laboratory, Ahmedabad-9*)

Received March 11, 1957

(Communicated by Professor Vikram A. Sarabhai, F.A.SC.)

I. Introduction

The study of the daily variation of cosmic ray intensity has grown in importance in recent years with increasing realisation that it provides a powerful tool for understanding the anisotropy of primary cosmic radiation as well as the electromagnetic state in interplanetary space. With the solar daily variation of cosmic ray intensity which arises due to the spin of the earth, it is possible to investigate the anisotropy in various directions by making suitable directional studies at different latitudes. A mass of data collected during the last three or four years as well as a re-examination of earlier data have brought to light numerous experimental facts which have been reviewed recently by Sarabhai *et al.*[1] The relevant facts may be stated as follows:—

1. The daily variation cannot at all times be satisfactorily described in terms of the diurnal component alone. It has been observed, however, that in general the first two harmonic components are adequate to represent fairly satisfactorily the main features of the daily variation.

2. The 12-monthly (annual) mean daily variation of meson intensity exhibits large long-term changes of amplitude and of the time of maximum of the diurnal as well as the semi-diurnal components.[2]

3. During several years the 12-monthly mean daily variation, particularly at low latitudes, exhibits two maxima instead of one (Fig. 8 of Ref. 2). Sarabhai *et al.*[3] have tried to show that the 12-monthly mean daily variation can be explained in terms of two types of variations, one having a maximum during the day at about 1100 to 1300 hours. and the other at night at about 0100 to 0300 hours. The relative contribution of these two types of variations changes from year to year and the data collected over the past twenty years is suggestive of a relationship of these changes with the 22-year cycle of solar activity. This makes the maximum of the diurnal component of the daily variation shift by as much as 10 to 12 hours over a number of years.

4. When data on individual days are examined, there is a tendency for the time of maximum of the diurnal component to occur either at noon or during the early morning hours.[4] Such days usually occur in groups that sometimes recur after 27 days. Some of the groups appear to be associated with active solar regions.

5. High values of C_p, daily geomagnetic planetary index, are normally associated with days having large amplitudes.[5] However large amplitudes are not always associated with magnetically disturbed days or the central meridian passage of solar regions of visible activity.[6]

The above facts lead to the conclusion that the daily variation and the anisotropy of cosmic radiation either on individual days or averaged over a group of days is of a highly variable character. Our knowledge of the permanent anisotropy, if indeed it exists, is meagre at the present moment. Hence for the interpretation of the anisotropy it is appropriate for the time being to take into account only the variable anisotropy about which we have a number of well established facts regarding its form as well as its solar and terrestrial relationships.

In the past few years, several attempts have been made to explain some of the average characteristics of the diurnal component of the daily variation on a model involving the modulation of primary cosmic ray intensity by changes in the electromagnetic condition in interplanetary space. Brunberg and Dattner[7] have tried to explain an anisotropy which would produce a daily variation of average amplitude of 0·3% and a time of maximum near noon. They suggest that a tangential anisotropy in the 18-hour direction might be created in the solar system by the rotation of the magnetic field of the sun. Alfven[8] has moreover shown that the disturbance in this field by the solar emission of ionised matter can give rise to a radial anisotropy which would alter with solar activity and could therefore account for the 11 years variation in the time of maximum of the diurnal component shown by Sarabhai and Kane[9] and Thambyahpillai and Elliot.[10]

To explain the anisotropy on days when there is a magnetic storm, Nagashima[11] has studied in detail the implications of the suggestion made by Elliot and Dolbear[12] and Alfven[13] that the storm time anisotropy is due to the presence of a polarised beam of ionised matter in the vicinity of the earth. His analysis shows that this anisotropy in the primary radiation is directed along the 12-hour direction and explains for the first time the increase in amplitude and advancement of the phase of the diurnal variation on magnetically disturbed days.

Apart from the difficulty that arises due to the daily variation exhibiting characteristics markedly different from those assumed by Brunberg and Dattner,[7] none of the theories advanced so far accommodate the existence of the two main types of variable anisotropies which are responsible for the day and night maxima in the daily variation of cosmic ray intensity at low latitudes. In this paper an attempt has been made to understand the variable character of anisotropy by modulation of the primary cosmic ray intensity by ionized solar-matter as it is ejected from the sun carrying a frozen magnetic field. The anisotropy is derived from the measurements of the daily variation of meson intensity at low latitudes.

II. Characteristics of the Solar Corpuscular Emission

The recurring disturbances in the earth's magnetic field have been attributed by a number of workers[14] to the presence of streams of ionized matter emitted by the sun. Although a 27 days recurrence of these disturbances over two to three solar rotations suggests that the emission is active over a long period, individual disturbances last for a few days. This indicates that the earth is engulfed in the streams for only a few days. It is, therefore, assumed that a mass of gas ejected by the sun may be looked upon as a beam with parallel sides perpendicular to the plane of the ecliptic.

Alfven[15] has shown that a highly conducting medium moving out of a region having a high magnetic field tries to drag the field with it. A mass of gas which is expelled by the sun is ionized and he has suggested that it will carry with it the solar magnetic field. Recent work on the general magnetic field of the sun by Babcock and Babcock[16] puts a limit of 1 gauss to its magnitude and suggests that it is concentrated near the polar regions. In solar equatorial latitudes there are intense local magnetic fields associated with active regions on the sun. It is reasonable to expect that beams along the plane of the ecliptic are formed by solar corpuscular emission from solar equatorial latitudes and they would carry therefore a trapped field which is not derived from the general solar dipole field but from the local magnetic fields in the neighbourhood of active regions from which the ionized matter is supposed to be emitted. On this basis it would be possible to have the trapped field having no preferential orientation with respect to the solar dipole field. For simplifying calculations it is assumed that this field is uniform within the beam. Swann[17] has explained how such uniformly magnetised beams with no external magnetic field can be realised in practice.

The trapped magnetic field moves with the beam with the same velocity as the solar corpuscles and in a co-ordinate system moving with the cor-

puscles, there is only a magnetic field present. But an observer on the earth, with respect to which the magnetic field is in motion, observes in addition to a magnetic field a charge displacement in a direction perpendicular to the velocity of the beam and the magnetic field. The beam therefore appears to have crossed electromagnetic fields and cosmic ray particles traversing the beam gain or lose energy depending upon their orientation with respect to the electric field. An isotropic distribution of primary particles is disturbed and an anisotropy is created in some directions in space.

III. ANISOTROPY OF THE PRIMARY COSMIC RADIATION*

In evaluating the effect of a beam of solar ionized matter on the anisotropy of primary cosmic radiation we neglect the inclination of the axes of the sun and the earth with the ecliptic. For observing stations at low latitudes, the primary cosmic ray particles incident from the vertical come from directions close to the equatorial plane, and hence only the acceleration or deceleration of particles crossing the beam in this plane is of consequence. This is produced by an electric field which develops due to the component of the trapped magnetic field in a direction perpendicular to the plane of the ecliptic. With different orientations of the magnetic field within the beam, this component could be reversed in direction. In the present work, the effect of this component alone on the anisotropy of cosmic radiation is investigated, and the results are most closely applicable to observations at the equator with narrow angle telescopes pointing to the vertical. However omnidirectional instruments, such as the ionization chamber, measures in addition primary particles inclined to the equatorial plane. In this case, as well as for observations at high latitudes, the contribution of the component of magnetic field parallel to the ecliptic would also have to be considered.

Fig. 1 shows the cross-section of the beam in the plane of the ecliptic. The ionized matter in the beam is moving with a velocity v along the Y-axis. The beam has a width equal to b along the X-axis. It is supposed that the beam is situated symmetrically with respect to the plane of the ecliptic. The magnetic field trapped within it has a component H_z' along the Z-axis and is called positive along the positive direction of the Z-axis. To a stationary observer on the earth the beam will have a component of magnetic field $H_z = H_z'/(1 - v^2/c^2)^{\frac{1}{2}}$ along the Z-axis and an electric field $(v/c)\, H_z$ along the X-axis. The potential difference between the two parallel sides of the beam is therefore $(v/c)\, bH_z$ and cosmic ray particles of charge e crossing such a beam will change their energy by $(v/c)\, ebH_z$.

* Part of the analysis in this section is reproduced from the original paper by Nagashima.[11]

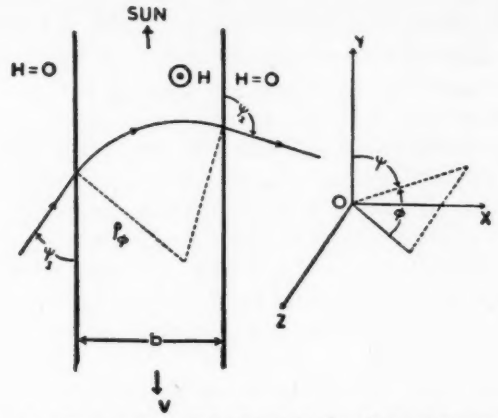

FIG. 1. Cross-section of the beam in the plane of the ecliptic.

The direction of the velocity of a particle in space can be uniquely determined by two angles ϕ and ψ where ϕ is the inclination to the plane of the ecliptic (XOY plane in Fig. 1) and ψ is the inclination in the plane of the ecliptic to the sun earth line (Y-axis in Fig. 1). If W_1, (ϕ_1, ψ_1) represent the energy and the direction of the particle before entering the beam and W_2, (ϕ_2, ψ_2), those of the particle after crossing the beam we get

$$\Delta W_b = W_2 - W_1 = (v/c)\, ebH_z \tag{1}$$

Since the velocity of ionized matter in the beam is much less than the velocity of light, $v \ll c$. Also if $\Delta W_b < W_1$ the direction of the particle with respect to the plane of the ecliptic is not appreciably altered. In consequence

$$\phi_2 \approx \phi_1$$

The particle is however deflected in the plane of the ecliptic and as shown in Fig. 1 if ϕ is not very large

$$\begin{aligned} \cos \psi_2 &= \cos \psi_1 - b/\rho_\phi \\ &= \cos \psi_1 - \sec \phi\, (ebH_z)/W_1 \end{aligned} \tag{2}$$

where ρ_ϕ is the projection of the radius of curvature on the plane of the ecliptic.

It is seen from Eq. 2 that if $b > 2\rho_\phi$, $\cos \psi_2 < -1$ and ψ_2 is imaginery. Such particles are not able to cross the beam but after entering the beam are deflected so as to emerge with unchanged energy on the same side of it from which they entered. Particles having $b < 2\rho_\phi$ can cross the beam only if

they enter it in favourable directions. The energy W of a proton which can cross the beam of width b in a direction ϕ is given by

$$W = W_{min}(\phi, b) = \tfrac{1}{2} ebH_z \sec \phi \qquad (3)$$

In Fig. 2 have been shown the deflections in the plane of the ecliptic of particles having energy less than $W_{min}(0, b)$. It is noticed that if initially there is an isotropic distribution of such particles, the deflections within the beam do not alter the intensity of these particles in any direction outside the beam. Thus the isotropy of cosmic radiation of energy less than $W_{min}(0, b)$ is not disturbed by the beam when an observer is outside it. If, on the other

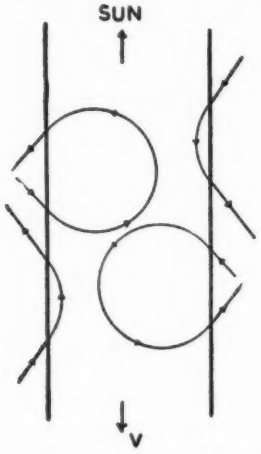

FIG. 2. Deflections of low energy cosmic ray particles $W < W_{min}(0, b)$ in the magnetic field within the beam.

hand, the earth is within the beam, the particles have to cross only a part of the beam to reach the earth. Since the strength of the magnetic field is the same as before but the width is reduced, the minimum energy of particles which can reach the earth is reduced and the anisotropy therefore extends to particles with energy less than $W_{min}(0, b)$. When the earth is at a distance x from one side of the beam, the minimum energy of the anisotropic radiation $W_{min}(0, x)$ is given by

$$W_{min}(0, x) = \tfrac{1}{2} exH_z \text{ or } \tfrac{1}{2} e(b - x) H_z \qquad (4)$$

whichever is smaller.

The anisotropy of cosmic rays also depends on the position of the earth with respect to the beam. The distance between the earth and the beam

changes due to the spinning of the sun and the motion of the earth along the ecliptic. Beams approach the earth in the same direction as the motion of the earth, but soon overtake it. We have to consider three cases; firstly when the beam approaches the earth, secondly when it envelops the earth and finally when it recedes from the earth. In Fig. 3 we show the effects in each case when H_z is positive. When the observer is on the right side of the beam, particles of energy W after crossing the beam from left to right gain an energy ΔW_b and have their final velocity directions lying in the shaded region in Fig. 3 (*a*). This region of acceleration extends from ψ_b^{acc} to π where ψ_b^{acc} is given by Eq. 2 as

$$\psi_b^{acc} = \cos^{-1}\left(1 - 2 \sec\phi \frac{W_{min}(0, b)}{W}\right) \tag{5}$$

There will be an increase of intensity of particles arriving in directions lying in this region, while those arriving from other directions either have not passed through the beam or, if passed through, have not crossed the beam and therefore do not undergo any change in their energy or intensity.

In Fig. 3 (*b*), the earth is enveloped in the beam but is at a distance x from the left side of the beam. The beam can now be considered as made up of two parts, one having width equal to x and the other $(b - x)$. Particles arriving from the left side are accelerated and gain an energy by $\Delta W_x = (v/c)\, exH_z$ and those coming from the right are decelerated and lose energy by $\Delta W_{(b-x)} = (v/c)\, e\,(b - x)\, H_z$. Due to the deflection of particles within the beam, the region of acceleration extends from ψ_x to $\psi_{(b-x)}$ while that of deceleration from $\psi_{(b-x)}$ to ψ_x where

$$\psi_x = \cos^{-1}\left(1 - 2 \sec\phi \frac{x}{b} \frac{W_{min}(0, b)}{W}\right) \text{ and } \pi > \psi_x > 0 \tag{6}$$

$$\psi_{(b-x)} = \cos^{-1}\left(-1 + 2 \sec\phi \frac{b - x}{b} \frac{W_{min}(0, b)}{W}\right) \text{ and } 2\pi > \psi_{(b-x)} > \pi \tag{7}$$

When the earth is in the centre of the beam, *i.e.*, $x = b/2$, ψ_x and $\psi_{(b-x)}$ are separated by 180°. We thus see that when the earth is within the beam, all directions in space, as viewed from the earth, are divided into either accelerated or decelerated regions. The intensity of the particles will therefore be more or less according as the instrument points to the region of acceleration or deceleration respectively.

In Fig. 3 (*c*) the earth is on the left side of the beam and particles of energy W while crossing the beam lose their energy by ΔW_b and appear in a shaded region bounded by ψ_b^{dec} and 2π where

$$\psi_b{}^{dec} = \cos^{-1}\left(-1 + 2\sec\phi\,\frac{W_{min}(0, b)}{W}\right) \text{ and } 2\pi > \psi_b{}^{dec} > \pi \qquad (8)$$

In this region the intensity of the particles is below normal.

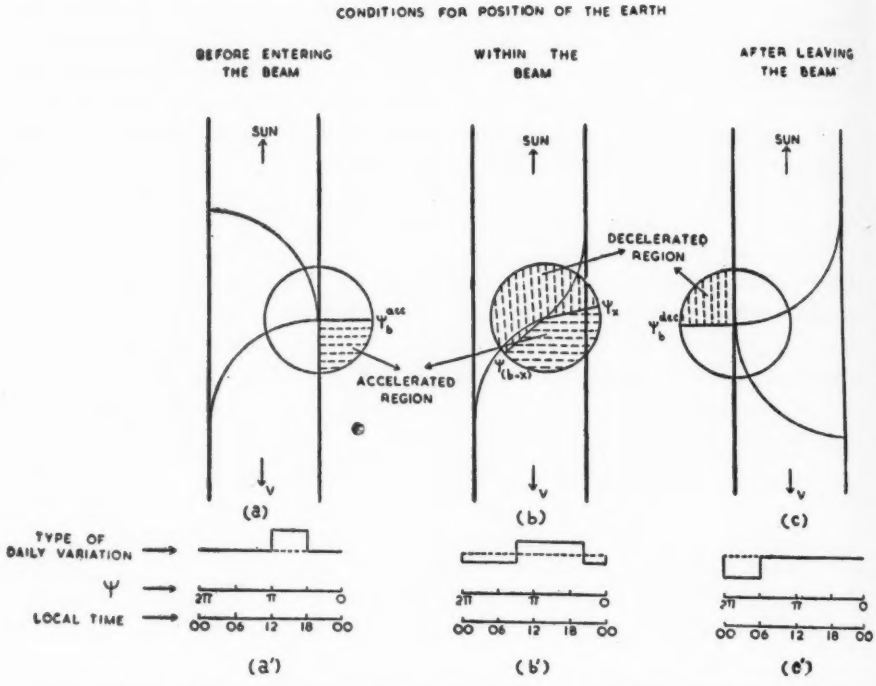

FIG. 3. Deflections of primary particles of energy $\approx 2W_{min}(0, b)$ and anisotropic region when the earth is (*a*) on the right side, (*b*) within and (*c*) on the left side of the beam. The component of the trapped magnetic field H_s is positive and the type of daily variation as a function of local time is measured by an instrument on the spinning earth in the absence of the geomagnetic field.

Because of the spin of the earth, a fixed telescope at a low latitude station would scan all directions in the plane of the ecliptic and would thus view during each day the regions where the isotropy of cosmic radiation is disturbed. The intensity measured by the telescope would therefore exhibit a solar daily variation. Taking the walls of the beam along the sun-earth line, *i.e.*, 12-hour direction and neglecting the influence of the earth's magnetic field, we show in Fig. 3 ΔW_x as a function of local time T on which is dependent the type of daily variation to be expected in each of the three cases. There is an increase of intensity from 12 hours to $(2\pi - \psi_b{}^{acc})/15$ hours in Fig. 3 (*a'*), while a decrease from 00 hours to $(2\pi - \psi_b{}^{dec})/15$ hours in

Fig. 3 (c'). The time of occurrence of the increase in case 3 (a') and the decrease in case 3 (c') is separated by 12 hours. The maximum of the daily variation therefore occurs between 12 and 18 hours irrespective of the relative position of the beam and the earth. When the earth is within the beam, this maximum, as shown by Nagashima,[11] is shifted towards 12 hours but is still between 12 and 18 hours.

We can summarise the influence of a beam with a positive component of the trapped magnetic field as follows. From the time when the beam is effective while approaching the earth, a region in space in which particles are accelerated is formed and this results in an increase in mean intensity in the afternoon. As the earth enters the beam, a new region of deceleration is created. This region goes on progressively decreasing but with increase in the amount of deceleration produced. The region of acceleration simultaneously increases but with a decrease in the amount of acceleration. The mean intensity therefore progressively decreases and attains its original value at the centre of the beam when both the regions are equal in width. As the earth leaves the beam, the region of acceleration disappears leaving behind a decelerated region and a decrease of mean intensity which returns to its normal value when the beam ceases to be effective.

In Fig. 4 we illustrate all these cases when H_z is negative, *i.e.*, directed opposite to what has been considered so far. The electric field is now directed from right to left so that in Fig. 4 (a) when the beam is approaching the earth we get a decelerated region from 0 to ψ_b^{dec} where

$$\psi_b^{dec} = \cos^{-1}\left(-1 + 2\sec\phi\,\frac{W_{min}(0, b)}{W}\right) \text{ and } \pi > \psi_b^{dec} > 0 \qquad (9)$$

In Fig. 4 (b) there is an accelerated region from ψ_x to $\psi_{(b-x)}$ and a decelerated region from $\psi_{(b-x)}$ to ψ_x where

$$\psi_x = \cos^{-1}\left(-1 + 2\sec\phi\,\frac{x}{b}\,\frac{W_{min}(0, b)}{W}\right) \text{ and } \pi > \psi_x > 0 \qquad (10)$$

and

$$\psi_{(b-x)} = \cos^{-1}\left(1 - 2\sec\phi\,\frac{b-x}{x}\,\frac{W_{min}(0, b)}{W}\right) \text{ and } 2\pi > \psi_{(b-x)} > \pi \qquad (11)$$

In Fig. 4 (c) when the earth leaves the beam we get an accelerated region from π to ψ_b^{acc} where

$$\psi_b^{acc} = \cos^{-1}\left(1 - 2\sec\phi\,\frac{W_{min}(0, b)}{W}\right) \text{ and } 2\pi > \psi_b^{acc} > \pi \qquad (12)$$

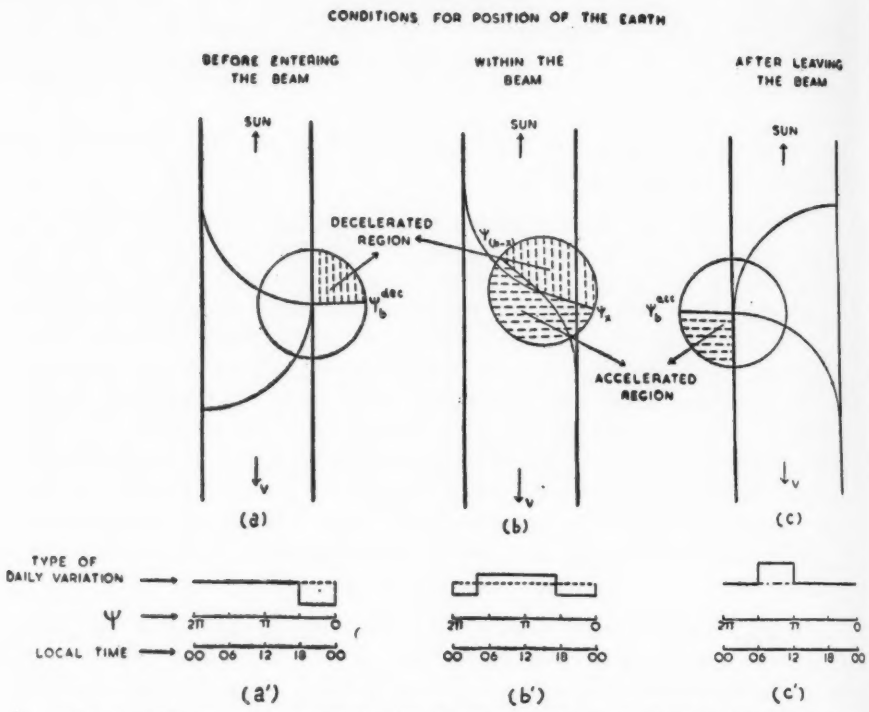

FIG. 4. Deflections of primary particles of energy $\approx 2W_{min}$ (0, *b*) and anisotropic region when the earth is (*a*) on the right side, (*b*) within and (*c*) on the left side of the beam. The component of the trapped magnetic field H_z is negative and the type of daily variation as a function of local time is measured by an instrument on the spinning earth in the absence of the geomagnetic field.

The type of daily variation recorded by an instrument on the spinning earth, neglecting the effect of the geomagnetic field, is illustrated in Fig. 4 (*a'*, *b'*, *c'*). When the earth is approaching the beam there is a decrease of intensity from $(2\pi - \psi_b^{dec})/15$ hours to 00 hours and when it leaves the beam there is an increase of intensity from $(2\pi - \psi_b^{acc})/15$ hours to 12 hours. The maximum of daily variation, when various energies of primary radiation are considered, is therefore expected to be between 06 and 12 hours.

The electromagnetic fields of the solar beams thus create anisotropy in the primary radiation which when the trapped magnetic field has a positive component gives rise to a maximum in the daily variation between 12 and 18 hours. With a reversed component of the magnetic field this maximum occurs between 06 and 12 hours. The times of maxima relate to the condition when the bending of the trajectories of cosmic ray particles in the geo-

magnetic field has not been allowed for. In the former case, when the beam is effective we should get an increase of mean intensity followed by a progressive decrease while in the latter case there should be a decrease of intensity followed by an increase.

IV. Diurnal Variation of Meson Intensity Produced by the Anisotropy of Primary Cosmic Radiation

The foregoing analysis gives the nature of the anisotropy that will be created by the electromagnetic fields in solar beams. The observable effect of the anisotropy in terms of a solar daily variation is however measured on cosmic ray secondaries produced by the primaries after they have suffered deflection in the geomagnetic field and interacted with matter in the atmosphere. Since the anisotropy, the deflection in the geomagnetic field as well as the interactions in the atmosphere are dependent on the energy of the primary particles, it is preferable for the purpose of evaluating the daily variation to consider the entire cosmic ray spectrum above the geomagnetic cut off rather than a mean energy of the primary radiation, as is usually done.

When the primary radiation is isotropic the intensity of cosmic radiation $I(\lambda, h)$ observed at an atmospheric depth h g./cm.^{2} and at geomagnetic latitude λ is given by

$$I(\lambda, h) = \int_{\alpha=0}^{\alpha=2\pi} \int_{\theta=0}^{\theta=\pi/2} \int_{E_{\lambda,\theta,\alpha}}^{\infty} m(E, h, \theta, \alpha)\, i(E)\, F(\theta, \alpha) \sin\theta\, d\alpha\, d\theta\, dE \qquad (13)$$

$F(\theta, \alpha)$ denotes the sensitive area of a recording apparatus at a zenith angle θ and azimuth angle α and $E_{\lambda,\theta,\alpha}$ is the corresponding cut-off energy at the geomagnetic latitude λ. $m(E, h, \theta, \alpha)$ and $i(E)\,dE$ are the overall multiplicity and differential energy spectrum respectively of the primary radiation.

If by the presence of the beams, primary particles of energy E gain an energy $\Delta E = \Delta W$ for a certain period of time, the change in the intensity ΔI is given by

$$\Delta I = \int_{\alpha=0}^{\alpha=2\pi} \int_{\theta=0}^{\theta=\pi/2} \int_{C_E}^{\infty} m(E, h, \theta, \alpha)\, i(E)\, g(E)\, \Delta E(T_{E,\theta,\alpha})\, F(\theta, \alpha) \times \sin\theta\, d\alpha\, d\theta\, dE \qquad (14)$$

where $C_E = E_{\lambda,\theta,\alpha}$ or $W_{min}(\phi, x)$ whichever is greater. The factor $g(E)$ is introduced to take into account the change in the differential energy spectrum of primary protons due to the additional energy gain and is given by Fonger[18] as

$$g(E) = \frac{1}{1+E}\left[\frac{2}{1-(1+E)^{-2}} + \beta\right] \text{ where } \beta = 2{\cdot}07 \qquad (15)$$

For meson intensity in the lower atmosphere, when $h > 700$ g./cm.^{2}, $m(E, h, \theta, \alpha)$ can be approximated as $m(E, h)\cos^2\theta$. The local time $T_{E,\theta,\alpha}$ refers to the direction of the particle outside the earth's magnetic field. Its relation with the local time $t_{E,\theta,\alpha}$ on the surface of the earth is given by

$$T_{E,\theta,\alpha} = t_{E,\theta,\alpha} + \psi_{E,\theta,\alpha} \tag{16}$$

where $\psi_{E,\theta,\alpha}$ is an angle through which a cosmic ray particle of energy E arriving at a zenith angle θ and azimuth angle α is deflected in the east-west plane (the plane of the ecliptic in the present work) in the earth's magnetic field. These values can be read out from the curves supplied by Brunberg and Dattner.[19] To evaluate the change of intensity at the surface of the earth $T_{E,\theta,\alpha}$ in Eq. 14 is replaced by $t_{E,\theta,\alpha}$. To obtain the diurnal variation, the values of $\Delta I/I$ are calculated by numerically integrating Eq. 14 at 24 local times, *viz.*, $t = 00, 01, 02, \ldots .$ 23 hours. For an ionization chamber $F(\theta, \alpha) = 1$. For counter telescope it can be evaluated by the formulæ given by Newell and Pressly.[20]

V. Numerical Evaluation of the Nature of the Solar Daily Variation of Meson Intensity

To compare the daily variation of meson intensity produced by the anisotropy of primary cosmic radiation with that observed experimentally, we must first examine some physical characteristics of the beam. The velocity of the ionized matter in the beam can be calculated from the time delay between the visible solar disturbances and the subsequent magnetic disturbances in the earth's magnetic field. A delay of about 24 hours when there is a large magnetic storm following a solar flare, indicates a velocity of 2,000 km./sec., while a delay from two to four days in the case of recurring magnetic disturbances suggest a velocity in the range of 1,000 km./sec. to 500 km./sec. We assume therefore that the velocity of the ionized matter at different times varies between 2,000 km./sec. and 500 km./sec.

The width of the beam is taken as $\sim 6 \times 10^{12}$ cm. With the synodic period of the sun as 27 days and the earth's orbital radius as $1{\cdot}5 \times 10^{13}$ cm., the earth will situate in the beam for about two days. The value is therefore consistent with inferences from geomagnetic data.

At the present moment there is no method by which we can determine the strength of the magnetic field in the beam. Parker[21] has recently shown that the value of the magnetic field in the beam is very insensitive to the density of the gas at the time of emission and with interplanetary density $\sim 10^{-21}$ g./cm.^{3} it should be less than $1{\cdot}4 \times 10^{-4}$ gauss. We assume that its value near the ecliptic varies between 2×10^{-5} gauss to 5×10^{-6} gauss. This

is necessary to produce an anisotropy compatible with experimental determination of the solar daily variation at low latitudes which has an amplitude of 0·3 to 1·0%.

With these values we show in Figs. 5 and 6 the expected daily variation of meson intensity at sea-level, *i.e.*, atmospheric depth $h = 1030$ g./cm.^{2} when the earth is just outside the beam and when the earth is within the beam at its centre respectively. For $m(E, 1030)\, i(E)$, the values given by Nagashima[22] using the primary spectrum given by Neher as

$$i(E) = \frac{0{\cdot}048}{E^{2/3}(1 + 0{\cdot}09\, E^{4/3})^{3/2}}$$

are used. The amplitudes and the times of maxima of the Fourier components of the daily variation are given in Table I. It must be emphasized that these values depend upon $i(E)\, dE$, the differential energy spectrum of the primary radiation and $m(E, 1030)$, the form of the multiplicity function. Recent evidence by Meyer and Simpson[23] and Neher[24] suggests that the differential energy spectrum varies during the course of years and a steeper spectrum than what is now assumed will give rise to larger amplitudes than those given in Table I. The precise value of the multiplicity function which is derived from the experimental determination of the latitude effect can be obtained for primary energies upto 15 Bev. For higher primary energies various authors have extrapolated it with different functions. Since at low latitudes primaries above 15 Bev. only are involved this extrapolation presents uncertainties. Hence the actual values at any time may be different from those given in Table I. However, they are not likely to differ much as to alter the picture presented therein.

An important point that emerges from Figs. 5 and 6 is that while a positive component of the trapped magnetic field within the beam gives rise to a diurnal variation at low latitudes with maximum shortly before noon, the reversal of this component will make the maximum in the daily variation shift to early morning hours. The daily variation in equatorial latitudes should therefore be expected to exhibit maximum either during night at about 03 hours or during day at about 11 hours. Beams emitted at different periods may not have identical characteristics and the time of maximum may vary within an interval of about an hour.

When the earth is at some distance from the beam, the walls of the beam will be inclined to the sun-earth line and the anisotropy in directions lying close to the walls of the beams is not accessible from the earth. The anisotropy of particles having energy near $W_{min}(0, b)$ is therefore not observed

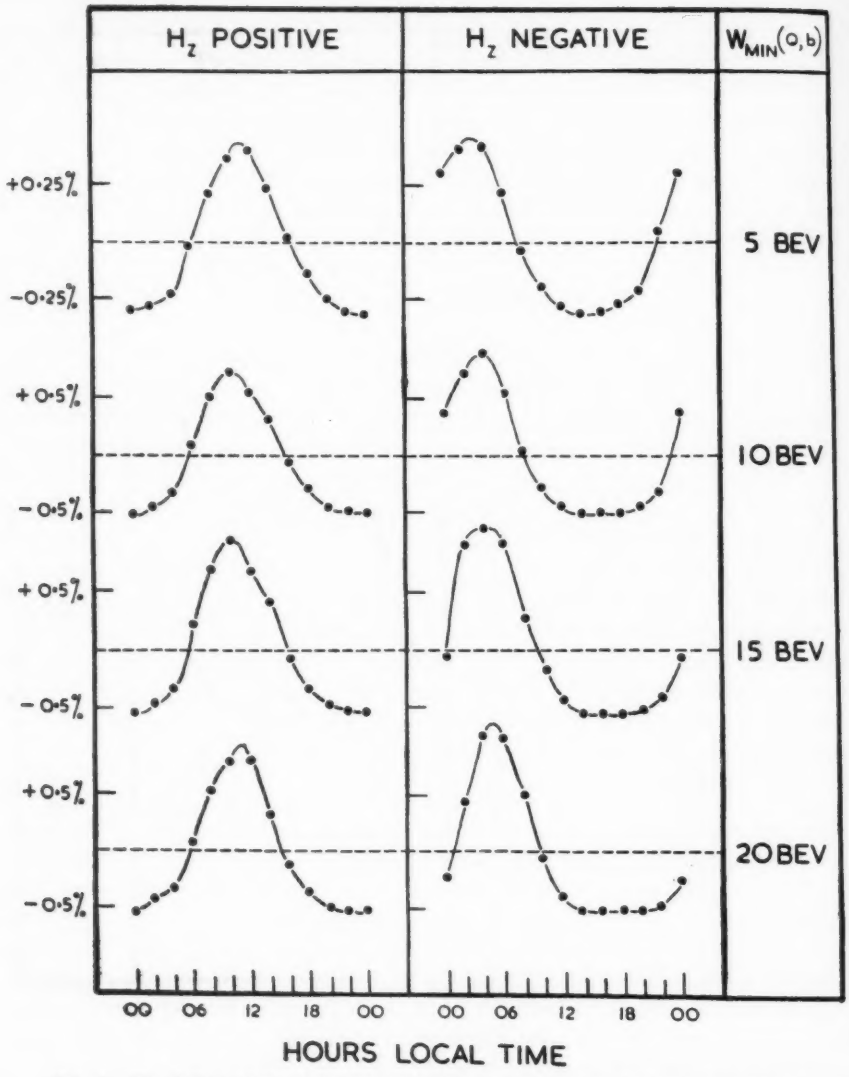

FIG. 5. The daily variation of meson intensity measured by an ionization chamber at sea-level in equatorial latitudes when the earth is just outside the beam of width $\sim 6\times10^{12}$ cm.

and the observed duration of the anisotropic region decreases. As the beam approaches the earth the accessible region increases, attains a maximum value within the beam and then decreases as the beam recedes from the earth.

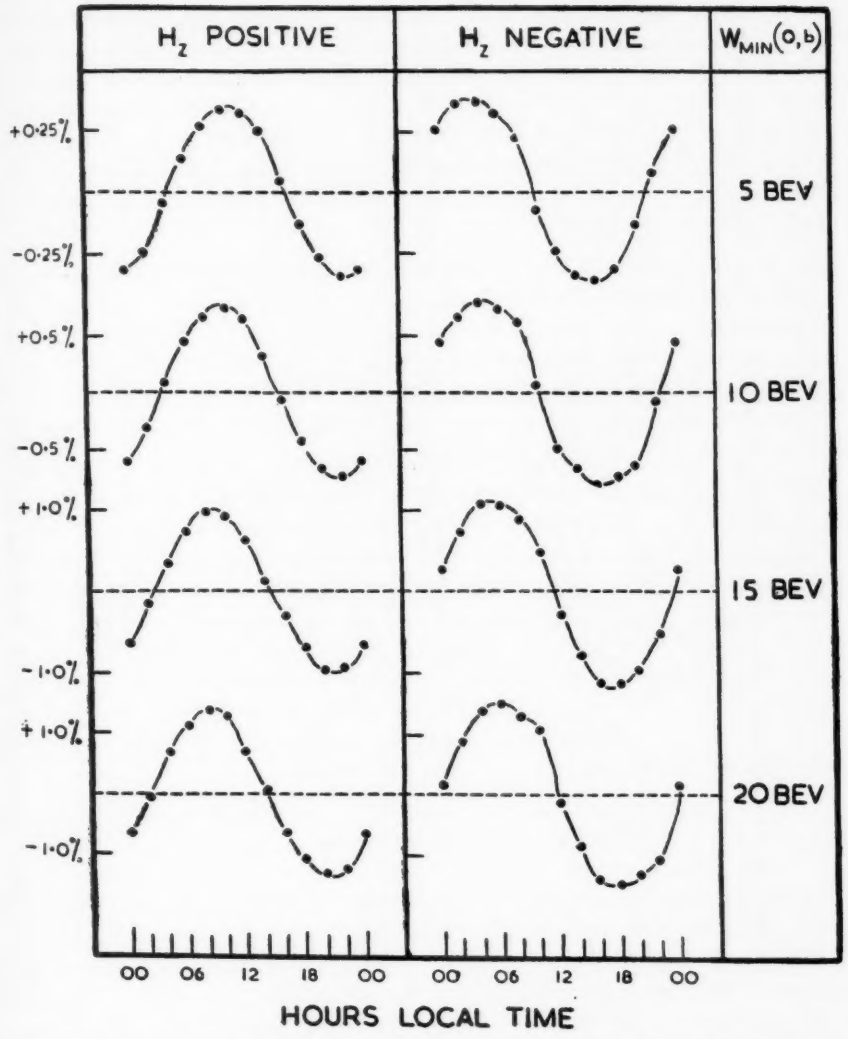

FIG. 6. The daily variation of meson intensity measured by an ionization chamber at sea-level in equatorial latitudes when the earth is at the centre of the beam of width $\sim 6 \times 10^{12}$ cm.

The amplitudes of the variation which depends upon the effective duration of the anisotropy increases for a few days, reaches a maximum when the earth is at the centre of the beam and then decreases progressively.

The limit of the region of acceleration or deceleration given by Eqs. 5–12 is expressed with reference to the walls of the beam. Their inclination to the sun-earth line introduces a correction to $T_{\theta, a}$. If we assume tentatively that the influence of the beam extends upto the time that it is within three days from the earth on either side of it, we have a maximum inclination of about 45° to the sun-earth line. The time of maximum would thus be displaced upto 3 hours on either side of the values indicated in Table I. Hence there should be a group of days when the time of maximum progressively shifts to later hours.

A further factor to be considered is the inclination of the walls of the beam to the sun-earth line due to the radial emission of solar matter from the spinning sun. Chapman and Bartels[25] have shown that the inclination would be by an angle of 12°, 24° and 48°, if the velocity of the matter is 2,000 km./sec., 1,000 km./sec. and 500 km./sec. respectively. The time of maximum would thus be further advanced by 12/15, 24/15 and 48/15 hours respectively.

It will now be realised that the daily variation observed on individual days will not always resemble the curves shown in Figs. 5 and 6, but these can still serve to represent the average characteristics of the daily variation. Analysis of Huancayo data by Sarabhai *et al.*[3] showing that the broad features of the daily variation of meson intensity at Huancayo can be explained in terms of the two types of variations, one having maximum at 1100 or 1300 hours and the other having a maximum at 0100 or 0300 hours can now be understood. The time of maximum on individual days will not always be sharply at the values given in Table I but will be grouped round these values. Observations by Sarabhai and Nerurkar[4] on the daily variation of meson intensity at Ahmedabad show similar characteristics.

The 12 monthly mean daily variation of meson intensity exhibits a 22-year cycle of change as observed at Huancayo. If this is due to change in the relative frequency of the variations with day and night maxima from year to year, the average orientation of the trapped magnetic field within beams should also have a similar variation. The most prominent feature on the sun which exhibits a 22-year cycle is the magnetic field associated with active solar regions. Maunder[26] has shown from a separate plot of sunspot areas for each hemisphere that there are comparatively large differences in the sunspot numbers of the two hemispheres as well as their time of maxima. One hemisphere appears to be more active than the other and remains so in the next sunspot cycle even though the reversal of the polarity of the magnetic fields associated with active regions takes place. If there is similar difference in activity between the North and the South hemispheres of the sun for

TABLE I

The per cent. amplitude and the time of maximum of the diurnal component of the daily variation of meson intensity measured by an ionization chamber at sea-level in equatorial latitudes by a beam of solar ionized matter of width $\sim 0{\cdot}66\times10^{13}$ *cm.*

Velocity of the beam v km./sec.	Component of the magnetic field H_z gauss	W_{min} $(0, b)$ Bev.	When the earth is just outside the beam						When the earth is at the centre of the beam					
			H_z positive			H_z negative			H_z positive			H_z negative		
			Ampl. %	Time of maximum		Ampl. %	Time of maximum		Ampl. %	Time of maximum		Ampl. %	Time of maximum	
				H.	M.		H.	M.		H.	M.		H.	M.
2000	5×10^{-6}	5	0·35	11	24	0·38	2	52	0·37	10	36	0·41	3	24
1000	5×10^{-6}	5	0·18	11	24	0·19	2	52	0·19	10	36	0·20	3	24
500	5×10^{-6}	5	0·09	11	24	0·09	2	52	0·09	10	36	0·10	3	24
2000	10^{-5}	10	0·61	10	48	0·67	3	40	0·75	9	40	0·84	4	24
1000	10^{-5}	10	0·30	10	48	0·38	3	40	0·37	9	40	0·42	4	24
500	10^{-5}	10	0·15	10	48	0·19	3	40	0·19	9	40	0·21	4	24
2000	$1{\cdot}5\times10^{-5}$	15	0·72	10	28	0·81	4	28	1·05	9	20	1·27	5	20
1000	$1{\cdot}5\times10^{-5}$	15	0·36	10	28	0·40	4	28	0·52	9	20	0·63	5	20
500	$1{\cdot}5\times10^{-5}$	15	0·18	10	28	0·20	4	28	0·26	9	20	0·32	5	20
2000	2×10^{-5}	20	0·68	10	36	0·75	5	12	1·44	8	12	1·70	6	00
1000	2×10^{-5}	20	0·34	10	36	0·37	5	12	0·72	8	12	0·85	6	00
500	2×10^{-5}	20	0·17	10	36	0·19	5	12	0·36	8	12	0·43	6	00

* Values reported at a symposium on Electromagnetic Phenomena in Cosmical Physics, Stockholm (1956) relate to the vertical intensity only.

corpuscular emission, and the coherent magnetic field trapped within the beam is in some way related to the local fields of active solar regions it would be possibleto have the 22-year cycle of change in the daily variation of meson intensity.

The amplitude of the daily variation on individual days can be as high as 0·7% for meson intensity as shown in Table I. It may be higher than 0·7% if the energy spectrum of the primaries is steeper. The amplitude averaged over a group of days, however, depends upon the number of days on which the beams are effective as well as the types of beams. Taking this number to be less than half it would be possible to account for the average amplitude of 0·1 to 0·3% for ionization chambers.

With a particular orientation of the magnetic field within the beam, the type of anisotropy and hence the daily variation is similar when the earth is on either side of it or within it. Each type of daily variation is thus expected to occur in groups of days. The recurrence tendency is a natural consequence of the persistence over several solar rotations of an active region responsible for a beam.

From a careful examination of geomagnetic disturbances and their association with solar phenomena in 1952–53, a period of low sunspot activity when the active regions were well defined and well observed, Pecker and Roberts[27] have shown that there is a minimum of geomagnetic activity about three days after the CMP of an active region. There are also definite maxima symmetrically situated at about 3 days from the minimum. They suggest that the solar active regions possess a magnetic field which deflects the ionized matter emitted by the region so that there is a deficiency of emitted matter at solar longitudes radially along the active centre. The ionized matter flows along lines of the magnetic field. At some distance above the centre of activity, the kinetic energy of the ions can be sufficient to overcome the magnetic field so that the guiding effect of the field of the active centre controls the ion flow only near the centre. The angle of aperture of this cone of avoidance may vary with the strength of the magnetic field of the active centre as well as that of the emission. With this picture of emission of ionized matter from the sun, we have in the plane of the ecliptic two beams separated on the average by about 5 to 6 days.

If the component of the trapped magnetic field perpendicular to the plane of the ecliptic is the same in both the beams and the earth is situated between them, it is seen from Figs. 3 and 4 that the earth receives accelerated particles from one beam and decelerated particles from the other. The amplitude of the daily variation can then be about double the values given in

Table I. If however this component of the magnetic field is different in both the beams, the earth receives accelerated or decelerated particles from each of them. Both types of anisotropies are simultaneously present. The resultant variation depends upon the distance between the two beams as well as the characteristics of them and in some cases it is possible to have a daily variation with two maxima. When the earth is on one side of both the beams, only the adjacent beam is effective and we have the resultant variation with only one maximum. It is thus possible to accommodate on the present model the existence of a daily variation with more than one maximum, such as is reported by Sarabhai and Nerurkar.[4]

VI. Conclusion

The creation of an anisotropy by the presence in the neighbourhood of the earth of beams of solar ionized matter with trapped magnetic fields derived from local fields related to active regions on the sun furnishes a plausible interpretation of several significant features of the daily variation of meson intensity. If one adopts the density and the velocity of ionized matter in the beams consistent with solar relationships of geomagnetic disturbances and assumes a strength of the trapped magnetic field compatible with electrodynamical considerations it is possible to derive a daily variation of meson intensity which, at low latitudes, would have a maximum just before noon or in the early morning. The two types of daily variation would occur in groups of days which would have a tendency of 27-day recurrence. The daily variation could have an amplitude upto 1% on individual days. The amplitude as well as the time of maximum of each type of daily variation would be expected to alter during each group. There would also be a possibility of daily variation with two maxima on some occasions.

The present interpretation does not deal with a permanent anisotropy of cosmic rays about which there is at present little experimental knowledge but which may nevertheless be present to a small degree. On the other hand it attempts to explain the observed features of a highly variable anisotropy in terms of a modulation of the primary cosmic ray intensity. Consequently the changes in the daily variation are linked with day-to-day changes in the daily mean intensity of cosmic radiation. A crucial test of the present interpretation would lie in the study of the correlated behaviour of the changes in the daily variation and in the mean intensity. This examination is in progress.

The author is deeply grateful to Professor V. A. Sarabhai for guidance and helpful discussions throughout the course of this investigation. The

author is also indebted to Professor H. V. Neher of California Institute of Technology for valuable discussions and critical comments during his visit to the laboratory. Grateful thanks are due to Mr. S. R. Thakore for computational assistance. The project under which this study was conducted is supported by Department of Atomic Energy, Government of India, for which the author is deeply grateful.

SUMMARY

The present status of knowledge concerning the daily variation of meson intensity is reviewed. A solar daily variation of a constant nature arising out of a permanent anisotropy in the cosmic radiation has not so far been established and even if it exists it may not exceed a few tenths of a per cent. However a number of features of a solar daily variation of a highly variable character having on the average a time of maximum on individual days either in the early morning or near noon are known. An attempt is therefore made to interpret the occurrence of a variable anisotropy of cosmic rays to which are attributed the principal experimental observations.

Beams of solar ionized matter with a frozen magnetic field derived from a solar dipole field have been earlier suggested to explain abnormal diurnal variation on magnetically disturbed days through an anisotropy in primary cosmic radiation created by them. The present paper considers that the variable anisotropy is due to such beams but the frozen magnetic field is derived from the magnetic field of the active solar regions and bears no preferential orientation in respect to the solar dipole field. With different orientations of the magnetic field in the beam, the component perpendicular to the solar equatorial plane could be reversed in direction. Depending upon the direction of this component, the anisotropy in the primary radiation gives rise to a daily variation at equatorial stations with maximum either in early morning hours or near noon for a group of days. With the strength of this component of the magnetic field in the range 10^{-4} to 10^{-6} gauss and the velocity of the beam between 500 km./sec. and 2,000 km./sec., the daily variation of meson intensity has amplitudes from 0·3 to 1·5%. The simultaneous presence of two such beams gives rise to double the amplitudes or a daily variation with two maxima.

Some further applications of this concept are discussed.

REFERENCES

1. Sarabhai, V., Nerurkar, N. W., Duggal, S. P. and Sastry, T. S. G. *Proceedings of a Symposium on Electromagnetic Phenomena in Cosmical Physics, Stockholm*, 1956.

2. Sarabhai, V., Desai, U. D. and Venkatesan, D. *Phys. Rev.*, 1955, **99**, 1490.
3. ———— *Proceedings of I.U.P.A.P.*, Cosmic Ray Congress, Mexico, 1955.
4. Sarabhai, V. and Nerurkar, N. W. *Ibid.*, 1955.
5. Sekido, Y., Yoshida, S. and Kamiya, Y. *Rep. Ionosphere Res., Japan*, 1952, **6**, 195.
6. Sittkus, A. .. *J. Atmos. Terr. Phys.*, 1955, **7**, 80.
7. Brunberg, E. A. and Dattner, A. *Tellus*, 1954, **6**, 73.
8. Alfven, H. .. *Ibid.*, 1954, **6**, 232.
9. Sarabhai, V. and Kane, R. P. *Phys. Rev.*, 1953, **90**, 204.
10. Thambyahpillai, T. and Elliot, H. *Nature*, London, 1953, **171**, 918.
11. Nagashima, K. .. *J. Geomag. Geoelec.*, 1955, **7**, 51.
12. Elliot, H. and Dolbear, D. W. N. *J. Atmos. Terr. Phys.*, 1951, **1**, 205.
13. Alfven, H. .. *Phys. Rev.*, 1949, **75**, 11.
14. Keipenheuer, K. O. .. *The Sun*, University of Chicago Press, 1954.
15. Alfven, H. .. *Cosmical Electrodynamics*, Oxford: Clarendon Press, 1950.
16. Babcock, H. D. and Babcock, H. W. *Ap. J.*, 1955, **121**, 349.
17. Swann, W. F. G. .. *J. Franklin Inst.*, 1954, **257**, 191.
18. Fonger, W. H. .. *Phys. Rev.*, 1953, **91**, 351.
19. Brunberg, E. and Dattner, A. *Tellus*, 1953, **5**, 269.
20. Newell, H. E. and Pressly, E. C. *Rev. Sci. Inst.*, 1949, **20**, 568.
21. Parker, E. N. .. *Phys. Rev.*, 1956, **103**, 1518.
22. Nagashima, K. .. *J. Geomag. Geoelec.*, 1953, **5**, 141.
23. Meyer, P. and Simpson, J. A. *Phys. Rev.*, 1955, **99**, 1517.
24. Neher, H. V. .. *Ibid.*, 1956, **103**, 228.
25. Chapman, S. and Bartels, J. *Geomagnetism*, 1940, **2**, Oxford: Clarendon Press.
26. Maunder, E. W. .. *Mon. Not. Roy. Astr. Soc.*, 1922, **82**, 534.
27. Pecker, J. C. and Roberts, W. B. *J. Geophys. Res.*, 1955, **60**, 33.

456–57. Printed at The Bangalore Press, Bangalore City, by C. Vasudeva Rao, Superintendent and Published by The Indian Academy of Sciences, Bangalore.

NOTICE TO AUTHORS

Scientific papers intended for publication in the *Proceedings of the Indian Academy of Sciences* can be accepted only when they are communicated by a Fellow of the Academy whose duty shall be to satisfy himself that such communications are fit to be read at the Meeting of the Academy and published in its *Proceedings*.

Papers should not ordinarily exceed fifty pages of foolscap. MSS. should be either typewritten or written in legible hand on one side of the paper. All papers should be carefully revised by the authors and should be absolutely in final form for printing. Position for text-figures should be indicated. Each paper shall conclude with a critical summary not exceeding 350 words.

Drawings, diagrams or other illustrations should be made on larger scale (preferably) twice the size than the ones in which they are intended to appear. They should be done in Indian ink on bristol board with lettering in pencil. Scale of magnification of camera lucida tracings should be indicated by the side of drawings. In certain special cases arrangements will also be made for monochrome lithographic and other colour plates. Reduction of illustrations desired should be indicated in pencil. Appropriate legends should accompany all drawings. Names of authors are to be marked in pencil on the left-hand corner of drawing sheets. Photomicrographs should be securely mounted with colourless paste.

All tables, quotations and footnotes which will be set hereafter (beginning from Vol. I, No. 2) in types smaller than the text, should be typewritten on separate sheets and placed with the text in proper sequence. Footnotes should be numbered in Arabic numerals.

References to literature in the text should be given, whenever possible, in chronological order, only the names of authors and years of publication, in brackets, being given. They should be cited in full after the summary, the authors' names following in alphabetical order. Thus,

Name or Names of author; Name of Journal (abbreviation) with a single underline; Year of publication; Number of Volume with a double underline, and lastly page. The following would be a useful illustration:—

Bergmann and Stather . . . . . Z. Physiol. Chem., 1926, 152, 189.

Two copies of slip-proof and wherever possible, a page proof for final revision will be sent to authors. All corrections are best made on the slip-proof which should be transmitted to the Office of the Academy. All proof corrections involve heavy expenses which would be negligible if the papers are carefully revised by the authors before submission.

Fifty free reprints including plates and with cover will be supplied for each paper. Additional copies can be supplied at cost on previous intimation.

Blocks appearing in the *Proceedings* will be available for purchase by their respective authors. Orders for the same should be sent along with the corrected proofs and in any case not later than one month after the date of publication of the paper. The price charged would be 25% of the actual cost of the blocks *plus* freight and despatching charges. If the blocks are reproduced in other journals or publications, due acknowledgment should be made in them to the *Proceedings*.

The original drawings and plates of blocks appearing in the *Proceedings* will be returned to such of the authors as may require them provided the cost of despatching such originals is borne by them.

CONTENTS

PAGE

The Specific Heats of Crystals and the Fallacy of the Theories of Debye and Born . . . . . Sir C. V. Raman 273

On Superposable Flows . . . . . P. L. Bhatnagar and P. D. Verma 281

A New Synthesis of Dalbergin and Methyl Dalbergin and a Synthesis of Allo-Dalbergin . . . . V. K. Ahluwalia, A. C. Mehta and T. R. Seshadri 293

Studies on the Dependence of Optical Activity on Chemical Constitution. Part XLVI. The Rotatory Dispersion of *d*-Camphor-β-sulphonyl-nitrophenylamides (*o*-, *m*- and *p*-), *d*-camphor-β-sulphonylphenylene-diamines (*o*- *m*-, and *p*-) and (*o*-, *m*- and *p*-) phenylene-*bis*-*d*-camphor-β-sulphonylamides . . . Bawa Kartar Singh and Shiva Mohan Verma 298

Multiple Processes in Electron-Photon Cascades . . . . . Alladi Ramakrishnan, S. K. Srinivasan, N. R. Ranganathan and R. Vasudevan 311

Inhibition of Shrinkage in Nuclear Emulsions . . . P. N. Krishnamoorthy 327

Non-Relativistic Approximation of Bhabha's Equation . . . . K. K. Gupta 336

An Interpretation of the Solar Anisotropy of Primary Cosmic Radiation . . . . . N. W. Nerurkar 341